

THE UNIVERSITY OF CALGARY

Force-Calcium Relation in Intact Rat Myocardium

by

Ellen Herdis Hollander

A THESIS

SUBMITTED TO THE FACULTY OF GRADUATE STUDIES

IN PARTIAL FULFILMENT OF THE REQUIREMENTS FOR THE DEGREE OF

MASTER OF SCIENCE

DEPARTMENT OF CARDIOVASCULAR/RESPIRATORY SCIENCES

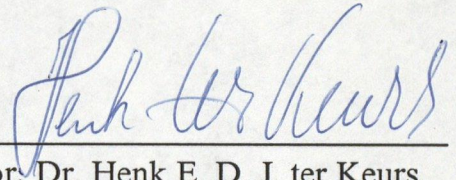
CALGARY, ALBERTA

APRIL, 1995

©Ellen Herdis Hollander 1995

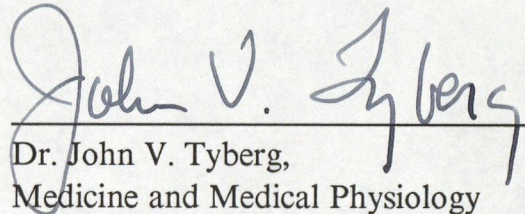
THE UNIVERSITY OF CALGARY  
FACULTY OF GRADUATE STUDIES

The undersigned certify that they have read, and recommend to the Faculty of Graduate Studies for acceptance, a thesis entitled "Force-Calcium Relation in Intact Rat Myocardium" submitted by Ellen Herdis Hollander in partial fulfilment of the requirements for the degree of Master of Science.



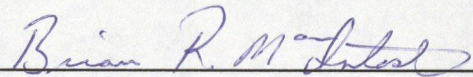
---

Supervisor, Dr. Henk E. D. J. ter Keurs,  
Medicine and Medical Physiology



---

Dr. John V. Tyberg,  
Medicine and Medical Physiology



---

Dr. Brian R. MacIntosh (external),  
Medical Sciences

April 7, 1995  
Date

## Abstract

Force-calcium relations were obtained in tetanized cardiac muscle at sarcomere lengths of 2.2  $\mu\text{m}$  and 1.8  $\mu\text{m}$ . Intracellular  $\text{Ca}^{++}$  concentration ( $[\text{Ca}^{++}]_i$ ) was estimated from the ratio of Fura-2 fluorescence collected at 510 nm and excited with 340 and 380 nm. Steady state levels of force were achieved with 12-15 Hz stimulation, in the presence of the sarcoplasmic reticulum  $\text{Ca}^{++}$ -ATPase inhibitor, cyclopiazonic acid. Maximal force ( $105.2 \pm 1.8 \text{ mN/mm}^2$ ) obtained at a sarcomere length of 2.2  $\mu\text{m}$  decreased by 25% when sarcomere length was shortened to 1.8  $\mu\text{m}$ . Although a marked decrease in force occurred, no concurrent changes in  $[\text{Ca}^{++}]_i$  were detected. Force- $[\text{Ca}^{++}]_i$  relations show reductions in maximal force, and a rightward shift of half-maximal  $[\text{Ca}^{++}]_i$  as sarcomere length decreases. This indicates that with decreasing sarcomere length and force generation, there is a reduction in  $\text{Ca}^{++}$  binding to myofilaments, due to decreasing myofilament sensitivity to  $\text{Ca}^{++}$ . Such a fundamental property of myocardium provides the basis for the Frank-Starling relation in the whole heart.

## Preface

Children of Happiness are not like ordinary children.  
A Child of Happiness always seems like an old soul living in a new body,  
and her face is very serious until she smiles,  
and then the sun lights up the world.  
*-for Bonnie Holtby, from the Daughters of Copper Woman*

I am always glad to touch the living rock again  
and dip my head in high mountain sky.  
*-for me, by John Muir*

Wisdom is knowing what to ask and whom to ask.  
You can learn grace from the panther, power from the bear, patience from the spider  
And of those three virtues, patience is the most important  
And the most difficult, Beloved Father  
*-Walk In My Soul*

So often it happens that we live our lives in chains  
and never know we have the key.  
*-The Eagles*

### On the Loose

On the loose to climb a mountain  
On the loose to where I am free  
On the loose to live my life the way, I think life should be  
Cause I've only got a moment and the whole world left to see  
I'll be searching for tomorrow on the loose  
Have you ever seen the sunrise, turn the sky completely red  
Slept beneath the moon and stars  
Pine bough o'er your head  
Can you sit and talk with friends, though not a word is said  
If you're like me, then you are on the loose.  
*-from Kati Beck's memorial (1994)*

## **Acknowledgments**

To begin I need to bring forth the names of the individuals that gave me skills (personally and academically) to continue on the path I have chosen. I need to always remember Mr. D.C. Lundy who gave me courage to have goals that you have to really work for. I will thank every day my teacher, mentor, and friend, Dr. V. Pat Lombardi. He has had so much faith in me and given me so many opportunities to learn and develop that I can accomplish any goal and overcome any obstacle that I may be faced with. Much of what he has done for me has made me what I am today and will help me become what I want to be tomorrow. My parents have always been my silent partner in anything I have ever chosen to do. Their support for all I have done has given me the security to risk trying harder and achieving more than I have ever thought I could. The unconditional love of my family is more than anyone could ever ask for and doesn't go unnoticed. I cherish it each and every day. I also can not do anything with out my best friend A.J., she has been with me nearly as long as my own family and is certainly a very significant part of who I am.

I need to thank the people that have helped me to start and complete the project presented here. The first to thank must be Hamid Banijamali, he has allowed me to inherit his set-up, and helped me to get started. Monica Scarabello has provided me with some desperately needed sanity, not to mention all the little things that I can still

think of and crack-up. Her advice and friendship have been invaluable in many of the things I have encountered while working in this lab. I must offer a thanks to my supervisor, Dr. ter Keurs, for allowing me the opportunity to complete this project, it has offered me with an education that extends beyond science. His efforts have challenged me to achieve a higher level of thinking, providing me with a means to grow. In conclusion, I would also like to extend my gratitude to my committee members Dr. J.V. Tyberg and Dr. B.R. MacIntosh for their much needed helpfulness and advice during the time Dr. ter Keurs was away on his sabbatical.

This thesis was written after a leave of absence where I went to attend to a tragedy. The friends that were involved were much more than a personal loss, but a loss for everyone as their contributions will never be fully achieved. They were people I have known while spending my summers doing the sweatiest, dirtiest, and best job I can do. I cared about each person and knew each in a different way. Their memories will never allow me to think I haven't been blessed. The other friends that were involved, but were fortunate enough to have gotten themselves out of danger, must also be thought of. Their continuing friendships will remind me again that I have been blessed and offer me a chance to appreciate what I have been allowed to have: a lot of very good friends.

In addition to the unfortunate events this past year, I would also like to include Suzanne Wilkins and Katie Eggleston. I miss them a lot.

## Table of Contents

	Approval Page .....	ii
	Abstract .....	iii
	Preface .....	iv
	Acknowledgements .....	v
	Table of Contents .....	vii
	List of Tables .....	x
	List of Figures .....	xi
Chapter 1	Introduction	
1.1	Prologue .....	1
1.2	Myofilament Sensitivity to $Ca^{++}$ .....	3
1.3	Co-operativity of the Thin Filament .....	4
1.4	Myofilament ATPase Activity .....	6
1.5	Force- $Ca^{++}$ Relations From Intact and Skinned Fibers .....	7
1.6	Inhibition of the Sarcoplasmic Reticulum .....	8
1.7	Objectives of the Study .....	10
Chapter 2	General Methods	
2.1	Muscle Preparation .....	12
2.2	Basic Experimental Set-Up .....	13
2.2.1	Placement of Muscle .....	13
2.2.2	Electrical Stimulation .....	16
2.2.3	Force Measurement .....	16
2.2.4	Sarcomere Length Measurement .....	16
2.3	$[Ca^{++}]_i$ Measurement .....	17
2.3.1	Autofluorescence and Background Light .....	18
2.3.2	Injection of Fura-2 into the Muscle .....	18
2.3.3	Path of Excitation Light to the Muscle .....	19
2.3.4	Path of Fluorescence Light from the Muscle .....	20
2.3.5	Fluorescence Ratio Conversion to $[Ca^{++}]_i$ Values .....	21
2.4	Data Acquisition .....	23
2.5	Force- $[Ca^{++}]$ Relations .....	26
2.6	Statistical Analysis .....	27
2.7	Solutions .....	27
2.7.1	Composition .....	27
2.7.2	Solution pH .....	28
2.7.3	Dissolving Cyclopiazonic Acid .....	31
2.8	Tetanic Contraction .....	34

Chapter 3	Effects of Cyclopiazonic Acid on Cardiac Muscle	
3.1	Introduction . . . . .	35
3.1.1	Hypothesis . . . . .	38
3.2	Methods . . . . .	38
3.2.1	Muscle Preparation . . . . .	38
3.2.2	Measurement of Recirculation Fraction . . . . .	39
3.2.3	Measurement of Force-[Ca <sup>++</sup> ] <sub>o</sub> Relations . . . . .	40
3.3	Results . . . . .	41
3.3.1	Twitch Force . . . . .	41
3.3.2	Recirculation Fraction . . . . .	46
3.3.3	Force-[Ca <sup>++</sup> ] <sub>o</sub> Relations . . . . .	46
3.4	Discussion . . . . .	57
3.5	Summary of Findings . . . . .	62
3.6	Potential Sources of Errors . . . . .	63
Chapter 4	Effects of Cyclopiazonic Acid on Cardiac Myofilaments	
4.1	Introduction . . . . .	64
4.2	Methods . . . . .	65
4.2.1	Chelexing . . . . .	66
4.2.2	Binding Constants . . . . .	68
4.2.3	Parent Solution . . . . .	70
4.2.4	EGTA Buffered Solutions . . . . .	70
4.2.5	Activating, Relaxing, and Skinning Solutions . . . . .	72
4.2.6	Ca <sup>++</sup> Solutions . . . . .	75
4.2.7	Protocol . . . . .	75
4.2.8	Curve Fitting . . . . .	76
4.3	Results . . . . .	76
4.4	Discussion . . . . .	82
4.5	Summary of Findings . . . . .	83
4.6	Potential Sources of Errors . . . . .	83
Chapter 5	Diastolic Fluorescence Measurements Before and After Fura-2 Loading	
5.1	Introduction . . . . .	84
5.2	Methods . . . . .	85
5.2.1	Muscle Placement . . . . .	85
5.2.2	Measurement of Muscle Fluorescence . . . . .	85
5.2.3	Measurement of Fura-2 Dye Leakage . . . . .	86
5.2.4	Measurement of Diastolic Ratios . . . . .	86

5.2.5	Twitch and Tetanus .....	86
5.3	Results .....	87
5.3.1	Autofluorescence .....	87
5.3.2	Dye Fluorescence .....	87
5.3.3	Dye Leakage .....	92
5.3.4	Diastolic 340/380 Ratios .....	95
5.3.5	Twitch and Tetanus .....	95
5.4	Discussion .....	100
5.4.1	Autofluorescence .....	100
5.4.2	Dye Fluorescence .....	100
5.4.3	Dye Leakage .....	101
5.4.4	Diastolic Fluorescence Ratio .....	101
5.4.5	Twitch and Tetanus .....	102
5.5	Summary of Findings .....	102
5.6	Potential Sources of Error .....	103
Chapter 6	Steady State Force-Fura-2 Fluorescence at Two Sarcomere Lengths	
6.1	Introduction .....	105
6.1.1	Hypothesis .....	106
6.2	Methods .....	107
6.2.1	Muscle Preparation .....	107
6.2.2	Fura-2 Loading and Muscle Stimulation .....	107
6.2.3	Force-[Ca <sup>++</sup> ] Relation .....	107
6.3	Results .....	108
6.3.1	Tetanus at Long and Short Sarcomere Lengths .....	108
6.3.2	Force-[Ca <sup>++</sup> ] <sub>o</sub> Relation .....	109
6.3.3	Force-[Ca <sup>++</sup> ] <sub>i</sub> Relation .....	117
6.3.4	Relationship Between [Ca <sup>++</sup> ] <sub>i</sub> and [Ca <sup>++</sup> ] <sub>o</sub> .....	123
6.4	Discussion .....	123
6.4.1	Tetanus at Long and Short Sarcomere Lengths .....	123
6.4.2	Force-[Ca <sup>++</sup> ] <sub>o</sub> Relation .....	128
6.4.3	Force-[Ca <sup>++</sup> ] <sub>i</sub> Relation .....	130
6.4.4	Relationship Between [Ca <sup>++</sup> ] <sub>i</sub> and [Ca <sup>++</sup> ] <sub>o</sub> .....	132
6.5	Summary of Findings .....	133
6.6	Potential Sources of Error .....	133
Chapter 7	Conclusion .....	135
References	.....	138

## List of Tables

Table 2-1	[Ca <sup>++</sup> ] for In Vitro Calibration of Fura-2 . . . . .	22
Table 3-1	F <sub>max</sub> , EC <sub>50</sub> , and Hill Coefficient (Force-[Ca <sup>++</sup> ] <sub>o</sub> ) . . . . .	56
Table 4-1	Binding Constants . . . . .	69
Table 4-2	Parent Solution . . . . .	71
Table 4-3	Activating and Relaxing Solutions . . . . .	73
Table 4-4	[Ca <sup>++</sup> ] Used in Activating Solutions . . . . .	74
Table 4-5	F <sub>max</sub> , EC <sub>50</sub> , and Hill Coefficient (Force-[Ca <sup>++</sup> ] <sub>free</sub> ) . . . . .	81
Table 6-1	F <sub>max</sub> , EC <sub>50</sub> , and Hill Coefficient (Force-[Ca <sup>++</sup> ] <sub>o</sub> ) . . . . .	116
Table 6-2	F <sub>max</sub> , EC <sub>50</sub> , and Hill Coefficient (Force -Ratio -[Ca <sup>++</sup> ] <sub>i</sub> ) . . . . .	122

## List of Figures

Figure 2-1	Illustration of Experimental Apparatus . . . . .	15
Figure 2-2	In Vitro Calibration of Fura-2 . . . . .	25
Figure 2-3	Effects of Increasing $[Ca^{++}]_o$ on pH . . . . .	30
Figure 2-4	Effects of Increasing DMSO or EtOH on Twitch Force . . . . .	33
Figure 3-1	Effect of [CPA] on Twitch Force Production . . . . .	43
Figure 3-2	Effect of [CPA] on Twitch Relaxation . . . . .	45
Figure 3-3	Twitch Force Decline From a Potentiated Beat with CPA . . . . .	48
Figure 3-4	Effect of [CPA] on Recirculation Fraction . . . . .	50
Figure 3-5	Effect of $[Ca^{++}]_o$ on Tetanic Force . . . . .	53
Figure 3-6	Force- $[Ca^{++}]_o$ Relation for the Twitch and Tetanus . . . . .	55
Figure 4-1	Skinned Fiber Force Tracings . . . . .	78
Figure 4-2	Force- $Ca^{++}$ Relations in Skinned Fibers . . . . .	80
Figure 5-1	Autofluorescence at 340, 360, and 380 nm . . . . .	89
Figure 5-2	Autofluorescence and Fura-2 Fluorescence . . . . .	91
Figure 5-3	Decline of Fura-2 Fluorescence Over Time . . . . .	94
Figure 5-4	Diastolic Fura-2 Fluorescence . . . . .	97
Figure 5-5	Force, Fluorescence, and $[Ca^{++}]_i$ for the Twitch and Tetanus . . . . .	99
Figure 6-1	Force and Fluorescence for Tetanus at the Short Length . . . . .	111
Figure 6-2	Force and Fluorescence for Tetanus at the Long Length . . . . .	113
Figure 6-3	Force- $[Ca^{++}]_o$ Relations at Short and Long Sarcomere Lengths . . . . .	115
Figure 6-4	Force- $R_{340/380}$ Relations at Both Sarcomere Lengths . . . . .	119
Figure 6-5	Force- $R_{340/380}$ Relations at Both Lengths with Raw Data . . . . .	121
Figure 6-6	Force- $[Ca^{++}]_i$ and Force- $[Ca^{++}]_o$ Relations at Both Lengths . . . . .	125
Figure 6-7	$[Ca^{++}]_i$ - $[Ca^{++}]_o$ Relation . . . . .	127

## Chapter 1

### Introduction

#### 1.1 Prologue

In the heart, all of the cells are contracting with each beat. The ability of these cells to respond to changes in pressure, volume, neural and humoral stimulation, substrate and oxygen availability, as well as other critical elements is vitally important to the health of an individual. Understanding activation and regulation of the cell's contractile machinery, the myofilaments, can be instrumental in the diagnosis and treatment of problems in this area. Moreover, since calcium ( $\text{Ca}^{++}$ ) is the primary activator of contraction, immediate modulation of its concentration could have substantial effects in response to the physiological demands that the heart can be subjected to.

Nearly 100 years ago, two important observations were made regarding the pressure and volume in the heart. These observations can be summarized as an increase in ventricular filling during diastole (preload) augments the ejection of blood during systole. The relation between end-diastolic volume and systolic performance is known as the Frank-Starling relation. This provides the heart with an important regulatory mechanism to allow the heart to respond to changes on a beat to beat basis. Preload can now be understood to effect end-diastolic fiber length which in turn has consequences at the level of the myofilaments. However, the specific mechanisms for this relation in regards to the contractile apparatus has yet to be established. The length-tension relation of isolated cardiac muscle introduces us to a view of the Frank-Starling relation without concern for ventricular geometry. Cardiac muscle operates in the range of sarcomere lengths from  $1.6\mu\text{m}$  to  $2.2\mu\text{m}$  (ter Keurs et al. 1980), which corresponds to the ascending limb of the length-tension relation, where the amount of

tension that is produced at constant activation increases with muscle length (Allen et al. 1974). Although cardiac and skeletal muscle are very similar in their myofilament arrangement their force-length relations are quite different. Shortening each muscle (cardiac and skeletal) to 80% of their optimal length, skeletal muscle can still produce 80-90% of its maximal force ( $F_{max}$ ), but cardiac muscle can only produce about 10% of maximal force. Such a length tension relation for skeletal has been explained by varying degrees of myofilament overlap (Gordon et al. 1966). Allen et al. (1974) suggested that the cardiac length-tension relation is influenced by other parameters in addition to thick and thin filament arrangements at lengths below optimal because of the observed differences in tension produced with various levels of  $Ca^{++}$ . Cardiac muscle is unable to achieve maximal force because of several limiting factors including the sarcolemma, SR, and sarcomeres (Schouten et al. 1990), unlike skeletal muscle. This would suggest that activation factors in relation to length must play an important role in steepness of the length-tension relation (Allen & Kentish 1985). The findings of Allen et al. (1974) provide a basis for subsequent investigations regarding the contractile behaviour of cardiac muscle.

In order to study potential factors contributing to the apparent length-dependant activation of cardiac contractile elements, multicellular preparations have been used. The ability to manipulate length in a multicellular preparation, allows tension and the effects of tension to be studied more specifically (Allen & Kentish 1985), as opposed to using a whole heart preparation. Activation of the myofilaments can be studied by skinning the muscle (permeabilization of sarcolemmal and subcellular membranes), through chemical means. The intracellular environment is controlled directly by manipulation of the solutions bathing the muscle (this is particularly important in controlling the  $Ca^{++}$  levels for myofilament activation) allowing a steady state level of force to develop at a given  $[Ca^{++}]$ . Indicators of intracellular  $Ca^{++}$  concentration

( $[Ca^{++}]_i$ ) provide a means to measure  $[Ca^{++}]_i$  in an intact (unskinned) preparation (Allen & Blinks 1978, Grynkiewicz et al. 1986).

## 1.2 Myofilament Sensitivity to $Ca^{++}$

In a study by Allen and Kurihara (1982) on intact cardiac muscle using an  $[Ca^{++}]_i$  indicator, the following were observed: 1) an increased rate of decline in cytosolic calcium from the peak immediately after the muscle was stretched; and 2) a rise in the  $Ca^{++}$  level was seen when the muscle was released (quickly shortened) in the middle of a contraction without a rise in tension. Using skinned cardiac muscle, in the presence of the same  $Ca^{++}$  indicator, a quick release during contraction also produced an rise of intracellular  $Ca^{++}$  ( $[Ca^{++}]_i$ ) (Allen & Kentish 1988). Such demonstrations of reduced affinity for  $Ca^{++}$  in a shortened muscle are further substantiated in force- $[Ca^{++}]$  relations at different sarcomere lengths (Hibberd & Jewell 1982, Kentish et al. 1986). It becomes apparent that as the muscle is stretched (longer sarcomere lengths), greater maximal ( $F_{max}$ ) and submaximal forces are achieved, in addition to a reduction in the amount of  $Ca^{++}$  necessary to achieve 50% of maximal force ( $EC_{50}$ ), and a larger increase in force for a given  $Ca^{++}$  increment to  $F_{max}$  (Kentish et al. 1986). Hofmann and Fuchs (1988) have compared force development in skinned fibers to the amount of  $Ca^{++}$  bound to troponin C (TnC) at two sarcomere lengths. This comparison shows a reduction in the amount of  $Ca^{++}$  bound to TnC at the shorter sarcomere length corresponding to a reduction in force. Support for the changes in the responsiveness of the myofibrils to  $Ca^{++}$  with changes in sarcomere length and force have been discussed by Allen and Kentish (1985) and Kentish, ter Keurs, and Allen (1988). Subsequent investigations have supported these findings and have revealed more information regarding the relation of the regulatory units of the thin filament to  $Ca^{++}$ , force, and length (review by Moss 1992).

It is difficult to attribute the observed change in the affinity of TnC for  $\text{Ca}^{++}$  to either alterations in muscle length or force development. The experiments of Allen and Kentish (1988) suggest that it is the generation of force, as opposed to sarcomere length changes, that affects  $\text{Ca}^{++}$  affinity of the myofilaments. In these experiments, a rapid muscle length change was imposed during contraction. After the quick length change, alterations in the  $\text{Ca}^{++}$  signal were followed much more closely by force changes than the length. In skeletal muscle, Guth and Potter (1987) found increases in TnC- $\text{Ca}^{++}$  affinity induced by myosin binding to actin, suggesting some "coupling" influence effects on the myofilaments. Further work by Sweitzer and Moss (1990) in skeletal muscle and Hannon et al. (1992) in cardiac muscle indicate force generation as the main factor controlling  $\text{Ca}^{++}$  sensitivity. In cardiac muscle, the amount of  $\text{Ca}^{++}$  bound to TnC, is an effect of myosin attachment (Hofmann & Fuchs 1987a) and force development (Hofmann & Fuchs 1987b), not sarcomere length alone. In summary, these studies of crossbridge binding and force development, show variations in the affinity of TnC for  $\text{Ca}^{++}$  can be attributed to the number of attached crossbridges and the amount of force generated (Allen & Kentish 1985). The positive feedback of force on  $\text{Ca}^{++}$  binding has been modeled by Landesberg and Sideman (1994).

### **1.3 Co-operativity of the Thin Filament**

Thin filament co-operativity occurs when  $\text{Ca}^{++}$  binds to TnC, allowing the formation of a crossbridge. The crossbridge attachment then increases the affinity of TnC to favor binding of another  $\text{Ca}^{++}$ . Again further  $\text{Ca}^{++}$  binding to TnC is enhanced by the formation of these crossbridges. The formation of strongly attached crossbridges increases  $\text{Ca}^{++}$  binding to the myofilaments (Brandt et al. 1987, Zot & Potter 1989, Metzger & Moss 1991, Hannon et al. 1992). A study using reconstituted fluorescent labelled TnC found that the TnC structure could be altered by strong attachment of

cycling crossbridges (Hannon et al. 1992). Such a conformational change may affect force development through an increased number of attached crossbridges by altering the affinity of the other TnC subunits along the regulatory strand to  $\text{Ca}^{++}$  (Brandt et al. 1987, Zot & Potter 1989, Metzger & Moss 1991), resulting in a "co-operative" effect of myosin attachment to actin. This interaction has been suggested to be an intrinsic property of the thin filament (Moss et al. 1985, Brandt et al. 1987). Tobacman and Sawyer (1990) found that binding of  $\text{Ca}^{++}$  to fluorescent labelled Tn was not co-operative in the absence of tropomyosin (Tm) and actin. Earlier results have shown an increase of thin filament-myosin ATPase rate with  $\text{Ca}^{++}$  (Holroyde et al. 1980) even in the presence of low myosin (Tobacman 1987). From this, they presented a model for "near-neighbour" Tn-Tm interaction, which suggests co-operativity may not be completely from crossbridges but to a large extent a part of the thin filament itself. Much support has been found for TnC as a primary regulator of contraction in the review by Zot and Potter (1987) with feedback from the crossbridges as a means of regulation (Hannon et al. 1992).

Work done by Pan and Solaro (1987) however, disputes the idea of co-operativity. In their experiments using a double-isotope technique ( $^{45}\text{Ca}$ ,  $^3\text{H}$ ) on skinned cardiac muscle where bound  $\text{Ca}^{++}$  was measured by the content of  $^{45}\text{Ca}/^3\text{H}$  in the effluence from the muscle sample, they saw little change in the  $\text{Ca}^{++}$ -TnC binding from freely or isometrically contracting muscle. Their conclusions were that co-operativity can not explain the force- $\text{Ca}^{++}$  relation, however, no new proposals have been made. Co-operative binding of  $\text{Ca}^{++}$  is supported by the work of Tobacman and Sawyer (1990) but when they directly measured  $^{45}\text{Ca}$  binding to native cardiac thin filament, they observed a non-co-operative effect similar to Pan and Solaro (1987). This technique was found to be very limited quantitatively, so a more quantitative method was used. Using cardiac TnC modified to fluoresce, observations of the light intensity could give

more evidence regarding of the location of  $\text{Ca}^{++}$  binding (TnC or whole troponin complex) (Johnson et al. 1980, Tobacman & Sawyer 1990). This method was able to give a better indication of any co-operative effects that may be occurring within the thin filament subunits.

There are large differences in the co-operativity and  $\text{Ca}^{++}$  sensitivity to Tn between cardiac and skeletal muscle. This difference is due, in part, to the number of low-affinity  $\text{Ca}^{++}$  specific binding sites there are available within the TnC in each muscle type. Cardiac muscle has one active and one inactive site, whereas skeletal muscle has two functional sites (Holroyde et al. 1980). Both muscle types have two high affinity sites for  $\text{Ca}^{++}$  and  $\text{Mg}^{++}$  (Potter & Gergely 1975) which are thought to play structural roles (Zot & Potter 1982). Thus there are only three TnC binding sites available for cardiac muscle whereas there are four available for skeletal muscle. The binding of  $\text{Ca}^{++}$  to the low-affinity sites are associated with crossbridge cycling (Holroyde et al. 1980, Johnson et al. 1980, Robertson et al. 1982). This can make studies of co-operativity in cardiac muscle more simple because co-operativity between sites can be eliminated.

#### **1.4 Myofilament ATPase Activity**

Stretching the muscle increases not only the apparent sensitivity of the myofilaments to  $\text{Ca}^{++}$  seen by a leftward shift of the force- $\text{Ca}^{++}$  relation, but also the ATPase activity of the skinned cardiac myofilaments (Kuhn et al. 1990, Kentish & Steinen 1994). The decline in ATPase rate with reductions in sarcomere length can be explained by the double overlap of thick and thin filaments (Kentish & Steinen 1994). An increase in the  $\text{Ca}^{++}$  binding to TnC with stretch could be used to account for the linear increase in both force and ATPase (Kuhn et al. 1990, Kentish & Steinen 1994). This could occur because the regulation by  $\text{Ca}^{++}$  of actomyosin ATPase activity has been associated with the two low affinity sites for  $\text{Ca}^{++}$  in TnC (Zot & Potter 1989),

similar to crossbridge cycling (Holroyde et al. 1980). Reductions in force with sarcomere length can not be solely defined by a decrease in ATPase rate, but also by an increase in opposing (restoring) forces (Kentish & Steinen 1994). Compared to a sarcomere length of 2.2  $\mu\text{m}$ , the ratio of generated force per mole ATP hydrolysed is reduced by 75% at sarcomere lengths of 1.6-1.8  $\mu\text{m}$  (Kentish & Steinen 1994). Decreasing sarcomere length corresponds to a reduction in both ATPase rate and force but the reduction in force is greater than the reduction in ATPase rate. Therefore, decreasing ATPase activity and opposing forces contribute to reductions in force as sarcomere length is reduced from optimal lengths.

### **1.5 Force- $\text{Ca}^{++}$ Relations From Intact and Skinned Fibers**

Using skinned muscle has been very useful in studying force development at varying  $[\text{Ca}^{++}]$ . It has been necessary to use the skinned preparations due to the difficulties of obtaining steady state relationships in the intact cardiac preparations. A main advantage using the skinning method is the ability to directly control the  $[\text{Ca}^{++}]$  with simultaneous force and sarcomere length measurement. Force- $\text{Ca}^{++}$  relations from intact and skinned muscles are different in  $\text{EC}_{50}$  and slope values, suggesting the intact preparation is more sensitive and co-operative to  $\text{Ca}^{++}$  binding (Yue et al. 1986, Gao et al. 1994).

In using skinned muscle, the difficulty arises when bathing solutions are being made to mimic the intracellular fluid of the intact muscle. Once the membranes have been disrupted, many components of the cell such as enzymes, proteins, peptides and regulatory messengers leak out. These components may or may not play a significant role in the aspects being studied of the contractile elements in the intact muscle. The preparation has now become an isolated system of contractile components that now requires the researcher to try rebuilding the system to resemble the intact preparation

through the addition of several components, some of which include salts, units of energy, and buffers. The ionic strength (defined as one half the sum of the concentration of ions in the solution multiplied by its charge squared; Atkins 1986) is a very important component that has been shown to affect the contractile system in several ways (Miller and Smith 1984). Due to the significant effects the ionic strength has on these types of experiments, this parameter must always be made note of.

Steady state relations in intact preparations are not without concern. The main obstacle is that development of steady state forces can only be achieved with pharmacological intervention. Another consideration regards activity-related changes in myofilament sensitivity during the time course of a tetanic contraction. Reductions in tetanic force have been seen although a steady level of  $[Ca^{++}]_i$ , which could be attributed to a reduction in myofilament sensitivity (Yue et al. 1986). Such alterations in  $Ca^{++}$  binding properties of the myofilaments could arise from inorganic phosphate ( $P_i$ ) or  $H^+$  accumulation (Kentish 1984) resulting from the tetanic contractions. Despite these differences, intact preparations have the significant advantage of maintaining native intracellular constituents that affect force generation and  $Ca^{++}$  binding properties of the myofilaments (Gao et al. 1994).

## **1.6 Inhibition of the Sarcoplasmic Reticulum**

In order to generate a tetanic contraction in cardiac muscle, the mode of pharmacological intervention must be considered. These interventions must alter some point of the excitation-contraction coupling process in order to allow  $[Ca^{++}]_i$  to reach a steady level that force can not only be generated but maintained, unlike the transient twitch. The main element in this process is the sarcoplasmic reticulum (SR) (reviewed by Wohlfart & Noble 1982, and Bers 1991), therefore, its elimination is crucial. Tetanization has been previously achieved in cardiac muscle in the presence of caffeine

(Forman et al. 1972) and ryanodine (Schouten et al. 1990, Backx 1989, Yue et al. 1986, Gao et al. 1994). Both caffeine and ryanodine affect the release portion of the SR so  $\text{Ca}^{++}$  cannot be sequestered in the SR (Endo 1975, Sutko & Kenyon 1983). Caffeine has the disadvantage of altering myofilament sensitivity (Fabiato & Fabiato 1973), but ryanodine does not (Fabiato 1985). It is not only desirable to eliminate the SR without side effects on myofilament  $\text{Ca}^{++}$  binding properties, but to eliminate unnecessary ATP use to minimize  $\text{P}_i$  and  $\text{H}^+$  accumulation during the tetanic contractions. With this in mind, inhibitors of the SR  $\text{Ca}^{++}$ -ATPase were considered. Elimination of this pump would allow more ATP to be available for use in steady state force generation. Three SR pump inhibitors are currently available: thapsigargin (Thastrup et al. 1990, 2,3-Di-(tert-butyl)-1,4-benzohydroquinone (DBH), and cyclopiazonic acid (CPA) (Goeger et al. 1988). The first two were not chosen because: 1) thapsigargin is a tumor promotor, and 2) DBH was not characterized in muscle. Hence, cyclopiazonic acid was chosen.

Cyclopiazonic acid is a mycotoxin that has been shown to effectively inhibit the SR ATPase in isolated skeletal SR vesicles (Goeger et al. 1988, Goeger & Riley 1989). In addition, it showed no effect on kidney nor gastric  $\text{Na}^+/\text{K}^+$  ATPase, mitochondrial  $\text{F}_1$ -ATPase, nor erythrocyte  $\text{Ca}^{++}$ -ATPase, suggesting that its effects are specific to  $\text{Ca}^{++}$ -ATPase activity on the SR and not actions on other ion transport enzymes (Seidler et al. 1989). CPA's inhibition of the SR  $\text{Ca}^{++}$ -ATPase activity is altered by ATP and  $\text{Ca}^{++}$  (Seidler et al. 1989). ATP and CPA appear to bind to the same site on the ATPase, therefore, as  $[\text{ATP}]$  increases, CPA inhibition decreases due to competitive binding. Increasing  $[\text{Ca}^{++}]$  causes an increase in the SR  $\text{Ca}^{++}$ -ATPase activity, this occurs even in the presence of CPA, however, the maximal ATPase rate is decreased by four-fold in the presence of CPA. Smooth muscle cells have shown additional effects from the application of CPA aside from its actions on SR  $\text{Ca}^{++}$  uptake. Most notably has been the inhibition of  $\text{Ca}^{++}$ -activated  $\text{K}^+$  current (Suzuki et al. 1992, Uyama et al. 1993).

$\text{Ca}^{++}$ -influx through voltage-gated  $\text{Ca}^{++}$  channels increased in ileal smooth muscle cells in the presence of 10  $\mu\text{M}$  CPA (Umayya et al. 1993) as did resting tension in aortic rings with 20  $\mu\text{M}$  CPA (Shima & Blaustein 1992). In skinned skeletal muscle, complete inhibition of SR  $\text{Ca}^{++}$ -ATPase activity was achieved with 10  $\mu\text{M}$  CPA (Kurebayshi & Ogawa 1991), however myofilament sensitivity was altered with [CPA] greater than 10  $\mu\text{M}$  CPA (Kurebayshi & Ogawa 1991, Huchet & Leoty 1993). The findings in skeletal muscle cause some concern regarding potential actions in cardiac muscle.

In cardiac muscle, dubious effects of CPA have not been found, in contrast to smooth and skeletal muscle. CPA has been shown to inhibit SR  $\text{Ca}^{++}$ -ATPase in isolated myocytes from the rat and rabbit (Hove-Madsen & Bers 1993) as well as rabbit trabeculae (Baudet et al. 1993). In the presence of CPA, reductions in force accompanied by prolongation of relaxation have been observed (Agata et al. 1993, Baudet et al. 1993). In addition, reductions in SR  $\text{Ca}^{++}$  content were observed in rabbit ventricle in the presence of CPA and known steric SR  $\text{Ca}^{++}$ -ATPase inhibitor thapsigargin (Baudet et al. 1993). Effects of CPA in cardiac muscle preparations appear to be highly specific for the SR  $\text{Ca}^{++}$ -ATPase and would be a likely candidate for eliminating SR uptake ability.

### **1.7 Objectives of the Study**

The first objective was to characterize effects of CPA on the properties of the twitch in cardiac trabeculae from the rat. Specifically, experiments were carried out to determine an appropriate CPA concentration that can be used to effectively eliminate the SR's role in the excitation-coupling process (chapter 1). Alterations in twitch force, relaxation rate, and  $\text{Ca}^{++}$  recirculating through the SR were studied. In addition, a protocol was developed to tetanize the muscle, and achieve a steady state, over a wide range of  $[\text{Ca}^{++}]_o$ .

The second objective was to check whether CPA affects the myofilament sensitivity. Force- $\text{Ca}^{++}$  relations in skinned fibers were done in the presence of  $30 \mu\text{M}$  CPA to evaluate changes from control in maximal force and  $\text{EC}_{50}$  (chapter 2).

The final objective was to measure intracellular  $\text{Ca}^{++}$  ( $[\text{Ca}^{++}]_i$ ) during steady state tetanic contractions of varying force at two sarcomere lengths. The  $\text{Ca}^{++}$  indicator Fura-2 (Grynkiewicz et al. 1986) was used to measure  $[\text{Ca}^{++}]_i$  in the experiments presented here. Chapter 5 evaluates the resting muscle's fluorescence characteristics in the presence and absence of Fura-2. The data presented in chapter 6 show fluorescence during tetani at a long and short sarcomere length over a wide range of  $[\text{Ca}^{++}]_o$  and are plotted as force- $\text{Ca}^{++}$  relations. Corresponding  $[\text{Ca}^{++}]_i$  measurements with length-induced changes of force in an intact preparation, presented in this chapter, provide evidence to confirm length-dependent activation as the basis for the Frank-Starling relation.

## Chapter 2

### General Methods

#### 2.1 Muscle Preparation

All of the work presented here has been performed on Lewis Brown Norway F<sub>1</sub> rats (Harlan Sprague-Dawley) 200-250 g of either sex, fed ad libitum. The rats were anaesthetized with diethyl ether. Once under anaesthesia, the heart must be quickly removed and perfused with an oxygenated physiological saline solution containing 15 mM 2,3-butanedione monoxime to block both Ca<sup>++</sup> release and one of the steps of the crossbridge cycle (Perreault et al. 1992). This can serve two purposes: 1) to protect the heart from damage by unnecessary ATP use, and 2) to reduce or eliminate contractions, therefore allowing dissection to proceed more easily. The physiological saline solution, used here for dissection and later for perfusion, is a modified Krebs-Henseleit solution which is described in section 2.8.1.

Initially, the right ventricle (RV) was opened from the pulmonary artery down along the anterior attachment of the RV to the septum to the apex and from the pulmonary artery to the atrioventricular (AV) ring, thus allowing the ventricular wall to lie flat on the bottom of the dissection chamber. The "ribbon-like" trabeculae used in these experiments are found coming out of the RV wall attached to the (AV) ring. Trabeculae that are uniform and minimally branched are preferred but less than optimal muscles have also been used here. These trabeculae ranged in size from 0.07 to 0.45 mm wide, 0.06 to 0.20 mm thick, and 2.0-5.0 mm long. The AV ring was cut below where the trabeculae inserts so that it can be released with some remaining portion of the tricuspid valve extending from the end of the muscle. The ventricular wall is dissected, forming a cube, by cutting around the area where the trabecula inserts.

## 2.2 Basic Experimental Set-Up

All experiments were done on the set up described below and seen in figure 2-1. The basic experimental set up can measure force, sarcomere length and muscle length with a heated superfusion system in place. The portion of the set up that is used for  $[Ca^{++}]_i$  measurements will be described separately.

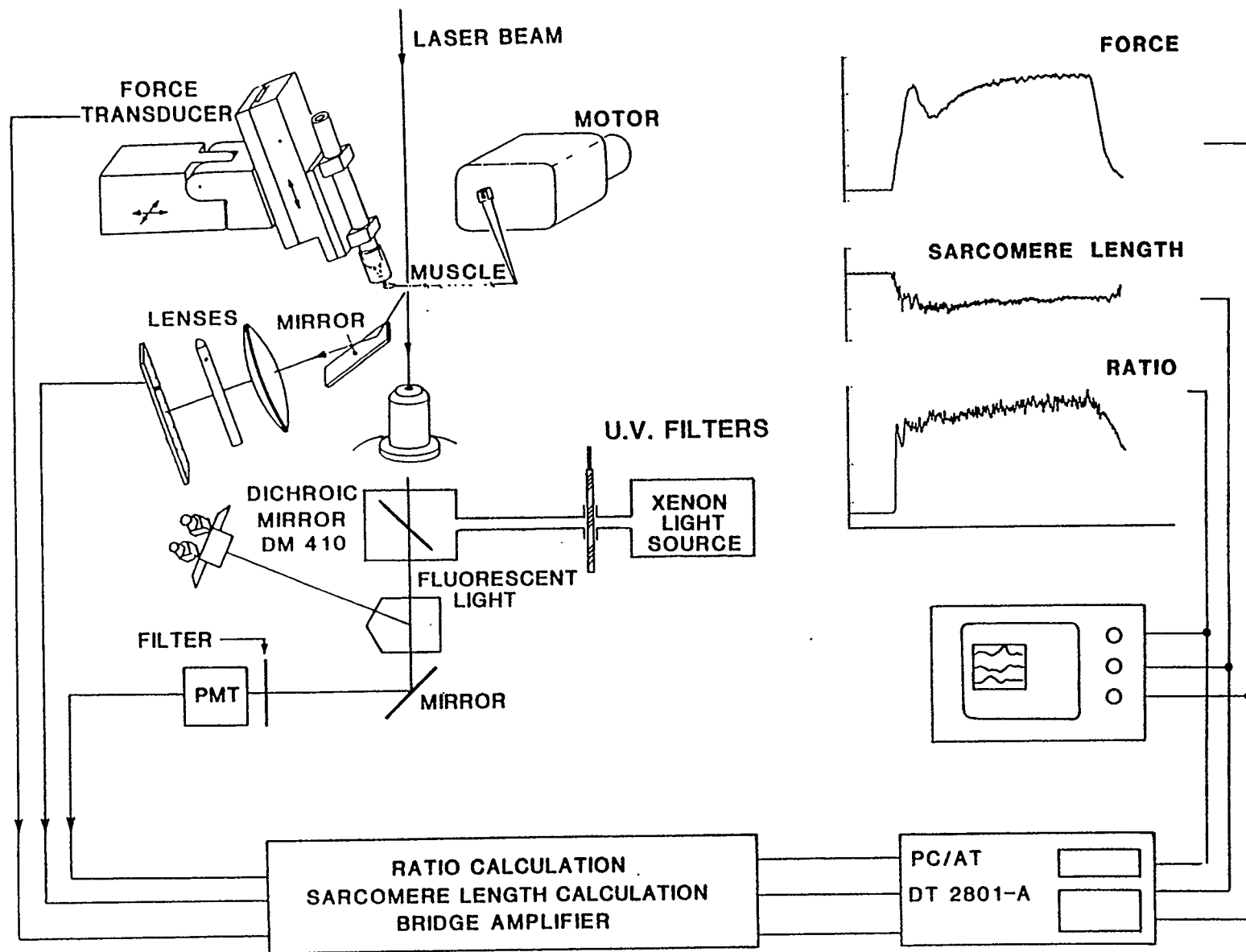
### 2.2.1 Placement of Muscle

The dissected trabecula was removed from the dissection chamber and placed in the bath of the experimental set-up filled with superfusion solution (modified Krebs-Henseleit solution without BDM). The ventricular cube was held by forceps so that the trabecula was hanging straight down. It was lowered through a platinum wire loop (basket) that had been glued onto the carbon extension arm of the force transducer in a perpendicular fashion. The loop's size (smaller diameter than the width of the cube) and position (horizontal) allowed the ventricular cube to rest on it while the trabecula hanged freely below the loop. The valvular end of the trabeculae was placed on a platinum hook extending from a servo motor (series 300 Cambridge Technology, Cambridge, MA). This arrangement placed the trabecula in a horizontal position within the bath. The adjustable arm could move toward or away from the force transducer to shorten or lengthen the muscle, thereby adjusting sarcomere length.

The force transducer and motor arm were lowered so the trabecula was suspended deep within the trough to the bottom of the bath. Once the trabecula was secured in the bath, superfusion began through the trough where Krebs-Henseleit solution was circulated from an oxygenated (95% O<sub>2</sub> and 5% CO<sub>2</sub>) reservoir through a glass heat exchanger. The superfusion ran at a flow rate of 15 ml/min. The experiments were done at 26°C and the  $[Ca^{++}]_o$  was varied as indicated.

**Figure 2-1: Illustration of Experimental Apparatus**

The apparatus is arranged to allow force to be measured simultaneously with either sarcomere length or fluorescence. Sarcomere length is measured with a He-Ne laser beam through the center of the muscle, and then reflected through a series of focusing lenses on to a measuring device. Fluorescence is measured after the muscle has been illuminated with UV light from the xenon light source. The muscle can be illuminated by three excitation wavelengths (340, 360, and 380 nm) by manually changing the UV excitation filters in front of the light source. Emitted fluorescence is collected at 510 nm on to a photomultiplier tube (PMT) and recorded. Details of force, sarcomere length, and fluorescence measurements can be found in the text.



### *2.2.2 Electrical Stimulation*

Stimulation of the muscle was conducted using two platinum electrodes attached to each side of the trough placed in the horizontal plane of the muscle. Stimulation pulses were derived from a pulse generator (Digitimer, model DS2, UK), that could be adjusted for voltage output and stimulus duration. Stimuli were triggered by a timing device (Digitimer, model D4030, UK) at 1 Hz for muscle equilibration, 0.2 Hz for steady state twitch measurements or as specified (i.e., tetanus, or extrasystole).

### *2.2.3 Force Measurement*

The force generated by a cardiac trabecula was measured using a modified silicon semiconductor strain gauge (model AE-801, Sensoror, Hortoen, Norway). As the muscle pulled on the strain gauge during a contraction or passive stretch, it deformed (or strained) the gauge changing the recorded resistance of the resistors on both sides of the gauge. The force transducer itself contains half of a balanced Wheatstone bridge with the other half in the amplifier. The resistance changes were read as a voltage output from the Wheatstone bridge. The voltage can then be converted to force (mN) based on the calibration with known masses. To avoid water and light affecting the transducer, a mixture of carbon and silicon dissolved in toluene was used to coat the force transducer.

### *2.2.4 Sarcomere Length Measurement*

The sarcomere length is measured using the laser diffraction technique (Krueger & Pollack 1975, ter Keurs et al. 1980). The beam of a 15 mW He-Ne laser light (Spectra-Physics model 106-2, Eugene, OR) (632.8 nm) is directed through the central part of the muscle. The muscle acts as a grating by the series arrangement of the sarcomeres. The grating creates orders of diffracted light beams away from the zero-

order beam, which is the light that has gone straight through the muscle. The light is collected on a 512-element linear photodiode array (model RC 105, Reticon, Sunnyvale, CA) which is scanned every 580  $\mu$ s. The angle between the diffracted order and the zero order indicates the grating constant (sarcomere length). The grating constant can be calculated by the following equation:

$$d = (\text{laser wavelength}) / \sin \alpha$$

In this equation  $d$  is the size of the grating (sarcomere length),  $n$  is the order of diffracted light and  $\alpha$  is the angle of diffraction between any order and the zero order. When the muscle is used as a grating, the first diffraction order is used and so  $n$  is equal to one. As the muscle shortens during a contraction the position of the diffracted light on to the array of photodetectors is shifted indicating a sarcomere length change. The median position of the first order is measured. This position of the first order in relation to the zero-order position is used to calculate sarcomere length based on a calibration using a known grating. Zero-order light is often scattered affecting the first-order signal. The zero-order light is subtracted by a single exponential decay function which begins at the start of the observation window which can be adjusted. Much of the scatter can be attributed to: 1) muscle thickness (i.e., multilayer diffraction grating), 2) mitochondrial content, and 3) variation in sarcomere length (Krueger & Pollack 1975, ter Keurs et al. 1980).

### 2.3. $[Ca^{++}]_i$ Measurement

In order to measure  $[Ca^{++}]_i$ , estimated by fluorescence, the muscle must first be loaded with the  $Ca^{++}$  indicator dye, Fura-2 pentapotassium salt (Molecular Probes, Eugene, OR). Once the dye is evenly distributed throughout the muscle, fluorescence measurements can be made. The dye will fluoresce at a wavelength of 510 nm when illuminated with UV light. After the fluorescence has been recorded and calibration

done, the  $[Ca^{++}]_i$  can be calculated. The following is an account of what must be done and what is happening in order to collect this kind of data.

### *2.3.1 Autofluorescence and Background Light*

The estimation of  $[Ca^{++}]_i$  is dependent on an accurate measurement of the Fura-2 fluorescence. To eliminate contribution of undesirable (non- $Ca^{++}$  related) light, several precautions have been taken. The fluorescence experiments were done in a dark room, with only red light to aid the experimenter. The portion of the set up, below the muscle bath, where the UV and fluorescent light paths are, has been covered with a black cover. In addition to undesirable light, the fluorescence the muscle emits in the absence of any dye, which is known as autofluorescence, must also be accounted for. Any ambient light that may have been detected was combined with the autofluorescence.

A major source of autofluorescence is mitochondrial NADH (Gueth & Wojciechowski 1986, White & Wittenberg 1993). This is measured prior to loading the muscle with Fura-2. Four measurements of ambient light and autofluorescence were taken: (1) no light through the system (UV shutter closed), (2) 340 nm illumination, (3) 360 nm illumination, and (4) 380 nm illumination. The values obtained were used later to subtract from the measured fluorescence in the presence of the dye. Once the measurements of autofluorescence and background light are taken, the fura-2 can be loaded into the muscle and accurately accounted for.

### *2.3.2 Injection of Fura-2 into the Muscle*

Fura-2 pentapotassium salt was dissolved in double-distilled water to a concentration of 4.0 mM. Microelectrodes used to inject the dye were made using a vertical puller (Kopf Instruments, model 750, Tujunga, CA). The tip of the filamentous glass microelectrode was made to have a resistance of at least 200 M $\Omega$ . The tip of this

microelectrode was filled with Fura-2, with the remainder of the electrode back filled with 140 mM KCl. The filled microelectrode was then placed in a holder with an Ag/AgCl half cell (WPI, Sarasota, FL) and attached to an amplifier (WPI Intra 767, Sarasota, FL). This amplifier then measures voltage or delivers current. The electrode was lowered into the bath and the junction potential was zeroed from around -10 mV. The tip of the microelectrode was impaled into a cell in the middle of a quiescent muscle. Impalement was indicated when the voltage being read from the microelectrode suddenly dropped to at least -50 mV. Once a successful impalement has been achieved, then the Fura-2, which is negatively charged, can be injected. This was done by sending a negative current (-7.2 to -8.2 nA DC current) through the microelectrode for approximately 10-20 minutes, depending on muscle size. The dye spread throughout the muscle from its single injection site by diffusion through gap junctions between cells (Backx & ter Keurs 1993). Once the muscle has been loaded with Fura-2 the microelectrode was removed and the muscle was stimulated at 1 Hz until a steady level of force and even distribution of the dye throughout the measurement site on the muscle was achieved. After this, steady state stimulation frequency was returned to 0.2 Hz. After this, the muscle was ready to be illuminated for data collection.

### *2.3.3 Path of Excitation Light to the Muscle*

A Xe lamp (model 6255, Oriel Corp., Stratford, CT), located behind the set up, and ignited by a power supply (model 68806, Oriel Corp., Stratford CT) was used to illuminate the fura-2 inside the muscle with UV light. The light from this lamp first must go through a biconvex lens, focusing the light, before going through a 340, 360, or 380 nm excitation filter (Melles Griot, Irvine, CA). A shutter is located just before the filters to block the UV light when fluorescence measurements are not being taken. A neutral-density filter is placed behind the 380 nm filter because of the greater light

intensity transmitted through this filter than through the 340 nm filter. Once the light has gone through the desired excitation filter, it hits a 400 nm dichroic mirror (400 DPLC, Omega Optical, VT). This mirror will reflect any light of a wavelength less than 400 nm at a 90° angle up to the muscle. Before the light can reach the muscle, from this point it must pass through a 10X UV-Fluor objective lens (Nikon, Canada). This focuses the light onto the muscle with a diameter of approximately 2 mm. This large area of illumination, relative to the muscle size, helps to minimize movement artifacts and errors resulting from differences in focus points between the three wavelengths.

#### *2.3.4 Path of Fluorescent Light From the Muscle*

The muscle, loaded with fura-2, will fluoresce optimally at a wavelength of approximately 510 nm when illuminated with UV light. The fluorescent light travels down through the 10X UV-Fluor objective lens to the same 400 nm dichroic mirror mentioned above. The light passes through the mirror, because the wavelength is greater than 400 nm. Once the light has passed through the mirror it passes through a 510 nm bandpass filter (Melles Griot, Irvine, CA) and falls on to a photomultiplier tube (PMT) (PMT-R2693 with a C1053-01 socket, Hamamatsu, Japan), which is used to detect the emitted light. The bandpass filter helps to minimize unwanted light. The duration of each fluorescence experiment was kept to a minimum (<1 hr) for two main reasons: diffusion of the dye out of the preparation and photobleaching (Roe et al. 1990, Becker & Fay 1987).

#### *2.3.5 Fluorescence Ratio Conversion to $[Ca^{++}]_i$ Values*

In order to measure  $[Ca^{++}]_i$  transients, the fluorescence emitted from both 340 nm and 380 nm illumination must be taken. This can only be done one at a time, and care must be taken to ensure that the force tracings for each are identical. Once fluorescent

measurements have been taken, the autofluorescence (which was measured before Fura-2 injection) must be subtracted, and the 340 and 380 nm signals can be ratioed (R). It is this ratioed signal that will be converted to an  $[Ca^{++}]_i$ . This conversion can be done through an equation derived by Grynkiewicz et al. (1986). The equation is as follows:

$$[Ca^{++}]_i = K'(R - R_{min}) / (R_{max} - R)$$

- $[Ca^{++}]_i$  = intracellular  $[Ca^{++}]$   
 $R_{min}$  = 340/380 nm ratio in the absence of  $Ca^{++}$ , after autofluorescence subtracted (from the in vitro calibration)  
 $R_{max}$  = 340/380 nm ratio with maximal  $Ca^{++}$  (pCa=4.56), after autofluorescence subtracted (from the in vitro calibration)  
 $R$  = 340/380 nm ratio (measured in the muscle during an experiment)  
 $K'$  = the true dissociation constant ( $K_d$ ) of Fura-2 multiplied by the ratio at 380 nm of the  $Ca^{++}$  free to the  $Ca^{++}$  bound forms ( $380_{min}/380_{max}$ ) ( $\beta$ ) (from the in vitro calibration) (i.e.,  $K' = K_d \times \beta$ )

The in vitro calibration necessary to obtain  $R_{min}$ ,  $R_{max}$ , and  $K'$  were done using a kit (Calcium Calibration Buffer Kit with Magnesium I; Molecular Probes, Inc., Eugene, OR). This kit contains two bottles of solutions (A & B). Solution A contained zero  $Ca^{++}$  with 1.0 mM  $Mg^{++}_{free}$ , 10.0 mM EGTA, 100.0 mM KCl, 10.0 mM MOPS, 1.0  $\mu$ M Fura-2, and a pH of 7.2. Solution B is the same except it has 39  $\mu$ M  $Ca^{++}_{free}$  included. Solutions of intermediate  $[Ca^{++}]$  (0 to 39  $\mu$ M) were made by mixing the two solutions in various proportions, as listed in table 2-1. This procedure is similar to mixing the relaxing and activating solutions as done for skinned fiber experiments, discussed in chapter 4. Each solution was placed in separate 100  $\mu$ L chambers mounted on the microscope stage where the bath for the muscle normally sits. This bath could hold two separate solutions at a time where measurement of the fluorescence would be accurate. Each solution containing bath was illuminated with 340, 360, and 380 nm light and the emitted fluorescence collected by the photomultiplier tube was recorded on chart record paper. The background fluorescence was measured by illumination of a chamber filled with solution B in the absence of Fura-2. The calculation of

**Table 2-1**

Solution combinations to make intermediate  $[Ca^{++}]$ 's between  $R_{max}$  and  $R_{min}$  for the in vitro calibration of Fura-2. Both solutions (A & B) contain 1  $\mu M$  Fura-2. Autofluorescence was taken with solution B without Fura-2 present.

Solution A ( $\mu L$ )	Solution B ( $\mu L$ )	$[Ca^{++}]$ ( $\mu M$ )	pCa
1000+CaCl <sub>2</sub> ( $R_{max}$ )	0	977.24	3.01
1000	0	27.54	4.56
990	10	21.38	4.67
970	30	7.76	5.11
960	40	6.03	5.22
950	50	4.79	5.32
900	100	2.34	5.63
875	125	1.82	5.74
850	150	1.48	5.83
800	200	1.05	5.98
750	250	0.78	6.11
700	300	0.62	6.21
650	350	0.49	6.31
600	400	0.39	6.41
500	500	0.26	6.59
450	550	0.21	6.67
400	600	0.17	6.76
300	700	0.11	6.96
200	800	0.06	7.19
100	900	0.03	7.54
0 ( $R_{min}$ )	1000	----	----

fluorescence at each wavelength first had the background fluorescence subtracted. The fluorescence measured at each  $[Ca^{++}]$  is shown graphically in figure 2-2. These points are fit with a sigmoidal curve fit (figure 2-2A) which nicely displays the fluorescence values from  $R_{min}$  to  $R_{max}$ . The curve fit is from a modified form of the Hill equation, which is described below in section 2.6. Although the sigmoidal fit through the fluorescence values can give the value for  $K'$ , a regression line through the linearized data provides a much more accurate estimation of  $K'$ . This is because the sigmoidal fit doesn't go through the data points very well at the low  $[Ca^{++}]$  range, but a much better fit can be made when the data are linearized (correlation coefficient = 0.996). The linearized data is plotted with  $-\log Ca^{++}$  (pCa) on the x-axis and  $\log (R - R_{min}) / (R_{max} - R)$  on the y-axis (figure 2-2B). The pCa value corresponding to 0 on the y-axis gives  $K'$  (5.06 pCa or 8.7  $\mu$ M).  $K'$  can then be broken down to give the dissociation constant ( $K_d$ ) by dividing  $K'$  with  $\beta$  (the ratio at 380 nm of zero  $Ca^{++}$  ( $380_{min}$ ) to saturating  $Ca^{++}$  ( $380_{max}$ )), ( $K' = 2.4 \mu$ M,  $\beta = 7.71$ );  $K_d$  is found to be 311 nM. This value is slightly higher than found by P. Backx ( $K_d = 265.0$  nM with 1.2 mM  $MgCl_2$  or 132.0 nM without  $MgCl_2$ ), but lower than H. Banijamali ( $K_d = 380.0$  nM,  $[MgCl_2]$  not mentioned). For the fluorescence experiments presented here (chapters 5 and 6), it is assumed that the value for  $K'$  is the same in vivo as it has been found here in vitro. This assumption ( $K'_{in vivo} = K'_{in vitro}$ ) is supported by calibration curves done in the presence of  $Mg^{++}$ , in vitro, being very similar to in vivo calibrations, as found by P. Backx (1989).

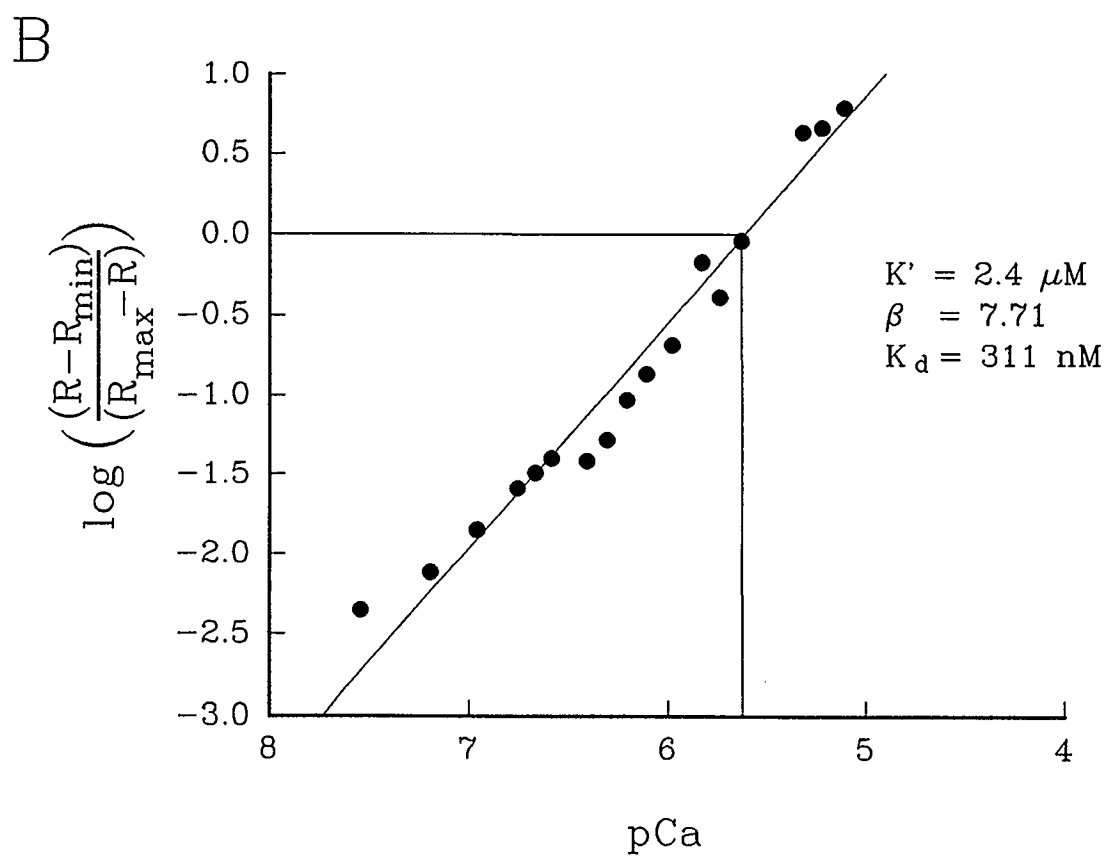
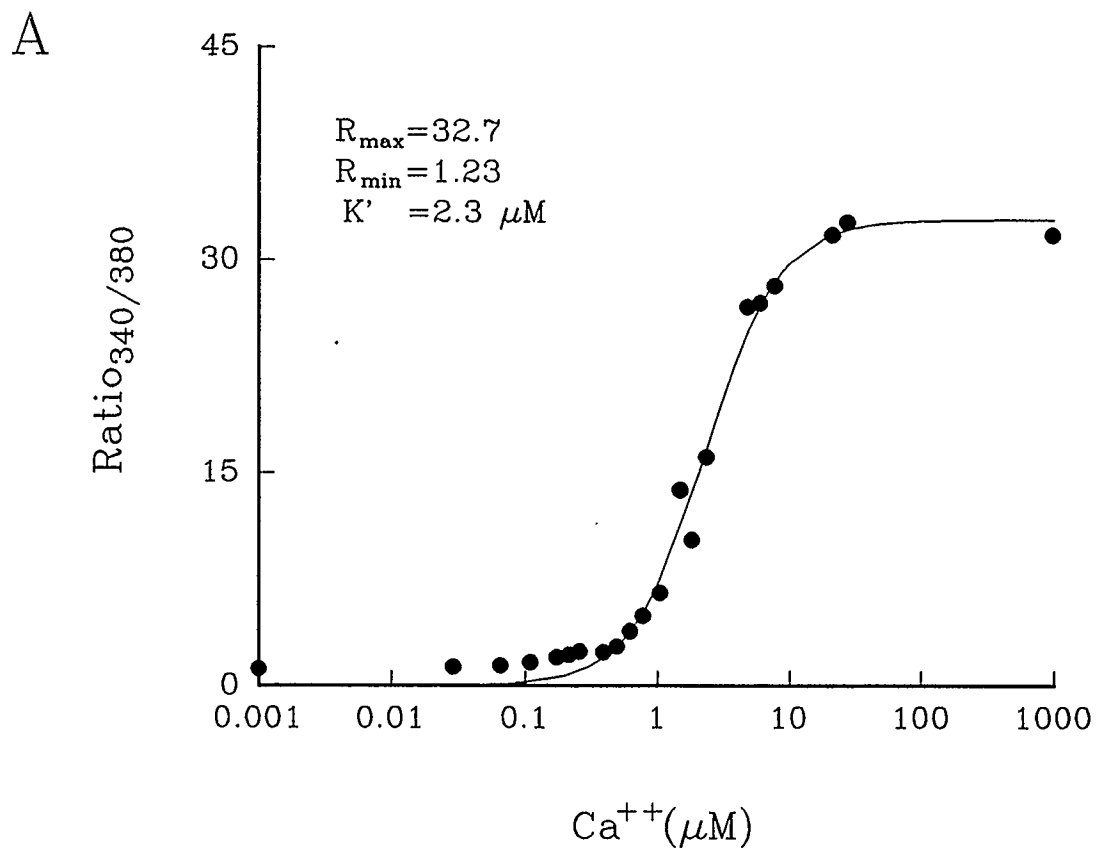
## 2.4 Data Acquisition

The muscle was positioned so that all measurements were taken near the center. Force, sarcomere length, and fluorescence measurements were recorded on an 8-channel chart recorder (Gould amplifier 2800S, 100kHz, Cleveland, OH) and sent to a computer (486 AST IBM compatible). The fluorescence signal from the PMT went to the

**Figure 2-2: In Vitro Calibration of Fura-2**

(A) Data points obtained from Fura-2 containing solutions illuminated with 340 and 380 nm light and fit with a modified Hill equation. This equation is described in section 2.6. The  $[Ca^{++}]$  corresponding to  $R_{340/380}$  at half of  $R_{max}$  is considered to be  $K'$ .

(B) Linearized form of the same data points, with a better fit of the regression line.  $K'$  is determined by the pCa corresponding to  $x=0$  when  $x=\log\{(R_{340/380}-R_{min})/R_{max}-R_{340/380}\}$ . The value of  $K'$  in the estimation of  $[Ca^{++}]_i$  is the value determined using this linearized graph.



computer via an A/D converter (2801A Data-Translation) and filtered at 100 Hz. All measurements were kept on a hard disk for data analysis.

## 2.5 Force-[Ca<sup>++</sup>] Relations

Force-[Ca<sup>++</sup>]<sub>o</sub> relations were made with intact muscle preparations with and without the SR inhibitor, cyclopiazonic acid (CPA). For all force-[Ca<sup>++</sup>]<sub>o</sub> relations, the same basic protocol was used. After equilibration in 0.7 mM [Ca<sup>++</sup>]<sub>o</sub>, the [Ca<sup>++</sup>]<sub>o</sub> was dropped to 0.1 mM. After the [Ca<sup>++</sup>]<sub>o</sub> was changed, at least 5 minutes was allowed for a steady state force to be achieved, then a measurement was taken which included both force and sarcomere length. Ca<sup>++</sup> was added to the superfusion solution to increase the [Ca<sup>++</sup>]<sub>o</sub>. The [Ca<sup>++</sup>]<sub>o</sub>'s that were used for the force-[Ca<sup>++</sup>]<sub>o</sub> relations were as specified in each chapter.

A modified Hill equation was used to fit, the relations obtained from the force-[Ca<sup>++</sup>] relations (Snedecor & Cochran 1967). These relations were sigmoidal when [Ca<sup>++</sup>] was plotted on a log scale. This equation was used for relations obtained with both intact and skinned muscle preparations as well as intracellular and extracellular [Ca<sup>++</sup>]. The modified Hill equation is as follows:

$$F = F_{\max} \times ([Ca^{++}]^n / ((EC_{50})^n + [Ca^{++}]^n))$$

F = force (dependent variable)

Ca<sup>++</sup> = [Ca<sup>++</sup>]<sub>o</sub> or Ca<sup>++</sup><sub>i</sub> (independent variable)

F<sub>max</sub> = maximum value that force (F) can be under the experimental conditions (i.e., sarcomere length, contractility)

EC<sub>50</sub> = amount of Ca<sup>++</sup> that corresponds to 50% F<sub>max</sub>

n = Hill coefficient (indicates steepness or slope of the curve)

The EC<sub>50</sub> and F<sub>max</sub> values are used extensively throughout this text for comparison between experiments. The value of n, however, is not fully understood and possible implications to the contractile proteins are discussed by Shiner and Solaro (1984).

## 2.6 Statistical Analysis

Statistical significance was determined when  $p$  values were less than 0.05. Most tests were traditional student's  $t$ -tests. However, when trends within experiments were reviewed in chapter 3 (effects of a drug with increasing concentration) and chapter 5 (Fura-2 dye loss) the Tukey-Kramer multiple comparison test was used.

Numbers listed in "methods" sections are given as an average  $\pm$  standard deviations, in order to give a distribution of the spread in that parameter (i.e., size, duration, amount). Numbers listed in "results" sections are given as an average  $\pm$  standard error of the mean, to give a spread of the data that can not be attributed to chance.

## 2.7 Solutions

For the experiments presented in this thesis, both Krebs-Henseleit and HEPES buffered solutions were used as superfusion solutions. The dose response curves and force- $[Ca^{++}]$  relations in chapter 3 are done using Krebs-Henseleit solution. In chapter 4, a series of skinned fiber experiments are presented and the details of the solutions used are presented in that chapter. The data presented in chapters 5 and 6 are done using HEPES buffered solution in order to better accommodate the high  $[Ca^{++}]_o$  used in the force- $[Ca^{++}]$  relations.

### 2.7.1 Composition

The solution used for perfusion (during dissection) and superfusion (in the muscle bath) of the muscle is a modified Krebs-Henseleit solution containing the following: 120.0 mM NaCl, 5.0 mM KCl, 1.1 mM  $MgCl_2 \cdot 6H_2O$ , 1.2 mM  $Na_2SO_4$ , 2.0 mM  $NaH_2PO_4 \cdot 2H_2O$ , 19.0 mM  $NaHCO_3$ , 10.0 mM glucose and  $[Ca^{++}]_o$  (BDH Chemical Co., Toronto, Canada) as indicated in the protocol for each chapter. This solution is

equilibrated with 95% O<sub>2</sub> and 5% CO<sub>2</sub>. The perfusion solution has 15 mM 2,3-butanedione monoxime added to protect the muscle during dissection as described above. The free [Ca<sup>++</sup>] to total [Ca<sup>++</sup>] in the Krebs-Henseleit solution is close to a linear relation with a slope of 0.7 (P. de Tombe 1989). For the fluorescence experiments, HEPES solution was used, because the high [Ca<sup>++</sup>]'s used would cause precipitation in Krebs-Henseleit solution. The HEPES solution contained the following: 137.2 mM NaCl, 5.0 mM KCl, 1.2 mM MgCl<sub>2</sub>, 2.8 mM Na<sup>+</sup>Acetate<sup>-</sup>, 10.0 mM HEPES, 10.0 mM Glucose, and [Ca<sup>++</sup>]<sub>0</sub> (BDH Chemical Co., Toronto, Canada) as indicated. NaOH was added to adjust the pH to equal 7.35. The HEPES solution was equilibrated with 100% O<sub>2</sub>. In the HEPES solution, free [Ca<sup>++</sup>] and total [Ca<sup>++</sup>] show a 1:1 relation when plotted against each other (P. de Tombe, 1989).

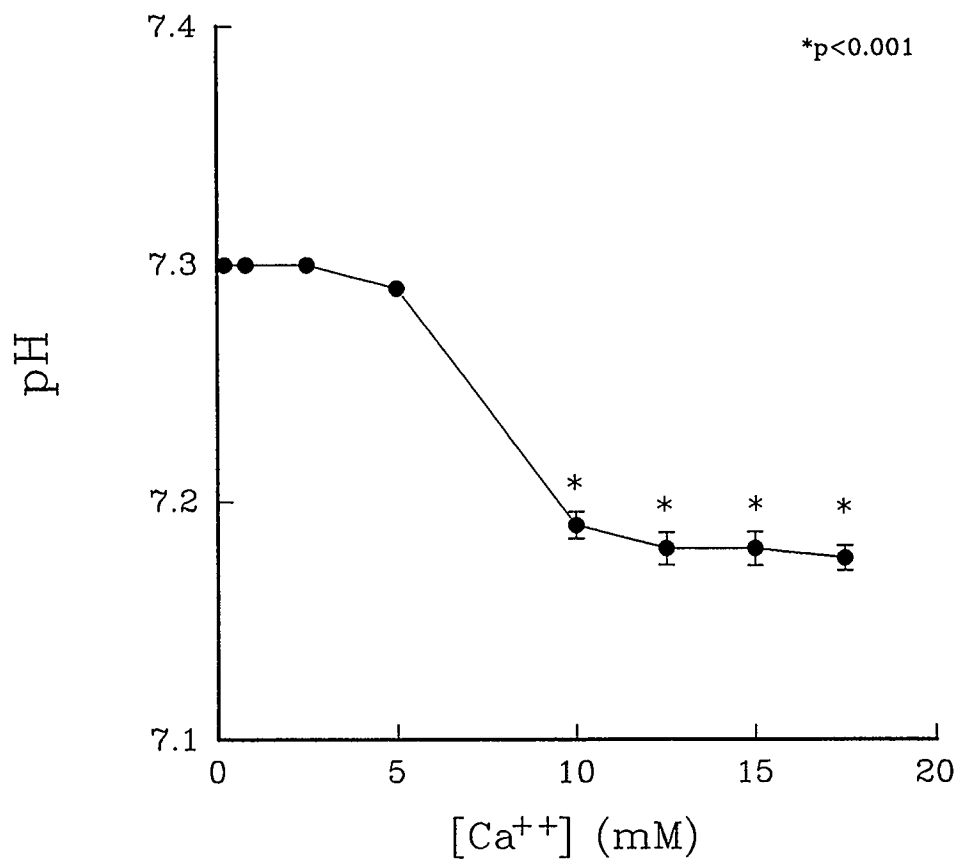
### *2.7.2 Solution pH*

When total [Ca<sup>++</sup>] is above 5 mM, in Krebs-Henseleit solution, the calcium salts of carbonate, phosphate and sulphate begin to precipitate. When precipitation occurs it becomes obvious that the Ca<sup>++</sup> buffering capacity of the solution is being exceeded and so pH changes would be expected. Changes of pH in the muscles bathing solution could have substantial effects on the muscles performance (Ricciardi et al. 1986), depending on the magnitude and duration of the pH change (Orchard & Kentish, 1990). Because of this concern, the pH of the Krebs-Henseleit solution was tested for the full range of [Ca<sup>++</sup>]'s used in the force-[Ca<sup>++</sup>]<sub>0</sub> experiments previously mentioned.

The Krebs-Henseleit solution was prepared and allowed to equilibrate for 15 minutes with 95% O<sub>2</sub> and 5% CO<sub>2</sub>. Ca<sup>++</sup> was then added to the solution and allowed to mix while at 26°C. The pH was taken after a few minutes, then the procedure was repeated after more Ca<sup>++</sup> was added. The [Ca<sup>++</sup>]'s (in mM) used were 0.2, 0.8, 2.5, 5.0, 10.0, 12.5, 15.0, 17.5. The results of 8 experiments indicate that pH is reduced by over

**Figure 2-3:** Effects of Increasing  $[Ca^{++}]_o$  on pH in Krebs-Henseleit Solution

Decline in pH as the  $[Ca^{++}]_o$  exceeds the buffering capacity of the solution, expressed as mean  $\pm$  standard error of the mean (n=8).



0.10 unit, at the highest  $[Ca^{++}]$ 's used, from the pH measured at low  $[Ca^{++}]$ 's. As seen in figure 2-3, the drop in pH is quite abrupt at the  $[Ca^{++}]$  where precipitation begins to take place and then plateaus, without showing any further reductions.

To eliminate any possible artifacts due to pH changes, HEPES solution was used in place of Krebs-Henseleit solution for the fluorescence experiments.

### *2.7.3 Dissolving Cyclopiazonic Acid*

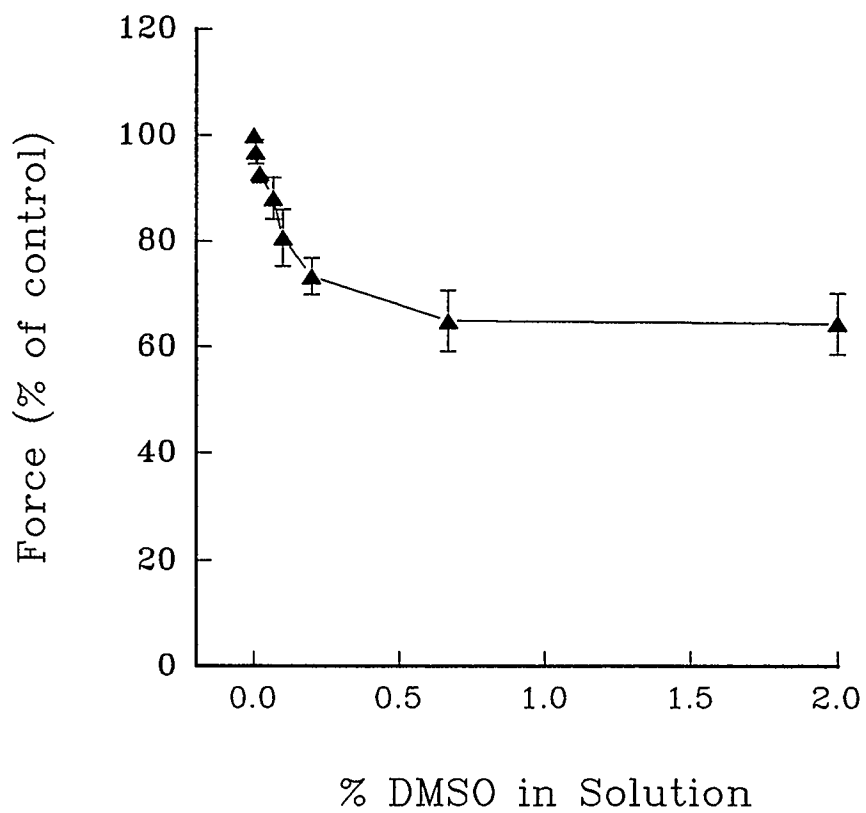
Cyclopiazonic acid (Sigma Chemical Co., St. Louis, MO) is not water soluble and therefore must be dissolved in dimethyl sulfoxide (DMSO). The amount of DMSO was kept as low as possible to avoid any possible side effects. A 29.8 mM stock solution of CPA was made. The majority of experiments presented here were done with 30  $\mu$ M CPA. The 29.8 mM stock solution was such that the DMSO did not exceed 0.01% at 30  $\mu$ M CPA in the superfusion solution. This amount of DMSO caused <5% reduction in twitch force (figure 2-4A). This has been tested in 5 muscles and shown with the standard error of the mean.

It was important to evaluate the solvent, ethanol (BDH Chemical Co., Toronto, Canada), in order to evaluate possible consequences on the muscle in the case the  $Ca^{++}$  channel agonist, Bay K-8644, was to be used. Bay K-8644 has been shown previously to aid the development of tetanic contraction (Yue et al. 1986, Gao et al. 1994) by augmenting the influx of  $Ca^{++}$  across the sarcolemma (Schramm et al. 1983). The effect of force with increasing ethanol levels in the solution can be seen in figure 2-4B. Based on this abrupt drop in force with ethanol, it was decided that the addition of Bay K-8644 would not provide enough advantage to overcome the negative effects to the muscle that would occur with the DMSO and ethanol in the solution.

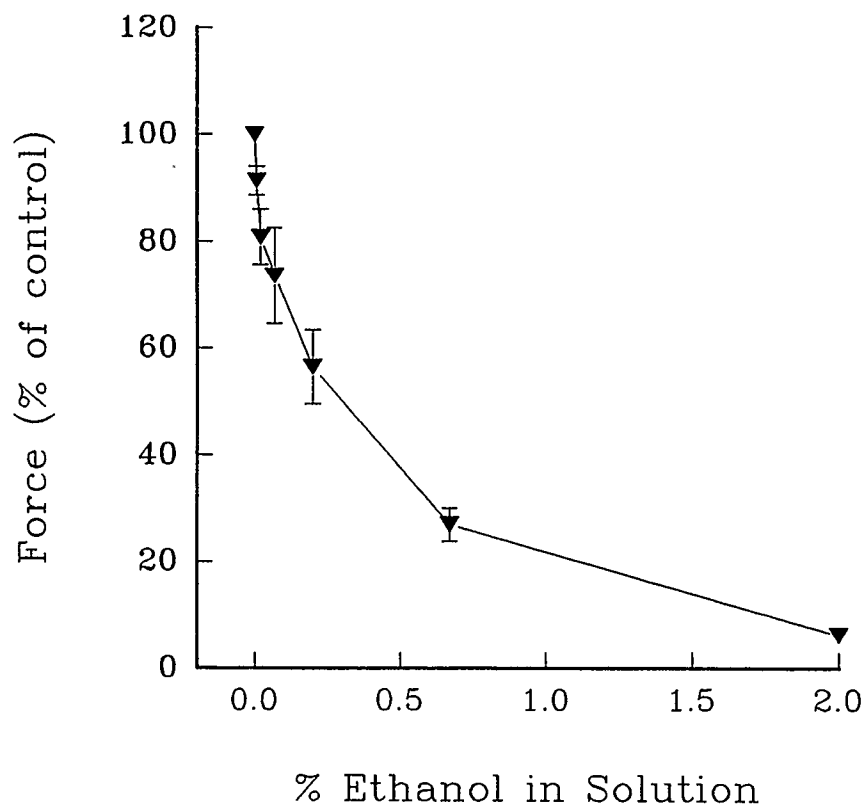
**Figure 2-4: Effects of Increasing Solvent Concentration of Twitch Force**

Decline in twitch force as [DMSO] (A) and [ethanol] (B) increases, expressed as mean±standard error of the mean (n=3).

A



B



## 2.8 Tetanic contraction

Tetanic contractions are not attainable in cardiac muscle without pharmacological intervention. The action potential is of a sufficiently long duration to prevent another stimulus from successfully activating the muscle before a substantial level of relaxation has occurred. This relaxation is achieved primarily by the sarcoplasmic reticulum (Bers & Bridge 1989). However, if the sarcoplasmic reticulum is rendered non-functional, then it would be possible that the next stimulation could occur before relaxation has been able to take place. This would enable more  $\text{Ca}^{++}$  to enter the cytosol and act on the myofilaments which would sustain the contraction for a longer period of time. Relaxation could only occur when the period of time between stimulations increased to allow the  $\text{Ca}^{++}$  extrusion mechanisms to reduce the elevated cytosolic  $\text{Ca}^{++}$  levels.

This sequence of events has been achieved with the aid of the SR inhibitor cyclopiazonic acid (CPA). 30  $\mu\text{M}$  CPA has been added to the superfusion solution and allowed to equilibrate to achieve maximal effectiveness. Once the force stabilized, a series of rapid stimuli at 12-15 Hz were initiated for no longer than 4.5 seconds and no less than 2 seconds. The stimuli were square wave pulses 40 ms in duration. This combination provided the means to consistently achieve a tetanic contraction at any sarcomere length or  $[\text{Ca}^{++}]_o$ . This is important to note because, tetanic stimulation was difficult to achieve at short sarcomere lengths or at low  $[\text{Ca}^{++}]_o$ .

## CHAPTER 3

### EFFECTS OF CYCLOPIAZONIC ACID ON CARDIAC MUSCLE

#### 3.1 Introduction

Twitches elicited in both cardiac and skeletal muscle are characterized by a rise in force followed by relaxation. The  $\text{Ca}^{++}$  transient associated with this mechanical response shows a rapid rise, the peak of which coincides with the maximum rate of force development, then the  $\text{Ca}^{++}$  transient declines as peak force is reached (Allen & Blinks 1979). The quantification of this relationship between  $\text{Ca}^{++}$  movement and force development is difficult because of the rapid movements and the kinetics of  $\text{Ca}^{++}$  binding to intracellular binding sites. In addition, the calcium-induced calcium release is not large enough to saturate the myofilaments (Fabiato 1985, Capogrossi et al. 1988, Schouten et al. 1990). Therefore, if the muscle can be made to maintain a given level of force, in turn, allowing  $\text{Ca}^{++}$  to also maintain a given level, then the relationship between the two can be more clearly defined. With the development of a steady force it would then be possible for  $\text{Ca}^{++}$  to saturate the myofilaments.

Tetanic stimulation in skeletal muscle is achieved simply by rapidly stimulating the muscle so that the twitches fuse together. When this occurs, the intracellular  $[\text{Ca}^{++}]$  ( $[\text{Ca}^{++}]_i$ ) is maintained at a high level due to the inability of the sarcoplasmic reticulum (SR) to completely pump the  $\text{Ca}^{++}$  out of the cytosol relative to the rate of  $\text{Ca}^{++}$  entering across the sarcolemma (Ruegg 1992). The amount of SR, and therefore the rate of  $\text{Ca}^{++}$  removal, in the cell determines how fast the muscle must be stimulated in order to maintain  $\text{Ca}^{++}$  levels high enough to maintain the tetanic force. This process is not possible in cardiac muscle because  $\text{Ca}^{++}$  entering through sarcolemmal channels is taken up by the SR for subsequent release (Drake-Holland et al. 1983, Cleeman & Morad 1991) but can not immediately release the  $\text{Ca}^{++}$  it has sequestered (Schouten 1985,

Schouten et al. 1987). This then allows time for the SR to remove enough  $\text{Ca}^{++}$  from the cytosol to induce myofilament relaxation before another substantial SR  $\text{Ca}^{++}$  release is possible. Although the action potential is recovered enough to allow another to take place, it is the SR " $\text{Ca}^{++}$  release compartment" that has not yet recovered (Schouten et al. 1987). If the SR was rendered non-functional, then the cytosolic  $\text{Ca}^{++}$  accumulation could take place by a sarcolemmal influx as a result of rapid stimulation. With a non-functional SR, the cytosolic  $\text{Ca}^{++}$  levels would remain high because the influx would be larger than extrusion mechanisms could handle. Therefore, enough  $\text{Ca}^{++}$  could enter the cytosol via sarcolemmal channels to saturate the cytosolic  $\text{Ca}^{++}$  binding proteins and allow a tetanic or steady state force to occur. An example of this is in the frog myocardium. The frog has very little SR relative to mammalian myocardium (Fabiato & Fabiato 1978) making extracellular  $\text{Ca}^{++}$  the primary source of activator  $\text{Ca}^{++}$  for the twitch (Morad et al. 1983). This makes it possible to tetanize just by increasing the frequency of stimulation and therefore,  $\text{Ca}^{++}$  influx (Mashima 1977).

It is the purpose of this chapter to develop a method of tetanization, in rat cardiac trabeculae, that will optimize and improve upon the techniques that are already in use (Yue et al. 1986, P. Backx 1989, Schouten et al. 1990, Gao et al. 1993). Traditionally, tetani in cardiac muscle have been executed by the use of caffeine (Forman et al. 1972) or ryanodine (Yue et al. 1986, Backx 1989, Gao et al. 1993) which eliminate the ability of the SR to sequester  $\text{Ca}^{++}$  by altering the SR's release channels. This allows  $\text{Ca}^{++}$  levels within the cytosol to rise. Often these interventions are accompanied by  $\text{Ca}^{++}$  channel agonists such as Bay K-8644 to facilitate  $\text{Ca}^{++}$  entry and subsequently force development to steady state levels (Yue et al. 1986, Gao et al. 1994). The duration of the tetanic contraction is much longer than in a twitch, which would logically result in an increased demand for ATP and subsequent elevated inorganic phosphate ( $\text{P}_i$ ) levels. It has been shown previously that  $\text{P}_i$  accumulation can reduce

force production and myofilament  $\text{Ca}^{++}$  binding (Kentish et al. 1991). Therefore, it would be much more advantageous to eliminate any unnecessary activities within the cell that consume ATP. Such an activity would be the pumping ability of the SR since it is the aim of the pharmacological intervention to eliminate its role in the first place. At the time these experiments were initiated, two main choices for elimination of the SR  $\text{Ca}^{++}$  pump were available: thapsigargin (Thastrup et al. 1990, Sagara & Inesi 1991, Lytton et al. 1991, Wrosek et al. 1992, Janczewski & Lakatta 1993) and cyclopiazonic acid (Goeger et al. 1988, Goeger & Riley 1989, Seidler et al. 1989, Baudet et al. 1993, Hove-Madsen & Bers 1993). The choice of cyclopiazonic acid (CPA) was more favorable, since thapsigargin promotes tumor development. Preliminary investigations were necessary to understand CPA's effects on cardiac muscle, because at the time there were no reliable studies dealing with this drug in cardiac muscle, particularly rat myocardium. In addition, an acceptable concentration had to be established which could provide the greatest amount of SR inhibition without adverse effects. Since CPA is very hydrophobic, it must be dissolved in dimethyl sulfoxide (DMSO), as discussed in chapter 2 section 2.8.3. The amount of DMSO in the superfusion solution must be maintained below 0.01% to minimize detrimental effects to force production (figure 2-4A), which provided another consideration for the maximum amount of CPA that could be used. For this reason, the  $\text{Ca}^{++}$  channel agonist (Bay K-8644) was not used in these studies to aid in tetanization, since Bay K-8644 must be dissolved in ethanol which has even more pronounced effects on the muscle's force production (figure 2-4B).

With all the considerations just mentioned and the goal of achieving steady state levels of force with minimum deleterious effects, the following experiments were devised. The primary aim was to achieve a steady state contraction under a wide range of extracellular  $[\text{Ca}^{++}]_o$ 's ( $[\text{Ca}^{++}]_o$ ).

### *3.1.1 Hypothesis*

Exposure to the SR  $\text{Ca}^{++}$ -ATPase inhibitor, CPA, would result in the following: 1) reduction in relaxation rate, 2) decreased recirculation fraction, and 3) would allow the cardiac muscle preparation to be tetanized with rapid stimulation. Since  $\text{Ca}^{++}$  extrusion through the  $\text{Na}^+$ - $\text{Ca}^{++}$  exchange is three to four fold slower than the SR, reductions in relaxation rate would be due to the  $\text{Na}^+$ - $\text{Ca}^{++}$  exchange having the principal role in relaxation after the SR  $\text{Ca}^{++}$ -ATPase was eliminated by CPA. Recirculation of  $\text{Ca}^{++}$  through the SR would be reduced because of its inability to sequester  $\text{Ca}^{++}$ , therefore allowing the sarcolemma to be the primary regulator of cytosolic  $\text{Ca}^{++}$  influx and efflux. Once an adequate level of SR inhibition has been attained, rapid stimulation would allow a sufficient amount of  $\text{Ca}^{++}$  to enter the cytosol, without being immediately taken up, to reach a steady state level allowing force to be sustained until cessation of stimulation.

## **3.2 Methods**

### *3.2.1 Muscle Preparation*

Trabeculae were dissected and mounted in the set-up, as described in chapter 2 (section 2.2). Each of the trabecula was first stimulated at 1 Hz and allowed to equilibrate for 30-45 minutes at 26°C in Krebs-Henseleit solution with 0.7 mM  $\text{Ca}^{++}$ . Then the trabecula was stimulated at 0.2 Hz, except where specified for brief interventions (i.e., extra-systoles or tetani). Muscle length was kept constant throughout these experiments at a resting sarcomere length of 2.15  $\mu\text{m}$ . However, the sarcomere length shortened during contraction due to the compliant ends of the preparation (Krueger & Pollack). There were two main series that were done: 1) force and recirculation fraction measurements with increasing [CPA], and 2) twitch and tetanic force, at one [CPA], with increasing  $[\text{Ca}^{++}]_o$ . These experiments helped to establish the

appropriate amount of CPA necessary to obtain maximal SR inhibition and to define the effect of CPA on cardiac muscle.

### *3.2.2 Measurement of Recirculation Fraction*

The measurement of recirculation fraction is an estimate of the amount of  $\text{Ca}^{++}$  that is taken up by the SR with each beat (Wohlfart 1982). These measurements of recirculation fraction, were done at 0.7 mM  $\text{Ca}^{++}$ ; the protocol can be visualized in figure 3-3. The trabecula was stimulated at 0.2 Hz for a variable amount of time, which was dependent on how long it took to achieve a steady, control level of force consistent for every twitch. Then a train of 10 stimuli at 3 Hz (extra-systoles) was imposed, followed by a 2 second rest period. Finally, the trabecula was again stimulated at 0.2 Hz. The twitch following the extra-systoles, is referred to as Beat 1. In this study, Beat 1 was observed to be potentiated compared to the control level of twitch force, prior to the extra-systoles. Beat 1 was followed, 5 seconds later with Beat 2 which is slightly less potentiated than Beat 1. Each twitch following Beat 1 was smaller than the one prior to it, declining in an exponential manner until the force returned to the level it was prior to the extra-systoles. The recirculation fraction can be estimated by plotting the force for each twitch ( $\text{Beat}_n$ ) against the next twitch ( $\text{Beat}_{n+1}$ ) following an extra-systolic potentiated beat (Banijamali 1994). When the forces from each of these beats are plotted in this manner, a linear regression can be made, suggesting that the same proportion of  $\text{Ca}^{++}$  reappears from one beat to the next. This can be best expressed as a percentage or fraction of  $\text{Ca}^{++}$  that continually recirculates through the SR from beat to beat. The slope of the linear regression is then taken as the recirculation fraction and expressed as a percent. This value is the percent or fraction of  $\text{Ca}^{++}$  that is recirculated through the SR.

This sequence was first performed under control conditions (i.e., prior to the

addition of CPA), then again for each addition of CPA. For each addition of CPA, force was allowed to stabilize (approximately 20 minutes) before the protocol was initiated. Measurements of twitch force were taken prior to the initiation of the extra-systoles and kept on the computer for further reference. However, most measurements of force were calculated from chart records.

### *3.2.3 Measurement of Force-[Ca<sup>++</sup>]<sub>o</sub> Relations*

The second series of experiments, measuring force-Ca<sup>++</sup> relations, was done at one [CPA] (30 μM). This [CPA] was determined from the first series of experiments. Once the muscle was equilibrated, as mentioned above, a control force-Ca<sup>++</sup> relation was done. This first involved decreasing the [Ca<sup>++</sup>] in the Krebs-Henseleit solution from 0.7 mM to 0.2 mM Ca<sup>++</sup>. Secondly, after the force had stabilized at the low [Ca<sup>++</sup>], a recording of the twitch was taken. Then Ca<sup>++</sup> was added to reach a final concentration of 0.4 mM Ca<sup>++</sup>. The muscle was allowed to equilibrate for about 5 minutes at this new [Ca<sup>++</sup>] before the next twitch measurement was taken. More Ca<sup>++</sup> was added and twitch measurements were repeated. The [Ca<sup>++</sup>]'s that were used were as follows: 0.2, 0.4, 0.8, 1.6, 2.5 mM (for the control force-Ca<sup>++</sup>) and 0.2, 0.4, 0.8, 1.6, 4.0, 8.0, 10.0, 12.5 mM Ca<sup>++</sup> (when CPA was present in the solution). Once maximal force was achieved, at 2.5 mM Ca<sup>++</sup>, the Krebs-Henseleit solution was changed to one containing 0.2 mM Ca<sup>++</sup> and 30 μM CPA. An exposure time of 40 minutes was allowed before force-Ca<sup>++</sup> measurements were taken. Force-Ca<sup>++</sup> records were taken for the twitch prior to tetanus (CPA twitch), and the tetanic contraction (described in chapter 2 section 2.9). The twitch after tetanus was also recorded. This sequence can be seen in figure 3-5. This sequence was repeated for each increment of Ca<sup>++</sup> until maximum tetanic force was achieved, at 12.5 mM Ca<sup>++</sup>. Force-Ca<sup>++</sup> relations were plotted for the control twitch, CPA twitch, and tetanus, all of which were normalized to the maximum force from the

control twitch (at 2.5 mM  $\text{Ca}^{++}$ ), and fit with a modified Hill equation (chapter 2).

### 3.3 Results

#### 3.3.1 Twitch Force

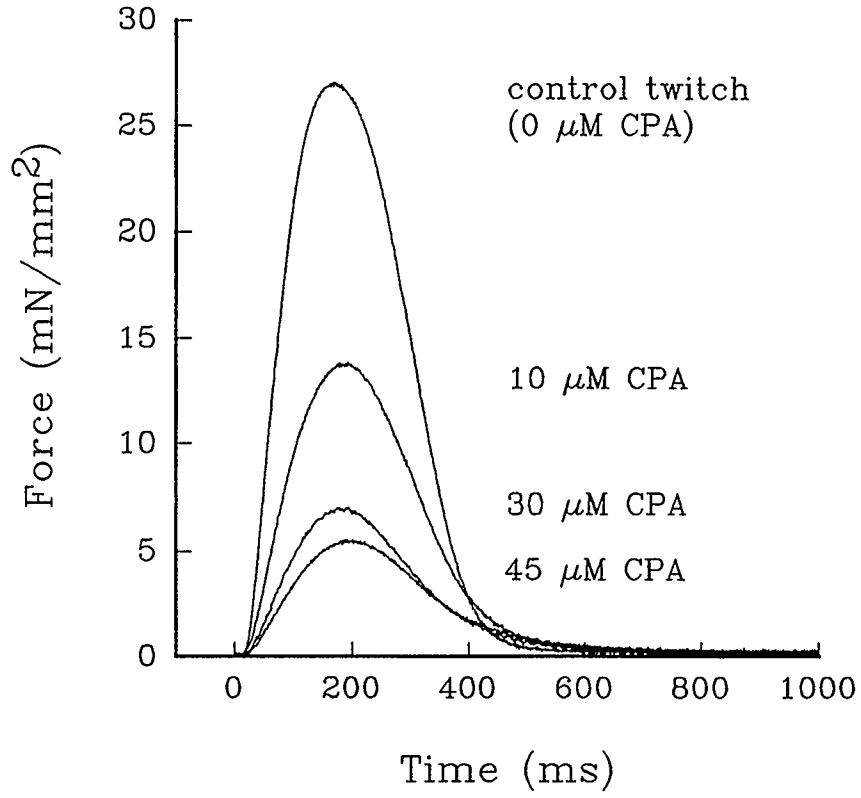
The effects of CPA on force production are shown in figure 3-1. Increasing [CPA] from 0 to 60  $\mu\text{M}$  decreased peak force by 82% ( $23.7 \pm 1.2$  to  $4.3 \pm 0.8$   $\text{mN/mm}^2$ ,  $p < 0.001$ ). Normalizing twitch force to control values, an obvious prolongation in relaxation is apparent, as seen in figure 3-2. Time to peak force increased significantly when compared within each experiment ( $p < 0.001$ ) from  $139 \pm 8.9$  ms at 0  $\mu\text{M}$  CPA to  $158.0 \pm 8.9$  ms at 30  $\mu\text{M}$  CPA with no further statistically significant increases at [CPA] above 30  $\mu\text{M}$ . The time to 75% relaxation increased with increasing [CPA] from  $197.7 \pm 17.1$  ms at 0  $\mu\text{M}$  CPA compared to  $223.2 \pm 10.4$  ms at 30  $\mu\text{M}$  CPA ( $p < 0.01$ ),  $226.7 \pm 8.9$  ms at 45  $\mu\text{M}$  CPA ( $p < 0.001$ ) with no statistically significant increase beyond 45  $\mu\text{M}$  CPA.

The increased relaxation time reported for CPA is quite underestimated when the reduction in twitch force is also considered. A very close relation between twitch force and relaxation time has been previously reported (Bucx et al. 1987). This relation indicates that reductions in twitch force are accompanied by reductions in relaxation time. Therefore, if the control twitch force is adjusted down to equal twitch force in the presence of CPA, a better evaluation of relaxation time changes can be made. Control twitch force was  $23.7 \pm 1.2$   $\text{mN/mm}^2$ , but the addition of 30  $\mu\text{M}$  CPA reduced twitch force by 64% to  $7.13 \pm 1.0$   $\text{mN/mm}^2$ . From this relation relaxation time is measured from the time at peak twitch force to 50% relaxation. The relaxation time for a control twitch ( $23.7$   $\text{mN/mm}^2$ ) was  $93.8 \pm 11.3$  ms. A 64% reduction in force corresponded to a relaxation time of 68 ms. Therefore, a comparison to the CPA twitch was done with the adjusted control force ( $7.13$   $\text{mN/mm}^2$  twitch force, and 68 ms relaxation time). The

**Figure 3-1:** Effect of [CPA] on twitch force production.

(A) The time course of a twitch in the presence of 0, 10, 30, and 60  $\mu\text{M}$ . (B) Decline of force with increasing [CPA], expressed as mean $\pm$ sem (n=5).

A



B

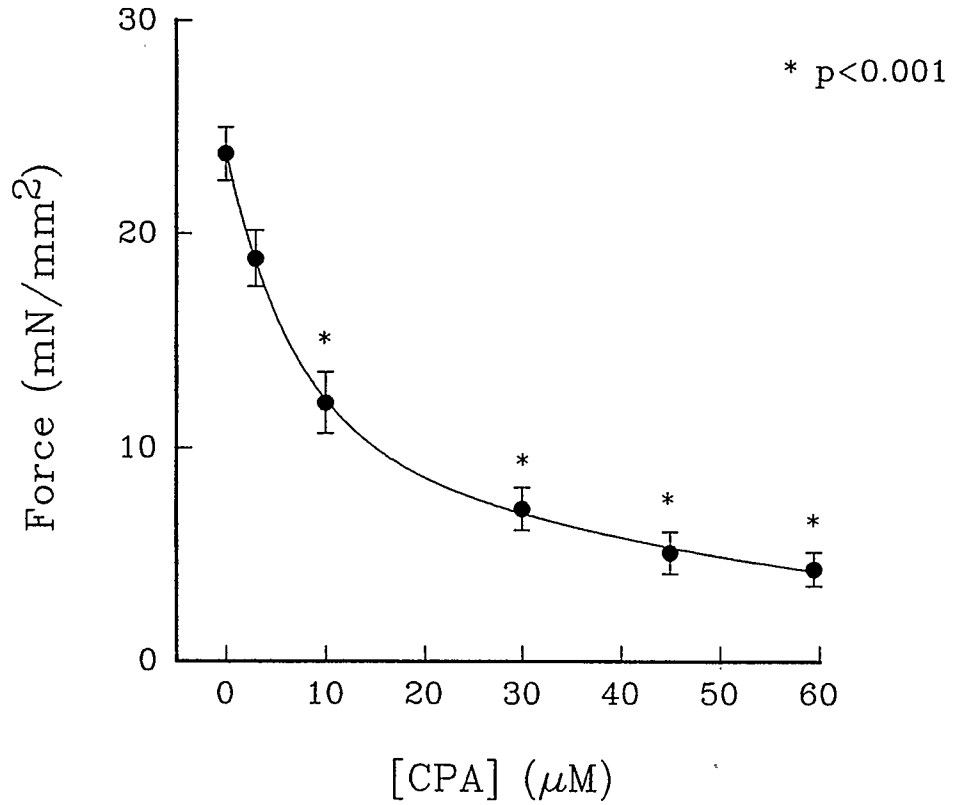
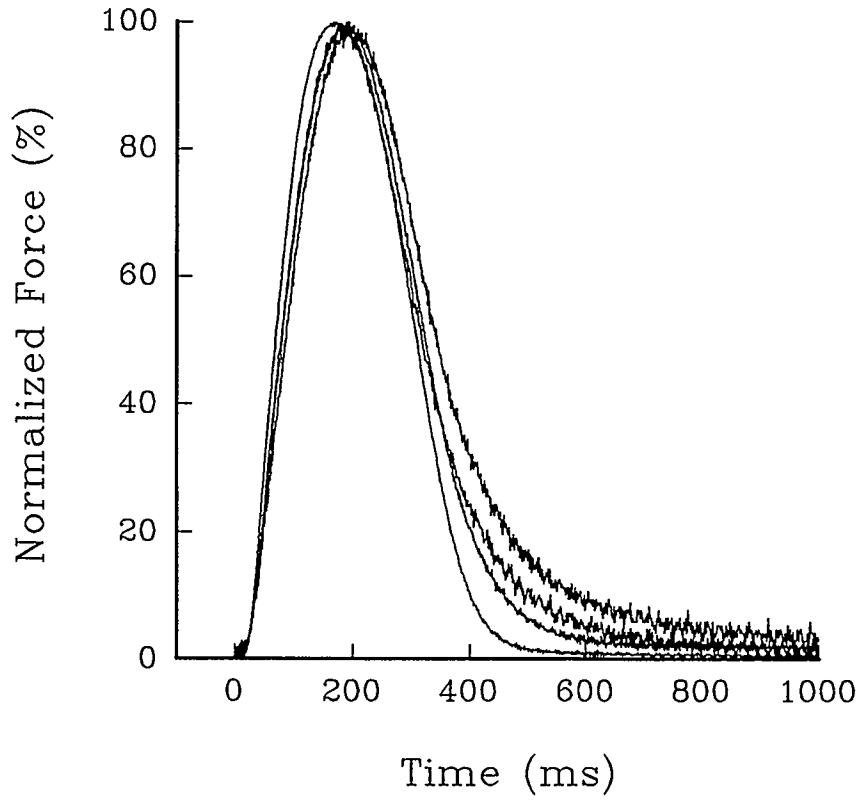


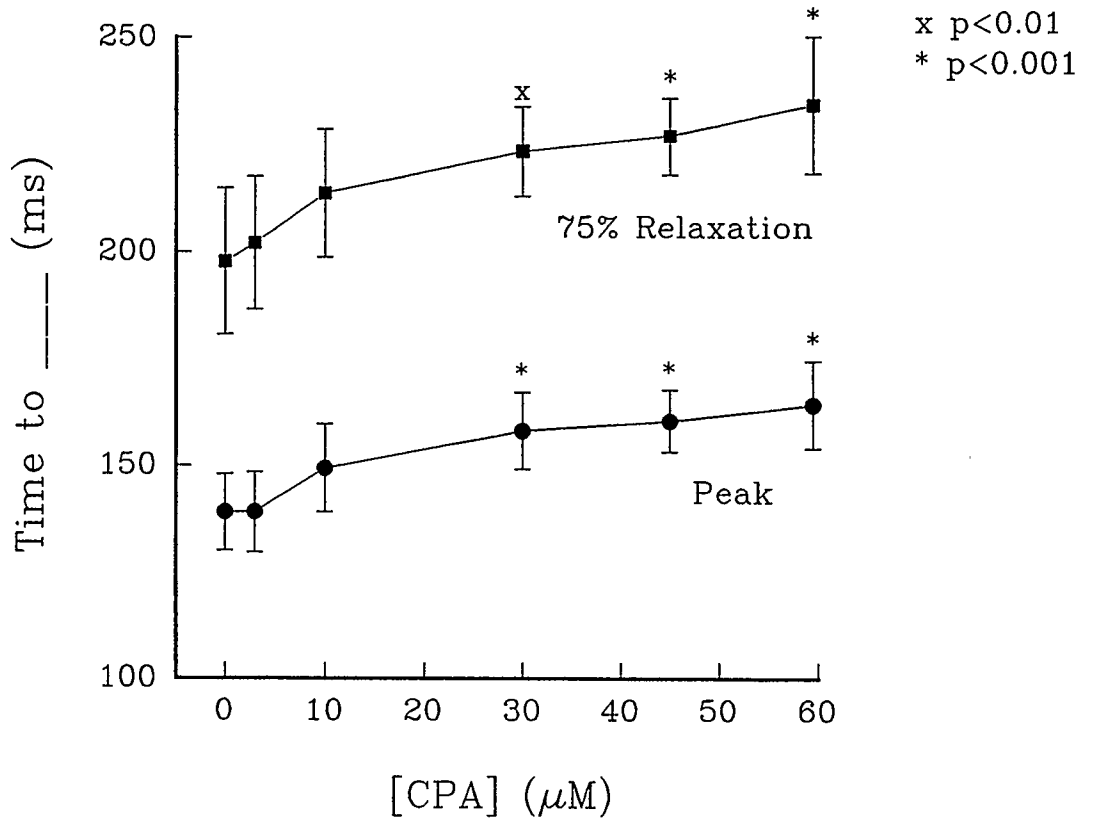
**Figure 3-2:** Effect of [CPA] on twitch relaxation.

(A) The time course of a twitch, normalized to control twitch force, in the presence of 0, 10, 30, and 60  $\mu\text{M}$ . These twitches are the same ones in figure 3-1A. (B) Time to peak twitch force and time to 75% twitch relaxation with increasing [CPA], expressed as mean  $\pm$  standard error of the mean (n=5).

A



B



CPA (30  $\mu\text{M}$ ) twitch had a relaxation time of  $109.5 \pm 17.1$  ms showing an increase of 62% from the adjusted control value. The comparison to the original control twitch ( $23.7 \text{ mN/mm}^2$ ,  $93.8 \pm 11.3$  ms) would only show an increase of 17%.

### 3.3.2 *Recirculation Fraction*

CPA (SR  $\text{Ca}^{++}$ -ATPase inhibitor) had been added to the cardiac muscle preparation in increasing doses to see its effect on the fraction of  $\text{Ca}^{++}$  re-taken up by the SR after it had been released. Figure 3-3 shows that the decline from the extra-systolic potentiated beat (Beat 1) became more rapid as [CPA] increased, suggesting that less  $\text{Ca}^{++}$  was recirculating through the SR and therefore less was available for the following beat. In addition, fusion of the high frequency priming pulses began to occur as [CPA] increases. Figure 3-4A is an example of the plotted data from one experiment, where the slope of each regression line decreased as [CPA] increases, demonstrating a reduction in the amount of  $\text{Ca}^{++}$  that was being recirculated through the SR. Figure 3-4B indicates the fall in the recirculation fraction with increasing [CPA] from a maximum value of  $68.6 \pm 2.8\%$ , under control conditions, down to a minimum of  $24.2 \pm 1.4\%$  at 30  $\mu\text{M}$  CPA. The change in the recirculation fraction from 30 to 60  $\mu\text{M}$  CPA was not statistically significant. It is apparent that 30  $\mu\text{M}$  CPA is the minimum amount of CPA necessary to obtain the maximum amount of SR inhibition, just as seen in the time to peak and time to 75% relaxation in the twitch.

### 3.3.3 *Force-[Ca<sup>++</sup>]<sub>o</sub> relations*

Effects of  $[\text{Ca}^{++}]_o$  on twitch and tetanic force production in the presence of 30  $\mu\text{M}$  CPA are shown in figure 3-5. In this figure, *a*, indicates the twitch prior to the initiation of the tetanus. This twitch is referred to as the CPA twitch through out this chapter. The force tracing of the tetani is indicated as *b*, with separate areas denoted as *b*<sub>1</sub>, *b*<sub>2</sub>,

**Figure 3-3: Effect of [CPA] on Force Decline From a Potentiated Twitch**

Exponential decline in force from a potentiated beat under control conditions (A), in the presence of (B) 30  $\mu\text{M}$  CPA, and (C) 60  $\mu\text{M}$  CPA. Each tick in the Timing tracing represents 10 seconds.

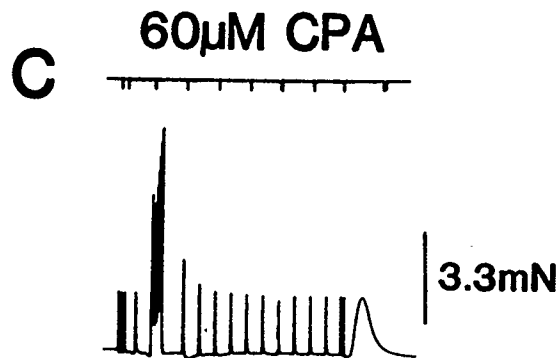
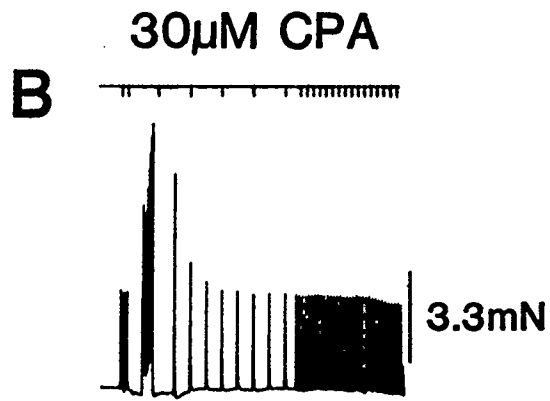
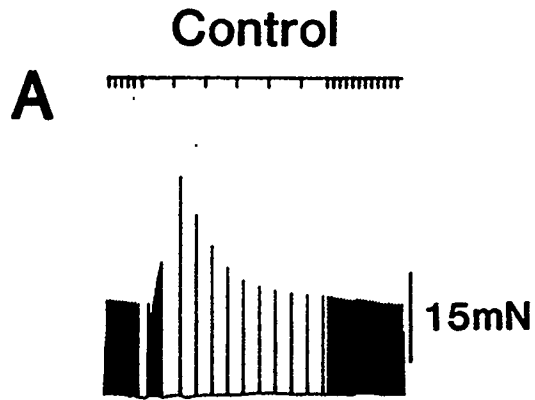
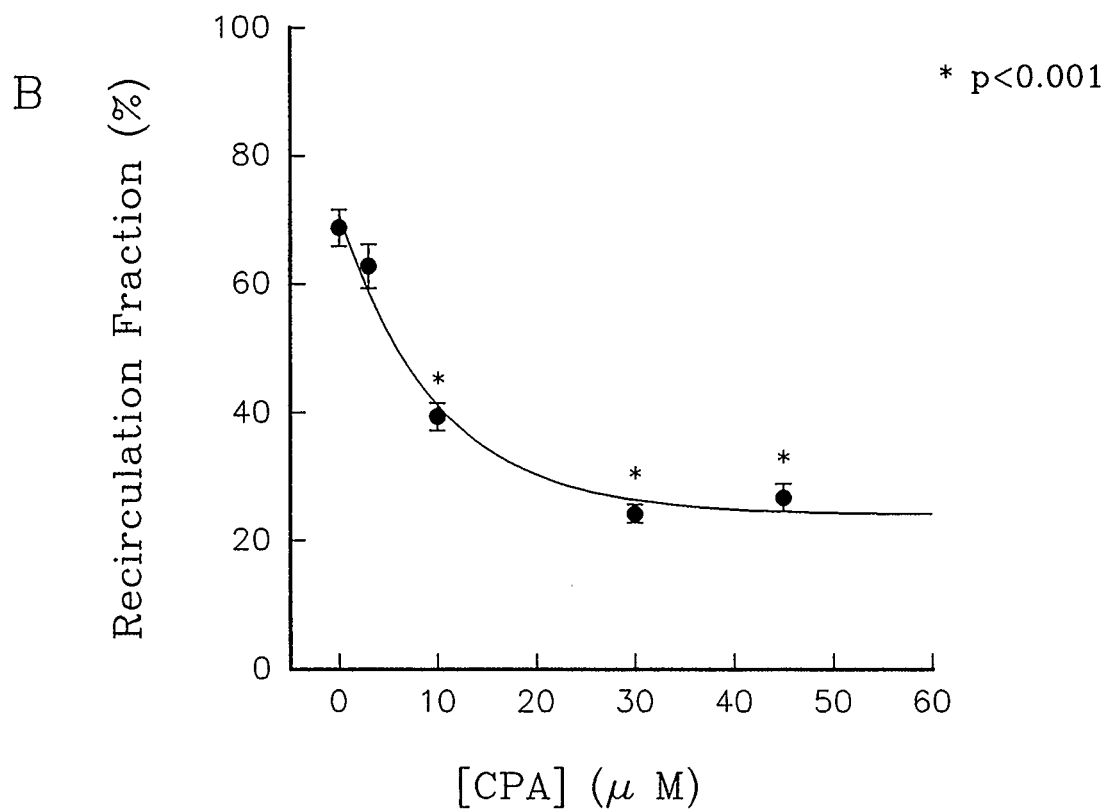
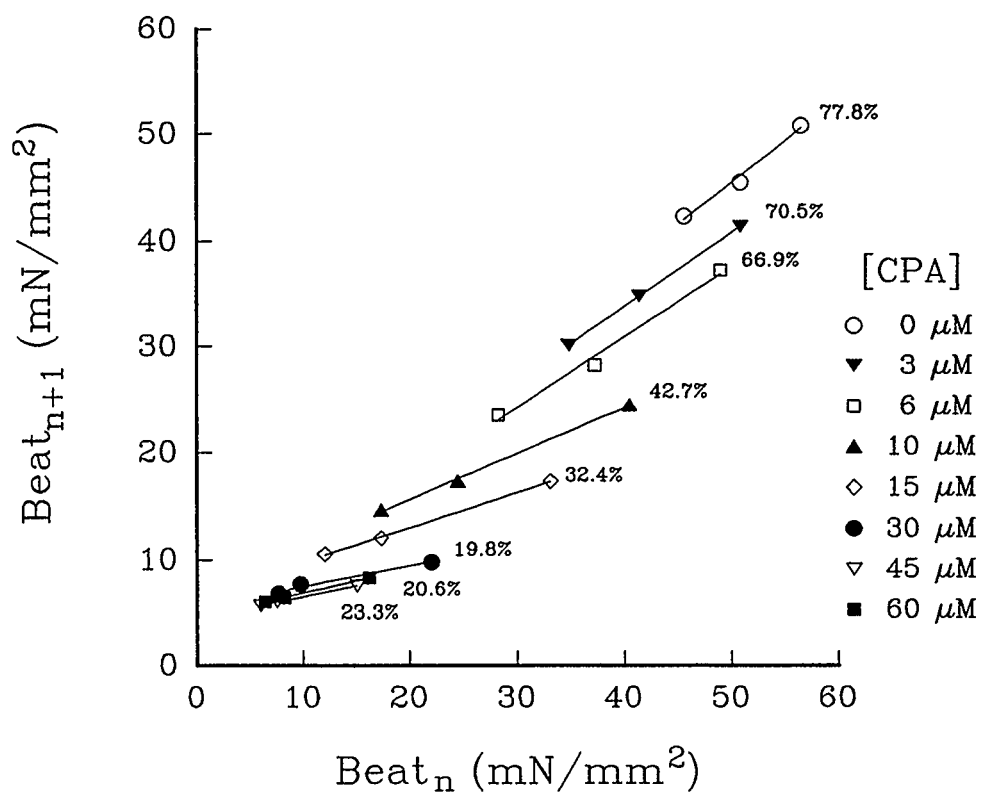


**Figure 3-4: Decline of Recirculation Fraction with Increasing [CPA]**

(A) Reduction in the slope with increasing [CPA] through a series of points from the decline in force from a potentiated beat (one experiment). (B) Decline in the recirculation fraction with increasing [CPA], expressed as mean $\pm$ sem (n=5).

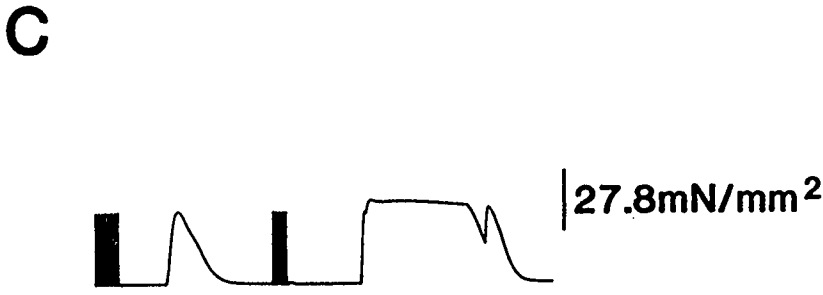
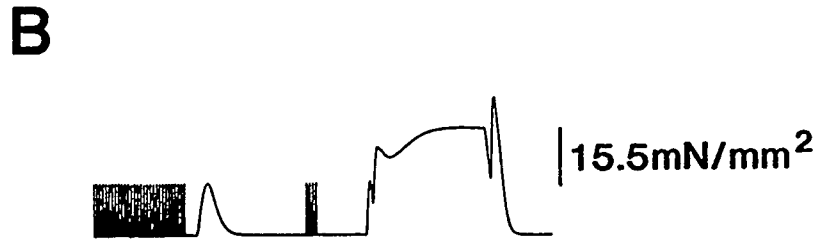
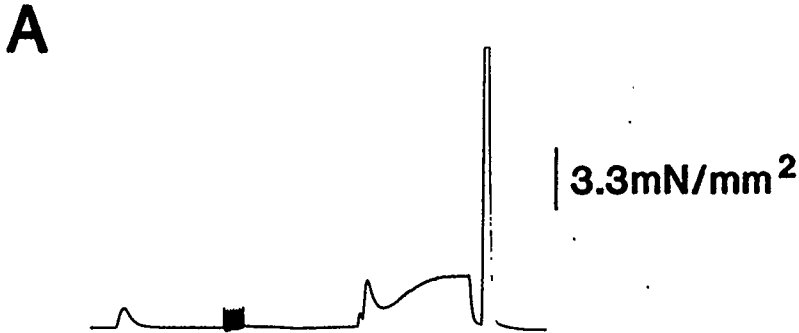


and  $b_3$ .  $b_1$  is the initial spike associated with the onset of the rapid stimulations.  $b_2$  indicates the drop or plateau in force (depending on  $[Ca^{++}]_o$ ), which also becomes less prominent as  $[Ca^{++}]_o$  increases. The last phase of the tetanus,  $b_3$  is most important since it is this point where the amount of entering  $Ca^{++}$  has reached a quasi-equilibrium with the buffering sites within the cytosol allowing steady state force to be reached. (This claim is further substantiated in chapter 6, where corresponding fluorescence measurements are made, indicating  $[Ca^{++}]_i$ ). The twitch after the tetanus shows a considerable amount of potentiation at lower  $[Ca^{++}]_o$ , however, the degree of potentiation relative to the tetanic force declines as  $[Ca^{++}]_o$  increases. The force of this potentiated post-tetanic twitch is quite close to  $F_{max}$ . This was not specifically studied since the interval between the end of the tetanic contraction and post-tetanic twitch varied not only between experiments, but often within a single experiment as well.

When the control twitch, CPA twitch, and tetanus ( $b_3$ ) were plotted as a force- $Ca^{++}$  relation, dramatic shifts in the curve were apparent, as seen in figure 3-6. The curve for the control twitch is located the farthest leftward with the CPA twitch the farthest rightward and the tetanus in between the two. These data points were fitted with a curve derived from the modified Hill equation, discussed in chapter 2 section 2.6. From the modified Hill equation, maximal force ( $F_{max}$ ) was  $104.1 \pm 1.3$  for the control twitch,  $93.0 \pm 4.9$  for the CPA twitch, and  $105.3 \pm 4.2$  for the tetanus, with no statistical difference between them ( $p > 0.05$ ). The  $EC_{50}$  showed a significant shift to  $1.44 \pm 0.22$  mM  $Ca^{++}$  for the CPA twitch and  $1.14 \pm 0.13$  mM  $Ca^{++}$  for the tetanic contraction from a control value of  $0.38 \pm 0.04$  mM  $Ca^{++}$ . The value for  $n$  was only significantly different for the CPA twitch because the slope is very shallow compared to the control twitch and tetanus. The values for these parameters are listed in table 3-1.

**Figure 3-5:** Effect of  $[Ca^{++}]_o$  on Tetanic Force

Time course of a tetanic contraction in the presence of 0.4 (A), 1.6 (B), and 10.0 (C) mM  $[Ca^{++}]_o$ . The tetanus is divided into phases, as indicated in (A). The phases are as follows, *a* is the twitch in the presence of CPA, and *b* refers to the tetanus which has three subheadings (*b*<sub>1</sub>, *b*<sub>2</sub>, *b*<sub>3</sub>) which are described in the text. The duration of each tetanus is 4.5 seconds.



time →

**Figure 3-6:** Force-[Ca<sup>++</sup>]<sub>o</sub> Relations for the Control and CPA Twitch, and Tetanus

Force-[Ca<sup>++</sup>]<sub>o</sub> relations curve fit by the modified Hill equation for the control twitch, tetanus, and twitch in the presence of 30 μM CPA, expressed as a mean ± standard error of the mean (n=5), as it is normalized to the maximum force (F<sub>max</sub>) attained in the absence of CPA.

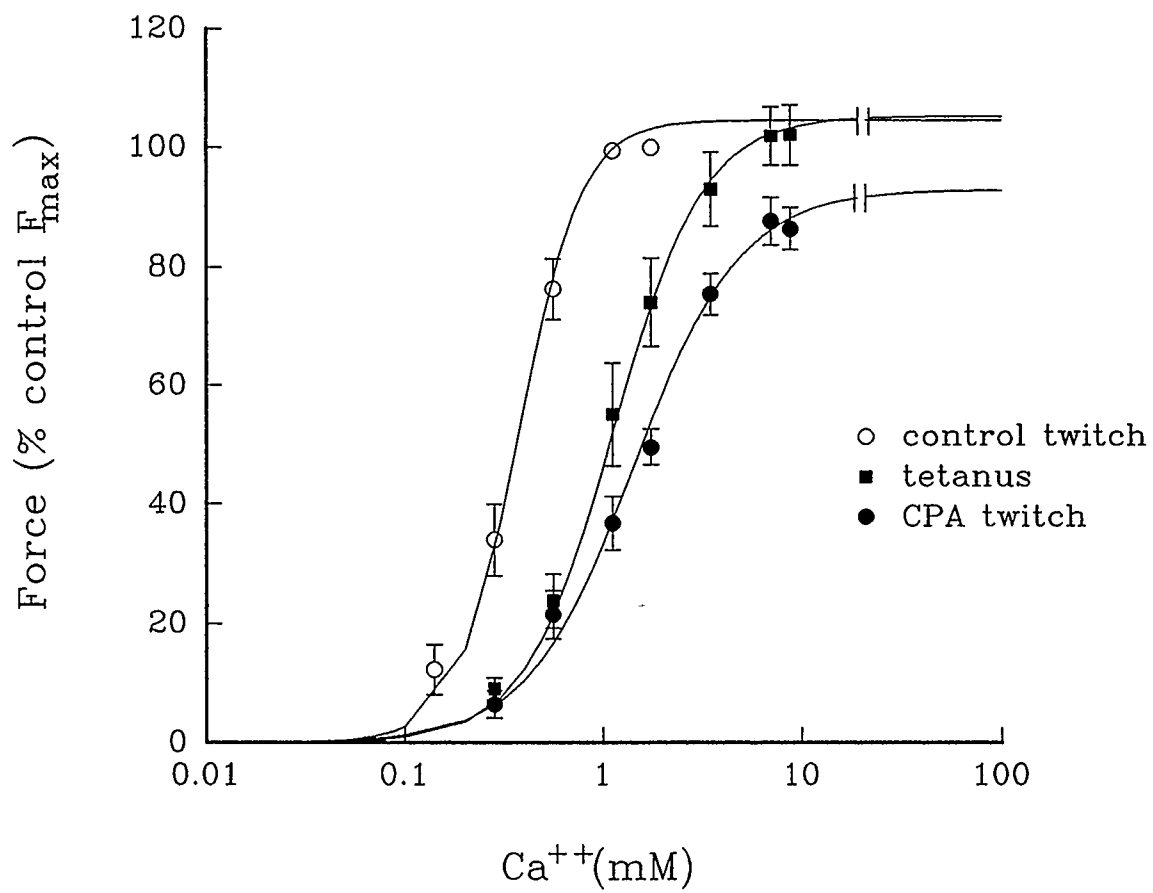


**Table 3-1**

Parameters from the modified Hill equation listed as mean values $\pm$ sem, taken from figure 3-6. (The modified Hill equation is described in detail in chapter 2).

	<i>n</i>	EC <sub>50</sub> (mM)	F <sub>max</sub>
Control Twitch	2.75 $\pm$ 0.39	0.38 $\pm$ 0.04	104.1 $\pm$ 1.3
CPA Twitch	1.62 $\pm$ 0.15*	1.44 $\pm$ 0.22*	93.0 $\pm$ 4.9
Tetanus	1.93 $\pm$ 0.22	1.14 $\pm$ 0.13*	105.3 $\pm$ 4.2

\* differences in these values from the control twitch are statistically significant,  $p < 0.05$ .

### 3.4 Discussion

The effect of CPA on the shape of the twitch was quite prominent. First, there was a reduction in peak twitch force with increasing [CPA] from 10 to 60  $\mu\text{M}$ . At concentrations above 30  $\mu\text{M}$ , peak force did not show any significant reductions (figure 3-1). Secondly, an increase in the time to peak force occurred at 30  $\mu\text{M}$  CPA (figure 3-2). This coincided with the increased impairment of the SR, and its reduced contribution to twitch force. Therefore,  $\text{Ca}^{++}$  influx across the sarcolemma became a more important contributor of  $\text{Ca}^{++}$  for force development. Lastly, prolongation of the time to 75% relaxation from peak twitch force became apparent as [CPA] increased to 30  $\mu\text{M}$  (figure 3-2). This demonstrated an impairment of the  $\text{Ca}^{++}$ -ATPase on the SR by CPA, slowing down  $\text{Ca}^{++}$  removal from the cytosol and thus twitch force relaxation. To show the prolongation of relaxation time with CPA, the comparison of twitch force in the presence of 30  $\mu\text{M}$  CPA and control force for 50% relaxation time were compared, showing an increase of 17%. However, when the control force and corresponding relaxation time was adjusted to match the peak twitch force of the CPA twitch a 62% increase in relaxation time was seen. This suggests not only does the addition of 30  $\mu\text{M}$  CPA result in a 64% reduction in twitch force but also a 62% increase in relaxation time. A prolongation in contraction with the addition of CPA has also been previously noted in adult rat hearts, but not in the neonatal hearts (Agata et al. 1993) Since the primary  $\text{Ca}^{++}$  removal mechanism, the SR, was being progressively eliminated,  $\text{Ca}^{++}$  extrusion was being increasingly dependent on the  $\text{Na}^{+}$ - $\text{Ca}^{++}$  exchange (Baudet et al. 1993). These effects on cardiac muscle have also been observed by Baudet et al. (1993) using cardiac muscle from a rabbit in the presence of 100  $\mu\text{M}$  CPA. Their work on rabbit muscle (with 100  $\mu\text{M}$  CPA), showed a greater increase in the time to peak force and relaxation, but the reduction in twitch force was greater in the experiments using rats (30  $\mu\text{M}$  CPA), presented here. This could be due to the greater

reliance on SR for force production and relaxation in the rat myocardium when compared to the rabbit (Bers 1985, Sutko & Willerson 1980, Bassani et al. 1994). In addition,  $\text{Ca}^{++}$  uptake and release by the SR, in the rat, has been found to be significantly faster than rabbit (Nayler et al. 1975), and the rat has a greater density of SR pump sites over rabbit myocytes (Hove-Madsen & Bers 1993).

Mammalian cardiac muscle contains a large amount of SR, especially the rat, and the EC coupling process is heavily dependent on this organelle (Fabiato & Fabiato 1978). When its operation is altered in any way, dramatic changes in the muscle's ability to perform are expected. As an inhibitor of the SR's ability to sequester  $\text{Ca}^{++}$ , reductions in the fraction of  $\text{Ca}^{++}$  that recirculates through the SR from beat to beat are expected, as seen previously with ryanodine (Banijamali et al. 1994). The results presented here in cardiac trabeculae, support the findings by Goeger et al. (1988) in isolated skeletal SR vesicles, that CPA is a potent inhibitor of the SR's ability to sequester  $\text{Ca}^{++}$ . At high [CPA], the recirculation fraction decreased as indicated by the rapid fall in force from the potentiated beat back to control levels. At [CPA] above 30  $\mu\text{M}$ , the drop in force back to baseline levels was so rapid, only two to three beats, at the most, could be attained (figure 3-3C), which made the estimate of recirculation fraction from the slope of the regression less reliable. Because of the difficulty in measuring the decline in force at these high [CPA]'s (45  $\mu\text{M}$  and 60  $\mu\text{M}$ ), the estimate of recirculation fraction even showed a slight, but not statistically significant increase. The recirculation fraction at 60  $\mu\text{M}$  CPA was not attainable in all the experiments done and therefore was not included in the graph of mean values (figure 3-4B). The smallest recirculation fraction was found with 30  $\mu\text{M}$  CPA, therefore, it was logical to use this amount of CPA to achieve the greatest effect. This is more clearly demonstrated in figure 3-2B. Baudet et al. (1993) studied the effects of SR  $\text{Ca}^{++}$ -ATPase inhibitors on a similar preparation using rabbit muscle. They found an acceleration in the rest decay

and a reduction in forces elicited by rapid cooling contractures of 76%, confirming that thapsigargin and CPA do indeed reduce the  $\text{Ca}^{++}$  content of the SR. This supports the findings presented here found by recirculation fraction measurements, that CPA effectively reduces the contribution of the SR by reducing the ability of sequester  $\text{Ca}^{++}$  and thus, the amount of  $\text{Ca}^{++}$  available for release.

The tetanic forces developed by the cardiac trabeculae presented here undergo striking shape changes throughout the duration of stimulation (figure 3-5). It is expected that inhibition of the SR by CPA should allow the cytosolic  $\text{Ca}^{++}$  to sufficiently rise to a steady level, leading to a steady state level of force, with minimal changes in pH (Marban et al. 1986). However, at low  $[\text{Ca}^{++}]_o$ , the force shows a dramatic drop ( $b_2$ ) before it rises to a steady state level ( $b_3$ ). This drop in force can be explained by the lack of complete inhibition of the SR  $\text{Ca}^{++}$ -ATPase, as has been found previously in a multicellular preparation (Baudet et al. 1993, Hove-Madsen & Bers 1993). Based on this finding, the following is an explanation of each phase of the tetanus:

$b_1$  With the SR  $\text{Ca}^{++}$  pumps still partially functional, the SR is able to sequester some  $\text{Ca}^{++}$ . As a fundamental component of the cardiac excitation-contraction coupling process, trans-sarcolemmal  $\text{Ca}^{++}$  can induce a SR  $\text{Ca}^{++}$  release (Fabiato & Fabiato 1975). This  $\text{Ca}^{++}$ -triggered SR release can then be seen as the  $b_1$  portion of the tetanus, similar to a twitch.

$b_2$  At low  $[\text{Ca}^{++}]_o$  after the initial  $\text{Ca}^{++}$  release from the SR along with incoming  $\text{Ca}^{++}$  through sarcolemmal channels, cytosolic  $\text{Ca}^{++}$  levels begin to drop due to the sequestering ability (albeit meager) of the functionally remaining SR  $\text{Ca}^{++}$  pumps, and  $\text{Na}^+$ - $\text{Ca}^{++}$  exchange activity (Bers & Bridge 1989). This drop in cytosolic  $\text{Ca}^{++}$  would correspond to  $b_2$ . At high  $[\text{Ca}^{++}]_o$ ,  $\text{Ca}^{++}$  entering the cytosol across the sarcolemma is much larger. This increased amount of

$\text{Ca}^{++}$  raises the cytosolic  $\text{Ca}^{++}$  levels to such a degree that the portion that is taken up by the SR is relatively insignificant and therefore no drop in force is seen. Fluorescence ratios (indicators of  $[\text{Ca}^{++}]_i$ ) just prior to the period of force decline, show a decline after the initial rise (figure 6-1). This is similar to  $[\text{Ca}^{++}]_i$  transients during a twitch (Backx & ter Keurs 1993), except  $[\text{Ca}^{++}]_i$  rises again to reach a steady state.

$b_3$      Redevelopment of force after  $b_2$ , at low  $[\text{Ca}^{++}]_o$ , occurs as a result of the SR pumps inability to keep up with the influx of  $\text{Ca}^{++}$  across the sarcolemma and  $\text{Na}^+$ - $\text{Ca}^{++}$  exchange. By this point, rapid stimulation has likely raised  $[\text{Na}^+]_i$  accompanied by a depolarization of membrane potential (Eisner et al. 1983, Eisner et al. 1984). The  $\text{Na}^+$ - $\text{Ca}^{++}$  exchange has been shown to reverse and contribute to contraction when  $[\text{Na}^+]_i$  is elevated (Bers et al. 1988, Harrison et al. 1992) and membrane depolarization can also alter the direction of  $\text{Ca}^{++}$  movement by the  $\text{Na}^+$ - $\text{Ca}^{++}$  exchange by exceeding its reversal potential (reviewed by Eisner & Lederer 1985). This inability to keep up allows cytosolic  $\text{Ca}^{++}$  to reach a steady level and subsequent steady state force generation can occur.

The tetanic forces achieved using CPA are different than found with ryanodine. The ryanodine tetani are not marked by a prominent initial spike ( $b_1$ ), but show a rise to steady state levels of force that continue for the duration of the stimuli (Yue et al. 1986, Gao et al. 1994). This could be because CPA only minimizes the ability of the SR to sequester  $\text{Ca}^{++}$  while ryanodine eliminates the ability of the SR to sequester  $\text{Ca}^{++}$ . Although the SR pumps are still able to take in  $\text{Ca}^{++}$ , ryanodine causes the  $\text{Ca}^{++}$  to leak out of the SR (Sutko & Kenyon 1983) so the  $\text{Ca}^{++}$  that is taken up goes right back out of the SR contributing to myofibril activation. Therefore, no initial spike is seen from a SR release of sequestered  $\text{Ca}^{++}$  ( $b_1$ ) or drop in force after the SR release ( $b_2$ ).

However, in the study presented here, the force developed during the steady state ( $b_s$ ) is comparable (slightly greater) to forces found with ryanodine assisted tetani.

The force- $Ca^{++}$  relations for the tetani, presented in figure 3-6, do not show increases in maximal force above the control twitch, which was not expected. In the intact muscle with a functional SR, maximal force only reaches 70% of the true maximal force the muscle can produce when it is skinned (Schouten et al. 1990). The SR is a major limiting factor (Capogrossi et al. 1988) in true maximal force development (Schouten et al. 1990), so with the addition of CPA, this protective role of the SR should be sufficiently eliminated. It should then be expected that force development, during repetitive stimulation in the presence of CPA, could reach levels near those found with skinned fibers. However, during the course of these experiments where  $[Ca^{++}]_o$  levels reached above 5.0 mM, a noticeable amount of precipitation (calcium salts of carbonate, phosphate and sulphate) began to form which increased as more  $Ca^{++}$  was added. This prompted a series of pH measurements that have been discussed in chapter 2 section 2.8.2. The results of these pH experiments in Krebs-Henseleit solution, showed  $[Ca^{++}]_o$ 's above 5.0 mM were associated with a sharp reduction in pH. Since pH has been shown to reduce force and myofilament sensitivity in skinned fiber's (Fabiato & Fabiato 1978, Ricciardi et al. 1986, Orchard & Kentish 1990), it could account for the underestimation of force and need for such high  $[Ca^{++}]_o$  in these experiments. To remedy this pH problem, HEPES buffered solution was used in subsequent experiments when high  $[Ca^{++}]_o$  were needed. Force- $[Ca^{++}]_o$  relations with HEPES solution can be seen in chapter 6, it is evident that tetanic contractions reach maximal forces that are much greater than has seen with tetani in Krebs-Henseleit solution. In addition, tetanic forces obtained in HEPES solution with CPA are approximately 20% greater than maximal tetanic forces in ryanodine treated trabeculae which were also done in Krebs-Henseleit solution with  $[Ca^{++}]_o$  up to 30 mM (Gao et al. 1994).

All of the effects of CPA on rat cardiac muscle presented here provide evidence for how the muscle can function with its principal  $\text{Ca}^{++}$  buffer eliminated. Tetanization was successfully achieved with 30  $\mu\text{M}$  CPA and rapid stimulation. The CPA sufficiently minimized the removal rate of  $\text{Ca}^{++}$  from the cytosol and the rapid stimulation allowed a sufficient amount of  $\text{Ca}^{++}$  to enter the cytosol, providing adequate means to tetanize the preparation at a wide range of  $[\text{Ca}^{++}]_o$ . The achievement of tetanization in this preparation has then provided the means to look at steady state  $[\text{Ca}^{++}]_i$  levels in the muscle during the tetanic steady state which are presented in chapter 6.

### 3.5 Summary of Findings

1. Twitch force decreased by 64% with a corresponding 62% prolongation of relaxation time, this compares well with previous work presented in the literature (Agata et al. 1993, Baudet et al. 1993, Perry-Man et al. 1993).
2. Recirculating  $\text{Ca}^{++}$  through the SR decreased, which explains prolongation of twitch relaxation. Measurement of recirculation fraction in the presence of CPA has not been done previously. Findings by Baudet et al. (1993) assessing  $\text{Ca}^{++}$  content of the SR, using rapid cooling contracture techniques, support the findings presented here. Their study showed SR  $\text{Ca}^{++}$  accumulation, in the rabbit, was diminished by 60% in the presence of 100  $\mu\text{M}$  CPA.
3. Tetanization, in cardiac muscle, was achieved using a SR  $\text{Ca}^{++}$ -ATPase inhibitor. Such a mode of tetanization has not been previously done, providing a means to achieve a steady state level of force without unnecessary ATP consumption. Reducing extraneous ATP use minimizes potential byproducts such as  $\text{P}_i$  and  $\text{H}^+$ , which could affect myofilament sensitivity (Lee & Allen 1993).

### 3.6 Potential Source of Errors

As mentioned previously, the estimation of the recirculation fraction with high [CPA] is difficult and sometimes unattainable. The force is not very potentiated to begin with because the SR  $\text{Ca}^{++}$  accumulation is so weak, therefore, only a few beats are needed for force to return to baseline levels. This is similar to frog cardiac muscle where there is very little SR and activating  $\text{Ca}^{++}$  is primarily from extracellular space (Morad & Goldman 1973). The problem with the high [CPA] measurements indicates that in order to reliably estimate the recirculation fraction, a decline of more than three beats is necessary.

## Chapter 4

### Effects of Cyclopiazonic Acid on Cardiac Myofilaments

#### 4.1 Introduction

Cyclopiazonic acid (CPA) is a mycotoxin that is considered to selectively inhibit the  $\text{Ca}^{++}$  ATPase of the sarcoplasmic reticulum (SR) in isolated vesicles from skeletal muscle (Goeger et al. 1988, Goeger & Riley 1989). This drug has been extensively characterized in smooth muscle (Shima & Blaustein 1992, Suzuki et al. 1992, Uyama et al. 1992, Gasgov et al. 1993, Uyama et al. 1993, Wantanabe et al. 1993) with some studies in cardiac muscle (Agata et al. 1993, Baudet et al. 1993), and skeletal muscle (Kurebayashi & Ogawa 1991, Huchet & Leoty 1993), as well as the plasma membrane (Mason et al. 1991, Wuytack & Raeymaekers 1992). In ileal smooth muscle strips, no effect on the contractile proteins were found (Uyama et al. 1992) but some effects on  $\text{Ca}^{++}$  sensitivity and maximal force production have been observed in both fast- and slow-twitch skeletal muscles (Kurebayashi & Ogawa 1991, Huchet & Leoty 1993). The effects of this inhibitor have not, however, been tested to see whether or not it has effects on the contractile elements in cardiac muscle. This inhibitor is used extensively in the experiments presented in this thesis and therefore any potential additional effects must also be evaluated. In each experiment presented in this thesis, force measurements are of fundamental importance and any effect of CPA on force production would be highly undesirable and undermine the ability to make any conclusions regarding mechanisms contributing to force development.

A practical method of assessing an effect of a drug on the contractile protein's or myofilament's ability to generate force at a given level of  $\text{Ca}^{++}$ , is to use a "skinned" muscle preparation (Smith & Miller 1985). "Skinning" a muscle conventionally involves the use of a biological detergent (i.e., Triton-X 100) to permeabilize lipid membranes,

such as the sarcolemma, SR, and mitochondria. Once the muscle is skinned, it is bathed in several solutions that mimic the intracellular milieu. The amount of force generated by the skinned muscle at a given level of  $\text{Ca}^{++}$  can be measured. Plotting force and free  $[\text{Ca}^{++}]$  results in a sigmoidal relation when  $[\text{Ca}^{++}]$  is plotted on a log scale. This relation provides a means to compare the force response of the myofilaments under a variety of parameter changes. For our purposes in the series of experiments presented here, comparisons will be made between the force- $[\text{Ca}^{++}]$  relation under control conditions and when exposed to 30  $\mu\text{M}$  CPA and its solvent, dimethyl sulfoxide (DMSO).

## 4.2 Methods

The final results of skinned fiber experiments depend heavily on the make up of the final solutions that bathe the muscle. These solutions must have the proper free ion concentrations ( $\text{Ca}^{++}$ ,  $\text{H}^+$ ,  $\text{Mg}^{++}$ ,  $\text{K}^+$ ,  $\text{Na}^+$ , etc.), since changes in the pH, ionic strength, and temperature can markedly affect the shape of the force- $\text{Ca}^{++}$  curve (Orchard & Kentish 1990), ionic strength (defined as one half the sum of the concentration of ions in the solution multiplied by its charge squared) (Harrison & Bers 1990). The specific preparations of each solution used are described in detail in the sections that follow. Because two force- $[\text{Ca}^{++}]$  curves are being compared in this series of experiments, it was of utmost importance to ensure that the basic solutions (control and CPA) were no different. For this reason these two solutions were prepared as one until the final  $\text{Ca}^{++}$  solutions were made up. The activating and relaxing solution used to make each  $\text{Ca}^{++}$  solution had 30  $\mu\text{M}$  CPA added. This way the only difference between each solution at each  $\text{Ca}^{++}$  was the CPA. Two possible sources of  $\text{Ca}^{++}$  contamination, are inadequately distilled water and the use of glassware. To minimize such contamination, only deionized water and plastic containers were used (Fabiato & Fabiato 1979), and the KOH, KBES (buffer), and potassium propionate ( $\text{KPr}$ ,  $\text{CH}_3\text{CH}_2\text{COO}^-\text{K}^+$ ) solutions

were chelexed to directly eliminate contaminant  $\text{Ca}^{++}$ .

#### 4.2.1 *Chelexing*

The first step in preparing the basic ingredients for skinning solutions must be removing any contaminate  $\text{Ca}^{++}$  by chelexing. The first solution to be chelexed was KOH. KOH was then used to make KBES and KPr as well as adjusting the pH for other solutions that were to be made. The 1.0 M KOH (pH near 13.9), 500 mM BES stock, and KPr were the solutions to be chelexed. This was also the order in which they were chelexed. The KOH was chelexed first because the BES buffer (HBES to KBES when the pH is fixed with KOH) and the KPr both required chelexed KOH to adjust their pH (at or slightly less than 7.1).

The purchased  $\text{Na}^+$ -Chelex was converted to  $\text{H}^+$ -Chelex then converted to  $\text{K}^+$ -Chelex which was the form used for contaminant ion removal.  $\text{K}^+$ -Chelex was the form of choice over the  $\text{H}^+$  form because the  $\text{K}^+$ -Chelex replaces the contaminant ions with  $\text{K}^+$  and did not alter the pH of the exiting solution from that of the entering solution. There were two methods used to convert the  $\text{H}^+$ -Chelex to  $\text{K}^+$ -Chelex form. The first method was used for chelexing the 1.0 M KOH. The second method was for the K-BES buffer and the KPr.

To convert  $\text{Na}^+$ -Chelex to  $\text{H}^+$ -Chelex, 150-175 ml of  $\text{Na}^+$ -Chelex beads and 100 ml of 1.0 M HCl were mixed together in a beaker with a teflon stir bar for 10 minutes. This mixture was then allowed to settle. Once the chelex beads had accumulated on the bottom of the beaker, the HCl was poured out. This was repeated with another 100 ml of HCl. After the second removal of HCl, the chelex beads were washed by adding 100 ml of double distilled water then mixing for 10 minutes. The water was removed in the same manner as the HCl. The washing with water was then repeated.

The conversion of the  $\text{H}^+$ -Chelex to  $\text{K}^+$ -Chelex using the first method (for

chelexing KOH) required that the  $H^+$ -Chelex be added to the column after half of the wash water was removed. This addition was enough for the chelex to reach near  $3/8$  of the total column height. The top of the column was inserted into place and the  $H^+$ -Chelex in the column was allowed to settle forming a bed. Once settled, the water was pumped out by a peristaltic pump. The KOH was allowed to begin entering the column at a rate of 1 drop/second once the water level had dropped to a level above the Chelex where the dripping of incoming solution would land in the solution already in the column and not disturb the bed. It is important for the bed to not be disturbed once the solution has begun running through it because the ion exchange distribution would be altered somewhat changing the efficiency of contaminant removal. The KOH solution was allowed to run through the column while the pH was checked periodically. As the KOH was being run through the column the Chelex was turning from the  $H^+$  form to the  $K^+$  form from the top downwards which caused the chelex to increase in size. The portion of the chelex that was still in the  $H^+$  form can be seen as a much more white color. When this color was no longer present, the Chelex bed had grown to its maximum at approximately  $3/4$  of the total column height and the proper pH could be obtained. When the pH of the exiting chelexed solution was the same as the entering unchelexed solution it was collected and saved for use in subsequent solutions.

The conversion of the  $H^+$ -Chelex to  $K^+$ -Chelex using the second method (for chelexing K-BES and KPr) required the  $H^+$ -Chelex to be adjusted at a pH of 7.1 with chelexed KOH. The adjustment of the pH turns the resin to the  $K^+$ -Chelex form. Once the pH is adjusted, the  $K^+$ -Chelex can be poured into the column reaching around  $3/4$  of the total column height. The entering and exiting pH's should be very similar from the start because the solutions and chelex has already had the pH adjusted to near the same value (at or slightly below a pH of 7.1). Some of the first solution (K-BES) was allowed to run through before collecting to ensure it was indeed the chelexed 500 mM

K-BES that was exiting the column. The second solution was the KPr. Because it is undesirable to have any of the K-BES buffer in with the chelexed KPr, the KPr solution was allowed to run through the column for some time (allow up to 150 ml to go through) to ensure all of the K-BES has exited the column before collecting the pure chelexed KPr. Another option that can be used to avoid any possible K-BES contamination is to chelex the KPr in a separate column.

#### *4.2.2 Binding Constants*

The components of the skinning solutions are the following: KOH, KBES buffer, KPr, MgCl<sub>2</sub>, Na<sub>2</sub>ATP, Na<sub>2</sub>CP, DTT, H<sub>4</sub>EGTA, and CaCO<sub>3</sub>. In order to properly calculate the amount of free ions in the final solution, accurate binding constants for each free ion must be known at the selected pH, ionic strength, and temperature of the experiments. Each compound must be accounted for as the binding constants found from chemistry tables are measurements taken at 20°C and 0.1 M ionic strength (Martell & Smith 1974), which are different values than those used in this study. Proper binding constants for each compound must be converted to 26°C and 0.2 M ionic strength and can be seen in table 4-1. The importance of accounting for ionic strength, as it has effects on maximal force development, has been shown by Kentish (1984). This conversion was done by a computer program using the Van't Hoff equation for temperature adjustment and the Debye-Huckel equation for ionic strength adjustment as described by Harrison and Bers (1989). However, this was not done for binding constants between EGTA or ATP to K<sup>+</sup> and Na<sup>+</sup> or for constants between CrP and Ca<sup>++</sup> or Mg<sup>++</sup> because these did not make any difference in final calculations of free ion and ligand concentrations. This is described in detail in P. Backx's thesis (1989).

Once proper binding constants have been determined, the amount of each compound needed to make the final solutions was calculated to give the desired free ion

**Table 4-1**

Binding constants for metals and ligands from Martell and Smith (1974) corrected for temperature (26°C) and ionic strength (0.2 M), as described in the text.

Ligand & Metal	Log K 20°C, I <sub>s</sub> =0.1M	Log K 20°C, I <sub>s</sub> =0.2M
<b>EGTA</b>		
Ca <sup>++</sup> <sub>(1)</sub>	10.97	10.532
Ca <sup>++</sup> <sub>(2)</sub>	14.76	14.402
H <sup>+</sup> <sub>(1)</sub>	9.47	9.348
H <sup>+</sup> <sub>(4)</sub>	8.85	8.767
H <sup>+</sup> <sub>(3)</sub>	2.66	2.704
H <sup>+</sup> <sub>(4)</sub>	2.00	2.083
Mg <sup>++</sup> <sub>(1)</sub>	5.21	4.968
Mg <sup>++</sup> <sub>(2)</sub>	12.83	12.593
K <sup>+</sup>	0.96	0.960
Na <sup>+</sup>	1.38	1.380
<b>ATP</b>		
Ca <sup>++</sup> <sub>(1)</sub>	3.77	3.439
Ca <sup>++</sup> <sub>(2)</sub>	8.46	8.223
H <sup>+</sup> <sub>(1)</sub>	6.51	6.493
H <sup>+</sup> <sub>(2)</sub>	4.06	4.009
Mg <sup>++</sup> <sub>(1)</sub>	4.06	3.811
Mg <sup>++</sup> <sub>(2)</sub>	8.61	8.373
K <sup>+</sup>	1.00	0.900
Na <sup>+</sup>	1.20	1.200
CrP	1.15	1.150

concentrations. It was important to maintain a pH of 7.1 and ionic strength of 0.2 M, while also keeping the free  $[Mg^{++}]$  between 1.02 and 1.03 mM.

#### *4.2.3 Parent Solution*

Using a FORTRAN computer program provided by Dr. Jon Kentish, ionic strength, pH, and free ion concentration were determined by trial and error from the imputed binding constants and total ion and compound concentrations for KOH, KBES buffer, KPr,  $MgCl_2$ ,  $Na_2ATP$ ,  $Na_2CP$  (this program is described by P. Backx (1989)). This process was done for a solution containing  $Ca^{++}$  (activating solution) and a solution with no  $Ca^{++}$  (relaxing solution). There is only one difference in the amount of added constituents between the activating solution and relaxing solution. The relaxing solution must contain a greater amount of  $MgCl_2$ , to make up for the absence of  $Ca^{++}$ , in order to maintain a constant free  $[Mg^{++}]$  between the two solutions (1.02 to 1.03 mM). This solution, without the additional  $MgCl_2$ , is referred to as the parent solution. The additional  $MgCl_2$  is added to the  $K_2H_2EGTA$  solution described below. Once the ingredients are gathered, the parent solution is made up as a 1.25X stock solution. The final concentrations for the parent solution are listed in table 4-2.

The parent solution contains  $Na_2ATP$ ,  $Na_2CP$ , DTT,  $MgCl_2$  and chelexed K-BES buffer, and KPr in the amounts indicated in table 4-2. DTT was added to maintain muscle health (Jewell & Kentish 1981). Once all the ingredients were added, KOH was used to adjust the pH just below 7.1. The parent was solution stored at  $-20^{\circ}C$  for no longer than six months.

#### *4.2.4 EGTA Buffered Solutions*

EGTA is used as a  $Ca^{++}$  buffer but several problems can arise with the miscalculation of EGTA purity. Any errors in the actual [EGTA] will result in errors

**Table 4-2**

Parent Solution at 26°C

<b>Compound</b>	<b>[X]<sub>nominal</sub> (mM)</b>	<b>[X]<sub>1.25X Stock</sub> (mM)</b>	<b>in 200 ml Stock (g)</b>	<b>in 200 ml Stock (mL)</b>
Na <sub>2</sub> ATP	6.80	8.50	1.01337	
Na <sub>2</sub> CP	10.00	12.50	0.86275	
DTT	1.00	1.25	0.03855	
BES	100.00	125.00	(0.5M BES)	50.0
KPr	54.00	67.50	(1.0M KPr)	13.5
MgCl <sub>2</sub>	5.95	7.4375	(1.0MMgCl <sub>2</sub> )	1.4875
+ MgCl <sub>2</sub> *	0.51			

(\* this MgCl<sub>2</sub> is added to the H<sub>2</sub>K<sub>2</sub>EGTA solution as described in the text)

in the calculation not only of bound  $\text{Ca}^{++}$  but more importantly free  $\text{Ca}^{++}$  (Fabiato & Fabiato 1983). It is with this in mind that the purity of the EGTA used for the experiments presented here has already been determined (T. Nguyen 1994). The purity of the EGTA was found to be the same as stated on the label, 97%.

Two 50 mM EGTA solutions ( $\text{H}_2\text{K}_2\text{EGTA}$  and  $\text{K}_2\text{CaEGTA}$ ) were made as follows. The  $\text{H}_2\text{K}_2\text{EGTA}$  solution was free of  $\text{Ca}^{++}$ . It was composed of 50.0 mM  $\text{H}_4\text{EGTA}$  dissolved in water adjusting the pH is at 7.0 with KOH. The additional  $\text{MgCl}_2$  that wasn't added to the parent solution, was added to this  $\text{H}_2\text{K}_2\text{EGTA}$  solution. The  $\text{K}_2\text{CaEGTA}$  solution consisted of 50.0 mM  $\text{H}_4\text{EGTA}$  and 50.0 mM  $\text{CaCO}_3$  dissolved and pH fixed at 7.0 with KOH. The formulation of  $\text{K}_2\text{CaEGTA}$  required more KOH to achieve a pH of 7.0 than was necessary for  $\text{H}_2\text{K}_2\text{EGTA}$ . This is because the added calcium displaces  $\text{H}^+$  from EGTA (Fabiato & Fabiato 1983). These solutions were set aside to be mixed with the parent solution, or stored at  $-20^\circ\text{C}$  for up to six months.

#### *4.2.5 Activating, Relaxing, and Skinning Solutions*

Now all of the basic solutions had been made and only the final combinations and the pH adjusting to 7.1 were left to do. There were three main groups of solutions that were used directly on the muscle: relaxing, activating, and skinning solutions. The basic two components in each of these solutions were an EGTA solution and parent solution mixed in a 1:4 ratio. The relaxing solution was essentially one part (i.e., 10 ml)  $\text{H}_2\text{K}_2\text{EGTA}$  solution mixed with four parts (40 ml) parent solution. The activating solution was then made with one part  $\text{K}_2\text{CaEGTA}$  and four parts parent solution. The skinning solution was just relaxing solution with 1% by volume Triton-X 100 added. Once these solutions were made, the final pH was fixed with KOH to 7.1. The final concentrations in the relaxing and activating solutions are listed in table 4-3. The

**Table 4-3**

Calculated ion and substrate concentrations for the final solutions made after Parent solution has been combined with  $\text{H}_2\text{K}_2\text{EGTA}$  (to make Relaxing solution) or  $\text{K}_2\text{CaEGTA}$  (to make Activating solution).

Substrate Metal or Ligand	[Relaxing] Total (mM)	[Relaxing] Free (mM)	[Activating] Total (mM)	[Activating] Free (mM)
BES <sup>-</sup>	100.00	0	100.00	52.93
HBES		47.07		47.07
EGTA <sup>-4</sup>	10.00	0.001	10.00	0.00001
Ca <sup>+2</sup>	00.00	0.00	10.00	0.029
ATP <sup>-4</sup>	6.80	0.71	6.80	0.705
Mg <sup>+2</sup>	6.46	1.03	5.95	1.031
Cl <sup>-</sup>	12.92	12.92	11.90	11.900
MgATP <sup>-</sup>		4.74		4.700
Propionate <sup>-</sup>	54.00	53.77	54.00	53.775
K <sup>+</sup>	140.00	139.21	140.00	139.221
Na <sup>+</sup>	33.60	33.23	33.60	33.229
HCP <sup>-2</sup>	10.00	9.80	10.00	9.795
DTT	1.00	1.00	1.00	1.000
Ionic Strength	208.84		208.35	
Ionic equiv.	174.95		174.54	
Net Charge	-0.00096		+0.000058	
pH	7.1		7.1	

**Table 4-4**

Divalent cation content of each  $\text{Ca}^{++}$  solution used to generate force- $\text{Ca}^{++}$  relations.

AS ( $\mu\text{L}$ )	RS ( $\mu\text{L}$ )	$[\text{Ca}^{++}]_{\text{total}}$ (mM)	$[\text{Ca}^{++}]_{\text{free}}$ ( $\mu\text{M}$ )	pCa	$[\text{Mg}^{++}]_{\text{total}}$ (mM)	$[\text{Mg}^{++}]_{\text{free}}$ (mM)
1000*	0	12.5	1063.28	2.787	5.950	1.467
1000	0	10.00	36.200	4.441	5.950	1.046
975	25	9.75	13.459	4.871	5.963	1.036
900	100	9.00	3.591	5.445	6.001	1.036
800	200	8.00	1.611	5.793	6.052	1.041
750	250	7.50	1.210	5.918	6.078	1.043
600	400	6.00	0.606	6.218	6.154	1.051
0	1000	0.00	0.000	0.000	6.460	1.079

\* 2.5 mM  $\text{CaCl}_2$  was added to the activating solution

relaxing and activating solutions were then divided in half. One half was set aside and the other half was used to add 30  $\mu\text{M}$  CPA. Now there was one activating and one relaxing solution for the control group and one of each for the CPA group.

#### *4.2.6 $\text{Ca}^{++}$ Solutions*

These are a sub set of solutions made from the activating and relaxing solutions that will be exposed to the muscle to obtain the force- $[\text{Ca}^{++}]$  relations. Activating, with 10.0 mM total  $\text{Ca}^{++}$ , and relaxing solution, with zero  $\text{Ca}^{++}$ , were combined in various proportions to get different  $[\text{Ca}^{++}]$ 's. The combinations of activating and relaxing solutions are listed in table 4-4, with the corresponding free-ion concentration of  $\text{Ca}^{++}$  and  $\text{Mg}^{++}$ . This procedure was repeated for the relaxing and activating solutions containing CPA.

#### *4.2.7 Protocol*

First, a very small and thin muscle was dissected and mounted in the apparatus (described in chapter 2). It was then exposed to the skinning solution for 20-25 minutes at 26°C. After this time the muscle was washed with relaxing solution and then stretched to a resting sarcomere length of 2.15  $\mu\text{m}$ . It is important to note that only resting sarcomere length was controlled for since, during contraction, the muscle pulled against the compliant ends of the preparation which allowed for some shortening. The muscle was activated by replacing the relaxing solution with an activating solution of a given level of free  $\text{Ca}^{++}$ . Once the force reached a steady state plateau, the activating solution was washed out of the bath, replaced with relaxing solution and the force declined. This procedure was repeated for each free  $[\text{Ca}^{++}]$ . A series of 6 muscles were used for the control and another 6 muscles were used with 30  $\mu\text{M}$  CPA in the activating solutions. In generating data for each series of solutions (control and CPA), it was

much more practical to do each series in a different muscle. This avoided any potential problems with CPA contamination as well as experimental run down effects. Force and sarcomere length records were measured from a chart recorder. The forces were normalized to maximal force obtained at  $1.06 \mu\text{M}$  free  $\text{Ca}^{++}$ .

#### *4.2.8 Curve Fitting*

The data obtained using control and CPA solutions were plotted as force- $[\text{Ca}^{++}]$  relations, where  $[\text{Ca}^{++}]$  is plotted on a log scale. The equation for the best fit through the data comes from a modified form of the Hill equation. Values from this equation ( $n$ ,  $\text{EC}_{50}$ ,  $F_{\text{max}}$ ) are averaged from five individual experiments and listed with standard error of the mean in table 4-5 for both control and CPA conditions. This equation is discussed in detail in chapter 2.

### **4.3 Results**

As the muscle was being exposed to the skinning solution, the first-order diffraction pattern indicating sarcomere length became very clear and well defined, as described by Kentish et al. (1986). Force development in activating solution are seen in figure 4-1. These tracings are typical for a control condition (figure 4-1A) and with  $30 \mu\text{M}$  CPA (figure 4-1B). When the muscle was exposed to an activating solution, force rose rapidly until a plateau was reached. Force decline to resting values occurred when the activating solution was replaced with relaxing solution. The force- $[\text{Ca}^{++}]$  relations obtained from both control and  $30 \mu\text{M}$  CPA solutions were fit nicely with the modified Hill equation, seen in figure 4-2A. It is quite obvious that CPA did not have any effect on the myofilaments, even when plotted in a linearized Hill form (figure 4-2B). This is numerically indicated by the lack of statistical significance, at the 95% confidence level, from control to CPA solutions for modified Hill equation parameters

**Figure 4-1: Skinned Fiber Force Tracings**

Force tracings under control conditions (A), and in the presence of 30  $\mu\text{M}$  CPA (B) at free  $[\text{Ca}^{++}]$ 's of 1063.3, 36.2, 13.5, and 3.6  $\mu\text{M}$ . The ticks in the time tracing represent 10 seconds.

**A**



**B**

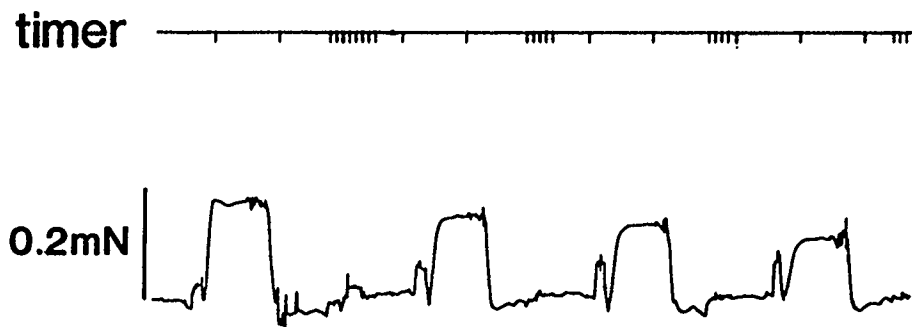
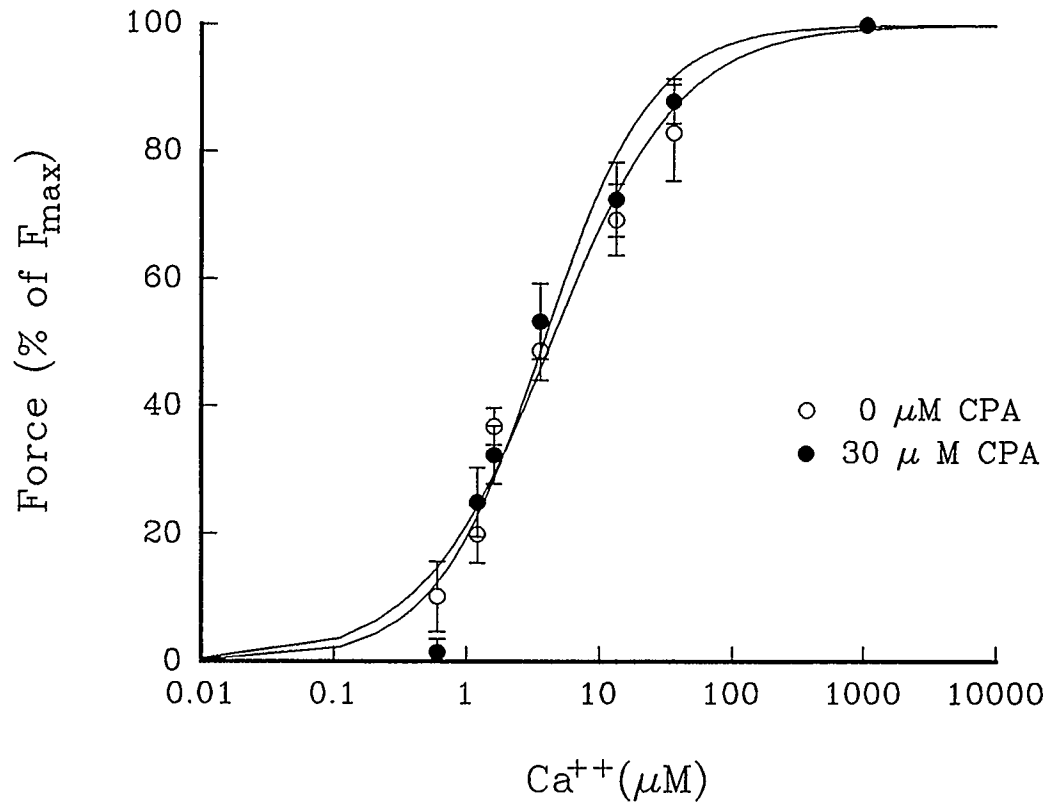


**Figure 4-2: Force-[Ca<sup>++</sup>] Relations in Skinned Fibers**

Force-[Ca<sup>++</sup>] relations from control and 30  $\mu$  M CPA solutions fit with the modified Hill equation (A). A linearized version of the data points with regression lines through the data. The point from the CPA solutions at the lowest [Ca<sup>++</sup>] is not included in the regression. All data are expressed as mean $\pm$ sem (n=5).

A



B

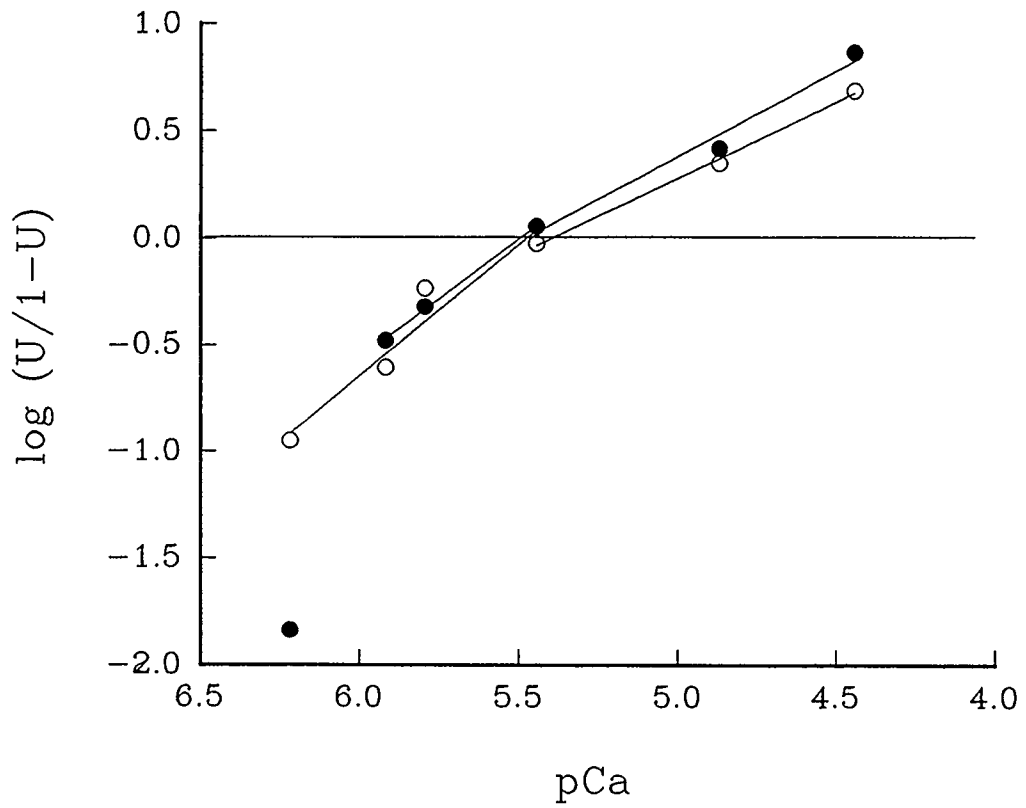


**Table 4-5**

Parameters from the modified Hill equation listed as averaged values with standard error of the mean, taken from figure 4-2. (The modified Hill equation is described in detail in chapter 2).

	$n$	EC <sub>50</sub> (μM)	F <sub>max</sub>
Control	0.89±0.13	4.33±0.62	52.3±17.5
30 μM CPA	1.07±0.18	3.79±0.92	49.7±10.94
$p$ value*	0.1	0.3	0.8

(\* significant difference if  $p < 0.05$ )

in  $n$ ,  $EC_{50}$ , or  $F_{max}$  values. These numbers are listed in Table 4-4, with their corresponding  $p$  values.

#### 4.4 Discussion

The force- $[Ca^{++}]$  relations found for the control and 30  $\mu$ M CPA (figure 4-2) indicate that CPA does not affect the steepness (co-operativity), the  $EC_{50}$  ( $Ca^{++}$  binding properties) nor the  $F_{max}$  (maximum force generating capacity) of the myofilaments. Despite the contrary results obtained in skeletal muscle, it can be concluded from this study that the use of 30  $\mu$ M CPA in cardiac muscle can be confidently used as a tool to block the  $Ca^{++}$ -ATPase and therefore eliminate the SR while trying to quantify the muscle's contractile activities.

The results of this study are not consistent with those found in both fast- and slow- twitch skinned skeletal muscle, where changes in the maximum force development (Huchet & Leoty 1993) as well as  $EC_{50}$  were observed (Kurebayashi & Ogawa 1991, Huchet & Leoty 1993) with [CPA] from 10 to 100  $\mu$ M. A possibility for the different findings is the amount of DMSO (solvent for CPA) in the solutions. In the experiments of Huchet and Leoty (1993), it was stated that DMSO did not exceed 0.5%, with Kurebayashi & Ogawa (1991) not exceeding 0.1%. These values are extremely high when looking at the decline in force with increasing DMSO content in the solution (chapter 2 section 2.8.3, figure 2-3A). In all of the experiments presented here, care was taken to not exceed 0.01% DMSO in any of the solutions. As seen in (figure 2-4, from chapter 2), excess DMSO in the solution can have substantial consequences on force production. A possible mechanism for this could involve an effect directly on the myofilaments. Any alterations in the  $Ca^{++}$  binding properties of the myofilaments or contractile activity with CPA could be seen here. Since no changes were seen with the addition of DMSO and CPA, then it can be concluded that the myofilaments are

unaffected and the steady state force- $\text{Ca}^{++}$  relations in any subsequent experiments presented in this thesis in the intact muscle are the result of all the innate cellular properties contributing to the generation of force and  $\text{Ca}^{++}$  handling in each cell.

#### **4.5 Summary of Findings**

The addition of 30  $\mu\text{M}$  CPA does not alter myofilament sensitivity in rat trabeculae. The assessment of cardiac myofilament sensitivity changes, in the presence of CPA, has not been previously reported in the literature.

#### **4.6 Potential Source of Errors**

As mentioned earlier, resting sarcomere length was controlled, but the amount of internal shortening during activation could vary due to the presence of elastic elements in series with the contractile elements (most notably the portion of the tricuspid valve used to hook on to the motor arm). This potential for error was minimized by choosing muscles that were very similar in size and cutting the valve portion as small as possible for each muscle. In addition, force measurements in these experiments were presented with a large standard error of the mean. The nonuniformity of many of the muscles used in these experiments made accurate measurement of cross-sectional area difficult and therefore resulted in large variances in stress measurements.

## Chapter 5

### Diastolic Fluorescence Measurements Before and After Fura-2 Loading

#### 5.1 Introduction

The use of calcium indicator dyes has provided a means to measure the intracellular calcium ( $[Ca^{++}]_i$ ) under a variety of conditions (Grynkiewicz et al. 1985). These dyes provide a direct evaluation of  $[Ca^{++}]_i$  as well as providing some information regarding the kinetics of the  $Ca^{++}$  movements through the cytosol. The dyes currently available that are most advantageous to  $[Ca^{++}]_i$  measurements are Indo-1 and Fura-2. These fluorescent indicators offer a  $Ca^{++}$  binding stoichiometry of 1:1, have a high signal to noise ratio, and offer an isosbestic point to minimize movement artifact and complications with dye loss (Grynkiewicz et al. 1985).

The experiments presented here were done using the  $Ca^{++}$  indicator dye Fura-2 in its salt form. The following properties of Fura-2 have been previously described in detail by Grynkiewicz et al. (1985). The quantum yield (0.49) allows a relatively low amount of dye to be used and still receive a large fluorescent signal. When Fura-2 binds to  $Ca^{++}$ , the intensity of fluorescence emission at 510 nm shifts from a minimum at 380 nm to a maximum at 340 nm. By measuring the emitted fluorescence at such a high wavelength (510 nm), the interference in the signal by autofluorescence (the intrinsic fluorescence of the preparation in the absence of any dye) is small since autofluorescence emits maximally around 450-460 nm (Gueth & Wojciechowski 1986, White & Wittenberg 1993). An isosbestic point at 360 nm is useful when the absolute amount of Fura-2 in the preparation is desired and not fluorescent changes associated with  $[Ca^{++}]_i$ . The fluorescence measured at the isosbestic point is insensitive to  $Ca^{++}$ . In addition, Fura-2 binds  $Ca^{++}$  much more avidly than to  $Mg^{++}$ .

It is the purpose of this chapter to establish the conditions of the muscle

preparation prior to and after loading of Fura-2. Prior to Fura-2 loading, it is important to accurately measure the autofluorescence of the muscle, which can vary between muscles. After Fura-2 is injected into the muscle preparation, it is important to evaluate that the dye did indeed enter the cells and responds to  $\text{Ca}^{++}$  fluxes associated with the twitch. In addition, it is important to monitor the condition of both the dye and the muscle throughout the duration of the experiment. Leakage of dye over the course of the experiment is common (Roe et al. 1990), but too little dye can result in an undesirable reduction in the signal to noise ratio. Over the course of the experiment it is also important to evaluate the health of the muscle. One valuable parameter is the ratio of fluorescence at 340 and 380 nm during diastole, which indicates an amount of  $[\text{Ca}^{++}]_i$  during the muscle's "rest" period. If this ratio (and therefore the  $[\text{Ca}^{++}]_i$ ) increases, then it is likely that the muscle is deteriorating.

## **5.2 Methods**

### *5.2.1 Muscle Preparation*

Trabeculae were dissected and mounted in the apparatus, as described in chapter 2. Each of the trabeculae was first stimulated at 1 Hz and allowed to equilibrate for 30-45 minutes at 26°C in HEPES buffered solution with 0.5 mM  $\text{Ca}^{++}$ . The procedure used to measure autofluorescence, inject the dye into the muscle, and record fluorescence values have all been described in chapter 2 (section 2.3).

### *5.2.2 Measurement of Muscle Fluorescence*

After the muscle has equilibrated, the HEPES solution superfusing the muscle is changed to one containing 0.2 mM  $\text{Ca}^{++}$  and 30  $\mu\text{M}$  CPA. After 10 minutes, the muscle's autofluorescence was recorded at each wavelength (340, 360, and 380 nm). Fura-2 was then injected into the muscle preparation for 15-30 minutes (time is

dependent on muscle size). After a sufficient amount of Fura-2 has been loaded into the muscle, the muscle was stimulated at 1 Hz until a steady level of force was achieved (approximately 5 minutes), then 0.2 Hz stimulation was resumed. It was after the muscle was again stimulated at 0.2 Hz that Fura-2 fluorescence measurements were taken.

### *5.2.3 Measurement of Fura-2 Dye Leakage*

The dye loss through the course of the experiment was determined by plotting the fluorescence at each wavelength over the time course of the experiment. The duration of each experiment was approximately 30 minutes. The fluorescence values were taken at the end of the 5 second interval (since the muscle is stimulated at 0.2 Hz). In figure 5-5, this period can be seen as the one second interval just prior to the initiation of the tetanus. The fluorescence was averaged by selecting this 1 second interval using a computer program created in our laboratory.

### *5.2.4 Measurement of Diastolic Ratios*

The diastolic ratios were measured in the same manner as described for Fura-2 dye leakage. The only difference is that each value presented in figure 5-3A&C, showing fluorescence values for 340 and 380 nm, are ratioed (340/380 nm). These ratios were then converted to an estimated  $[Ca^{++}]_i$  value using the calculations described by Grynkiewicz et al. (1986) and discussed in chapter 2 (section 2.3.5). The ratio of 340/380 nm is independent of the absolute amount of dye in the muscle, so it is unaffected by dye leakage.

### *5.2.5 Twitch and Tetanus*

Twitches were elicited at a rate of 0.2 Hz. To initiate a tetanic contraction,

stimuli (20-40 ms duration) are administered at a rate of 12-15 Hz for a period of 2.5 to 4.7 seconds. These parameters are adjusted for each muscle to optimize the achievement of a steady state as judged by the shape of the force tracing. A detailed description of the means to elicit twitches and tetani in the set-up used here can be found in chapter 2.

### **5.3 Results**

#### *5.3.1 Autofluorescence*

The autofluorescence of each trabecula is measured prior to Fura-2 loading. It was important to obtain accurate autofluorescence values, at each wavelength, prior to loading of the dye, Fura-2, so that it can be properly subtracted from the fluorescence signal of the dye. The autofluorescence was taken at a medium length (passive sarcomere length = 2.15  $\mu\text{m}$ , n=14), and at a short length (passive sarcomere length = 1.90  $\mu\text{m}$ , n=7), as shown in figure 5-1. The autofluorescence taken at the medium length was used to subtract from fluorescence measurements taken at medium and long lengths (passive sarcomere length = 2.30  $\mu\text{m}$ ). The autofluorescence taken at the short length was used to subtract from fluorescence measurements taken at the short length. However, there were no significant differences between the two lengths in autofluorescence values at each wavelength.

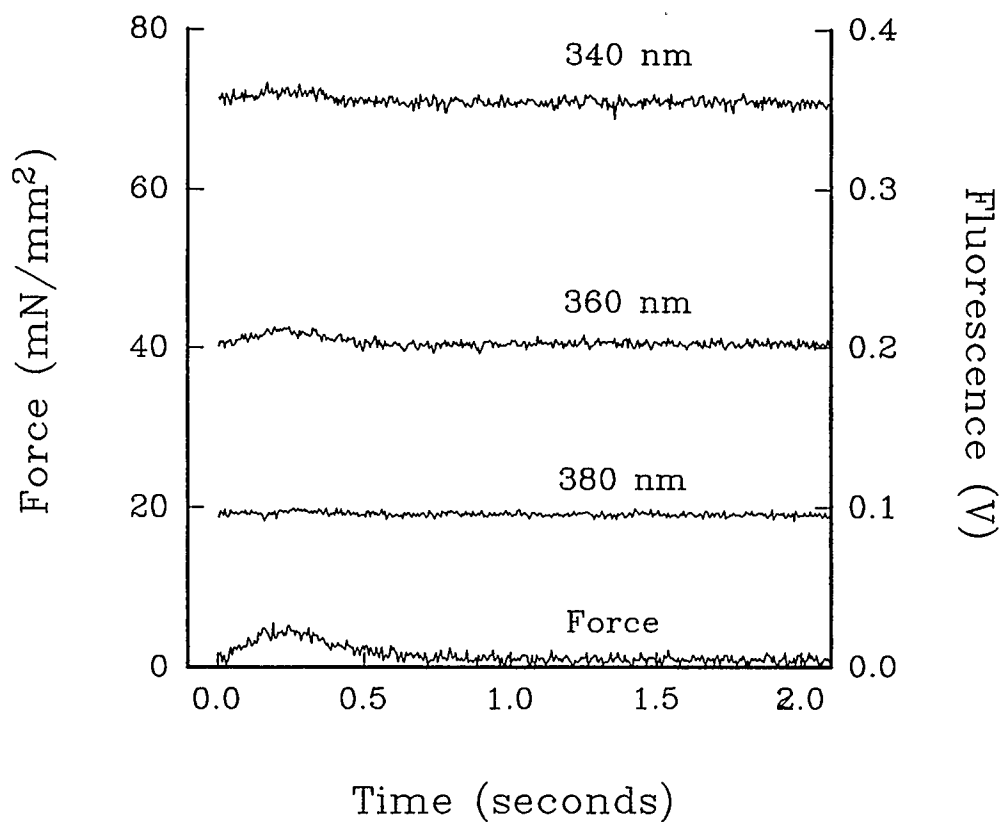
#### *5.3.2 Dye Fluorescence*

The muscle's emitted fluorescence taken at each wavelength (340, 360, and 380 nm) from one typical experiment is shown in figure 5-2. The fluorescence was measured before and after Fura-2 loading. Each fluorescence measurement is accompanied with its corresponding twitch force. Two twitches are shown in each graph, indicating the force transient before and after Fura-2 injection. A substantial reduction in force and

**Figure 5-1:** Autofluorescence at 340, 360, and 380 nm

Autofluorescence at 340, 360, and 380 nm are shown with their corresponding force tracing for the short sarcomere length (A), and the long length (B). These are taken from two separate experiments.

A



B

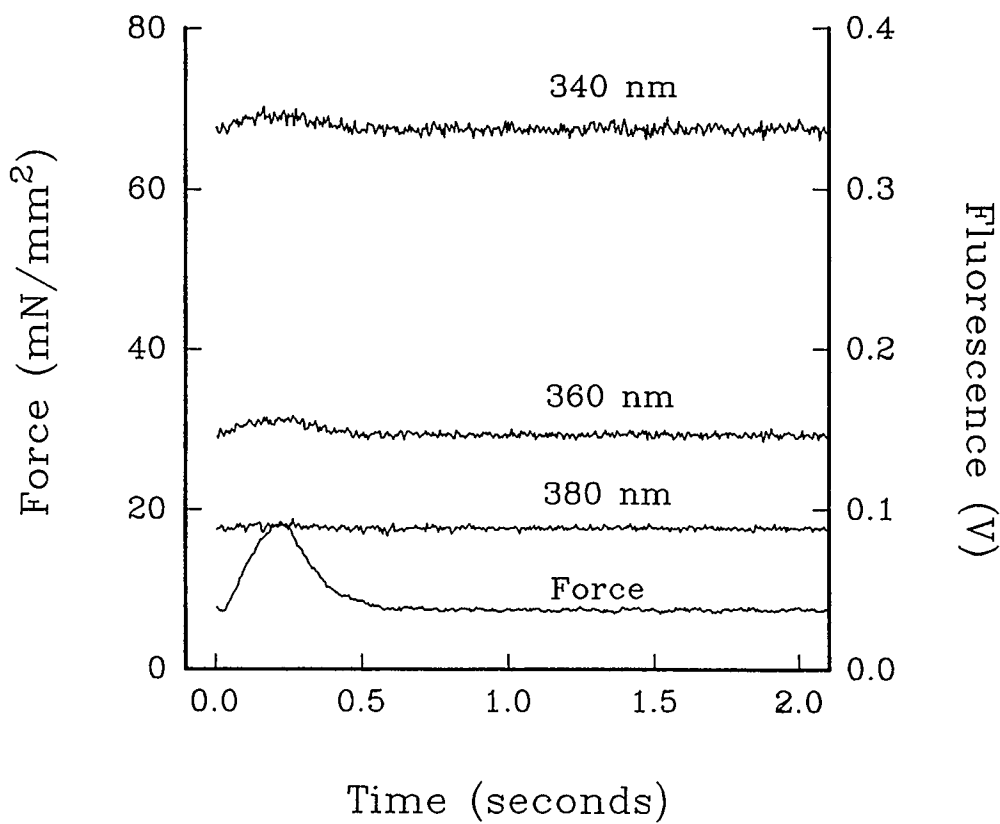
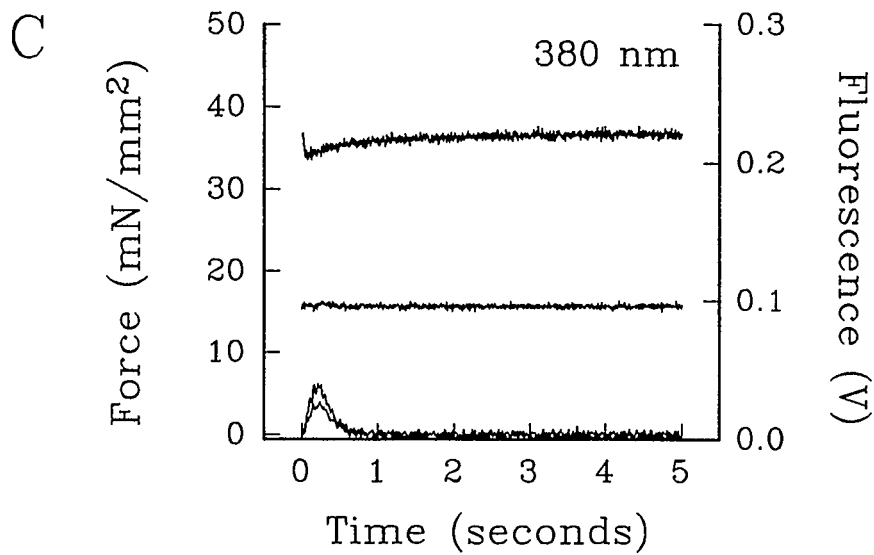
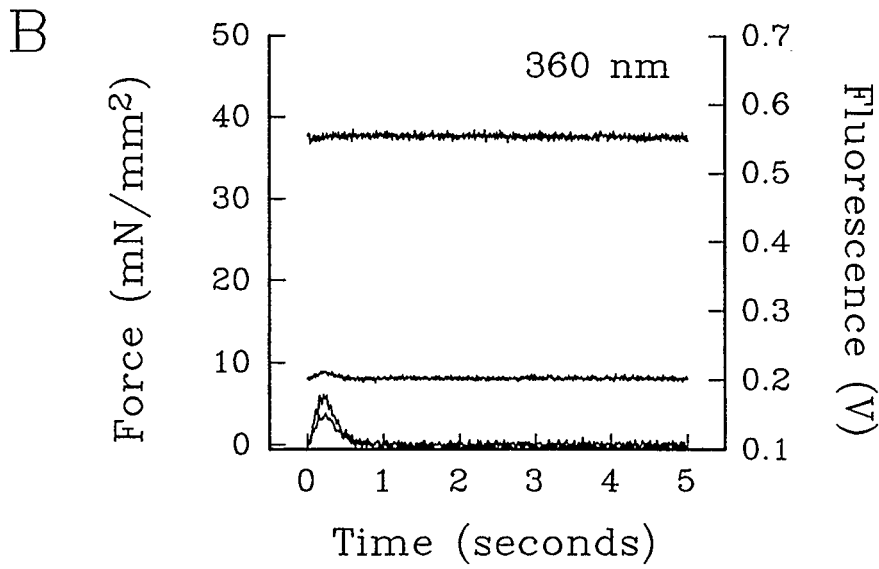
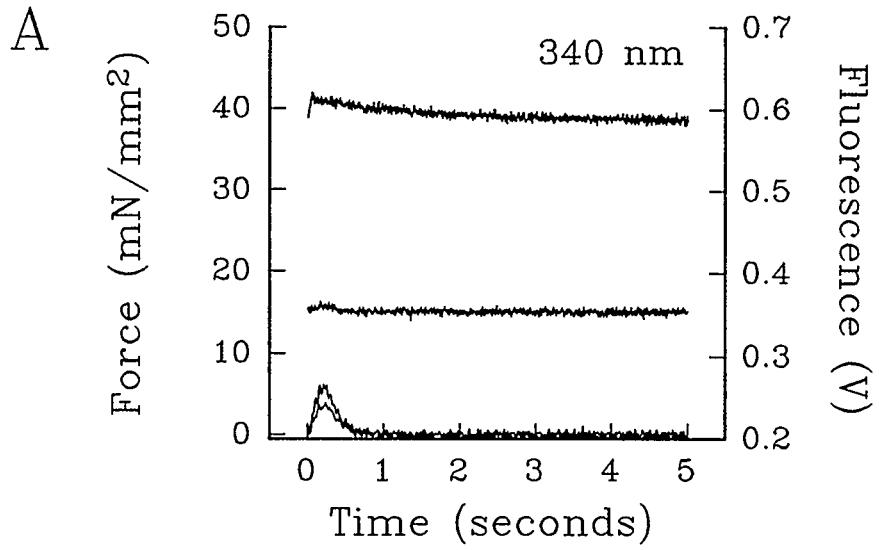


**Figure 5-2:** Autofluorescence and Fura-2 Fluorescence at 340, 360, and 380 nm

Autofluorescence and Fura-2 fluorescence at 340 (A), 360 (B), and 380 (C) nm are shown with their corresponding force tracing for the short sarcomere length. These tracings are from one typical experiment.



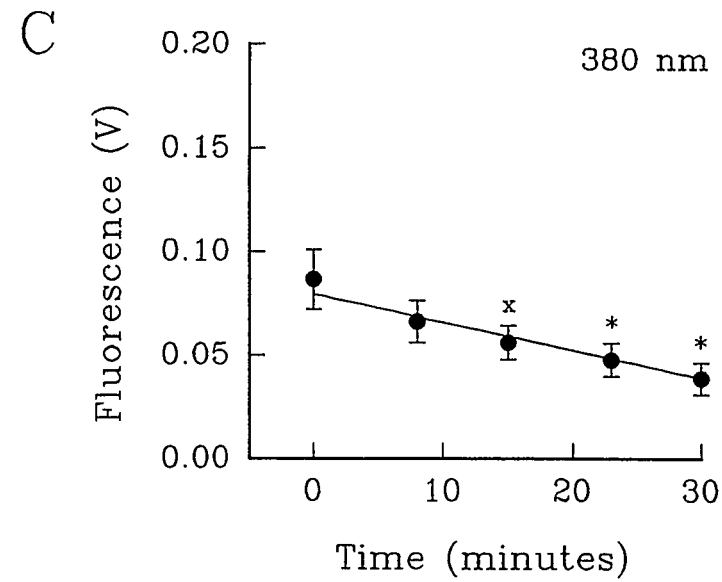
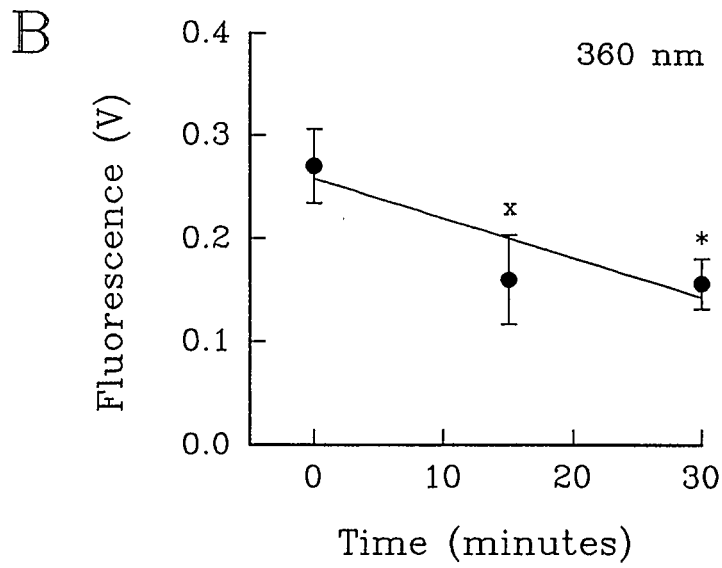
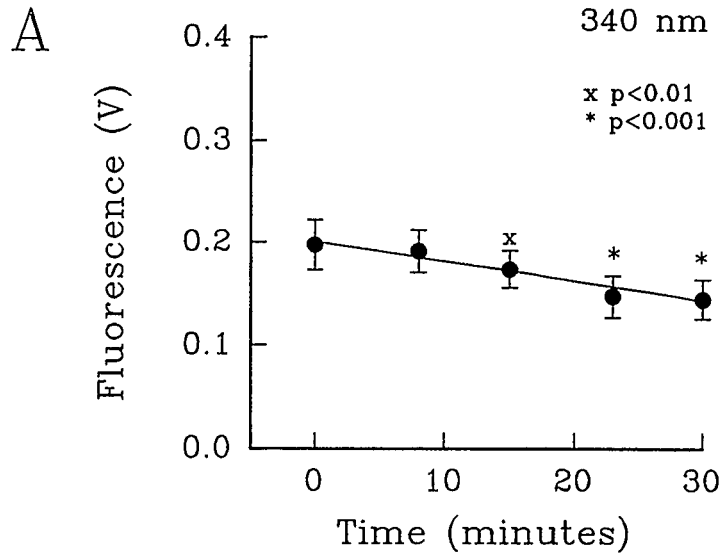
prolongation of relaxation relative to peak force production is apparent in one of the twitches from each graph. This twitch is taken after Fura-2 injection and reflects the effect on the muscle of cyclopiazonic acid (CPA), which is discussed in detail in chapter 3. It is apparent, for each wavelength, that the fluorescence level was dramatically increased after loading of the dye. The measured fluorescence after Fura-2 loading for 340 and 380 nm are marked by the presence of a waveform that is different in shape than the signal seen in the autofluorescence measurement. The waveform measured with Fura-2 is the fluorescence emitted from the dye due to  $\text{Ca}^{++}$  binding. The 340 signal shows a rapid initial rise then a slower decline back to baseline levels. The  $\text{Ca}^{++}$  transient waveform for the 380 nm signal is a rapid initial downward deflection with a slow rise back to baseline levels. There is not much change in the 360 nm signal from before to after loading of the dye except a slight modification in the movement artifact which is associated with the change in shape of the twitch force.

### *5.3.3 Dye Leakage*

Once the dye has been loaded into the muscle, the muscle was allowed a few minutes to equilibrate immediately followed by the experimental protocol. Quick execution of the protocol and proper design of the protocol minimizing the muscle's exposure to the UV light provided a larger fluorescence signal from the dye and a signal more representative of the  $[\text{Ca}^{++}]_i$  transient. These two requirements of the protocol (short overall duration and minimal UV exposure) were made because dye leakage out of the muscle over time could have reduced the signal to noise ratio in the recorded measurement (Roe et al. 1990, Tsien 1989) and long exposure to UV light could bleach the dye causing the bleached Fura-2 molecules to form an intermediate that still fluoresces regardless of the  $[\text{Ca}^{++}]_i$  levels (Becker & Fay 1987). The reduction in baseline levels of Fura-2 over the course of the experiment is represented in figure 5-3 at each

**Figure 5-3: Decline of Fura-2 Fluorescence Over Time for 340, 360, and 380 nm**

The decline of Fura-2 fluorescence at 340 (A), 360 (B), and 380 (C) nm are displayed over the time course of a typical experiment. There were no statistical differences between the slope of the regression lines through each set of data, expressed as mean  $\pm$  standard error of the mean (n=9).



wavelength. Although the total amount of dye loaded into each individual muscle varies, the relative decline in the signal with estimated time shows a similar pattern. The slope of the line fit through data points, from nine experiments, for each wavelength indicated the rate of dye loss at  $-1.9 \pm 0.8$  mV/min for 340 nm,  $-3.8 \pm 1.3$  mV/min for 360 nm, and  $-1.4 \pm 0.3$  mV/min for 380 nm (value of fluorescence is expressed as millivolts). There were no significant differences between the rate of dye loss at any of the wavelengths.

#### *5.3.4 Diastolic 340/380 Ratios*

Resting fluorescence ratios (340/380 nm) from trabeculae between stimulations (i.e., during diastole) are presented in figure 5-4. The points included in this figure are from both short and long lengths. In accordance with previous observations by P. Backx (1989), there were no differences between diastolic ratios at short and long sarcomere lengths. Diastolic ratios range from  $2.34 \pm 0.13$  at 0.25 mM  $[Ca^{++}]_o$  to  $2.62 \pm 0.18$  at 8.0 mM  $[Ca^{++}]_o$ , corresponding to  $[Ca^{++}]_i$  levels from 88.0 nM to 110 nM. However, as  $[Ca^{++}]_o$  increased to 16.0 mM, the resting  $R_{340/380}$  showed a significant ( $p < 0.05$ ) increase above values at 0.25 mM. This corresponded to contracture development when tetani were initiated. Therefore, no further data will be presented from measurements taken at this  $[Ca^{++}]_o$ .  $[Ca^{++}]_i$  estimates are found to be similar to previously reported values observed in resting myocytes by Spurgeon et al. (1992). As  $[Ca^{++}]_o$  in the presence of CPA (SR pump inhibitor) increased from 0.25 mM to 8.0 mM, there was no significant increase in the 340/380 ratio, suggesting the muscles large capacity to regulate  $[Ca^{++}]_i$  even under conditions of a compromised SR.

#### *5.3.5 Twitch and Tetanus*

Once autofluorescence has been accounted for and Fura-2 has been loaded into

**Figure 5-4: Resting Fura-2 Fluorescence**

Resting Fura-2 fluorescence ratios ( $R_{340/380}$ ) are displayed for  $[Ca^{++}]_o$  from 0.25 to 16.0 mM. There is a statistical differences between the data points of 0.25 and 16.0 mM  $[Ca^{++}]_o$ . The data are expressed as mean  $\pm$  standard deviation to show the spread in the data (n=9).

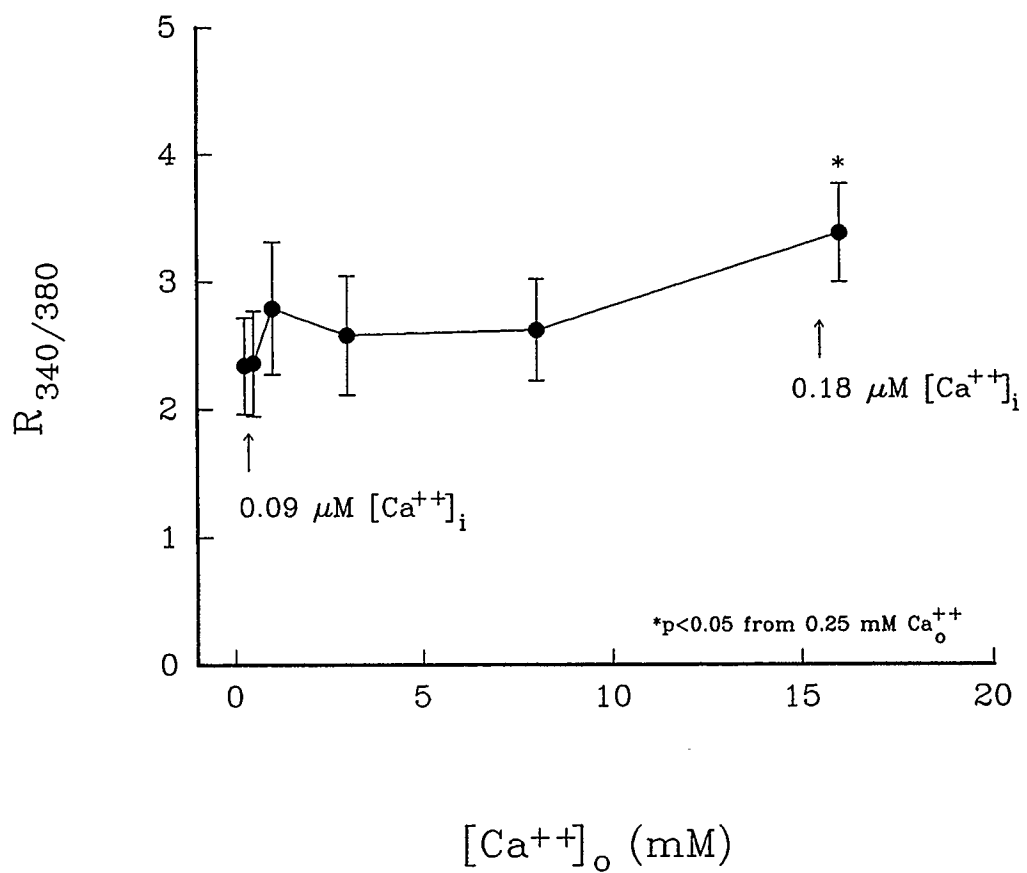
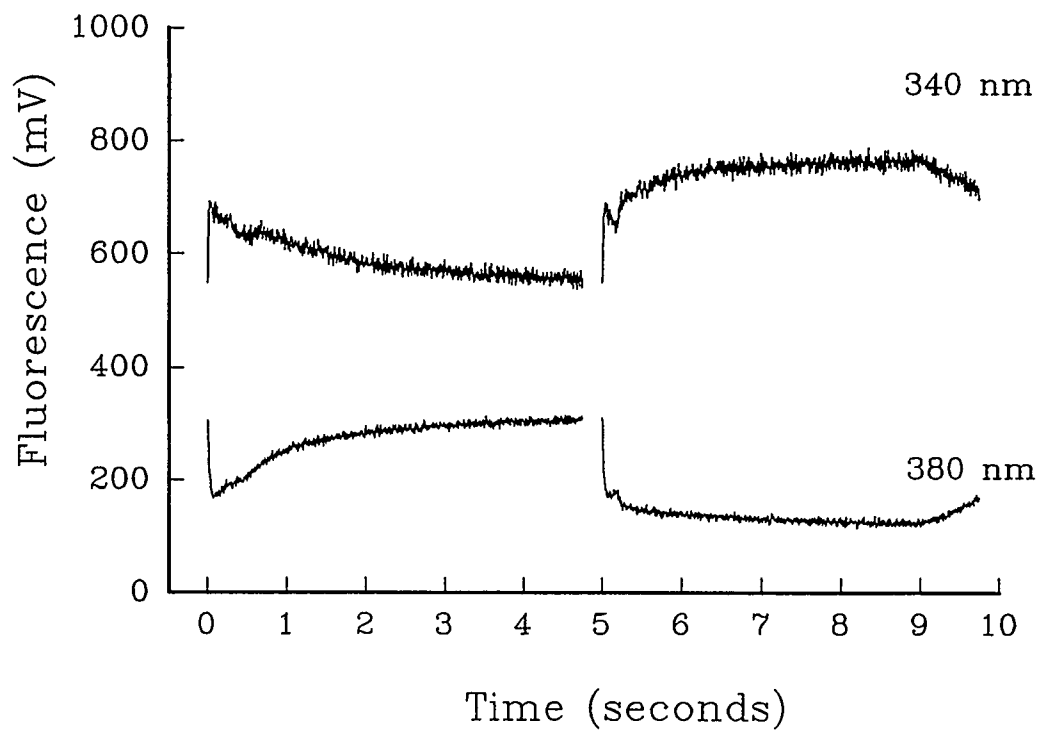
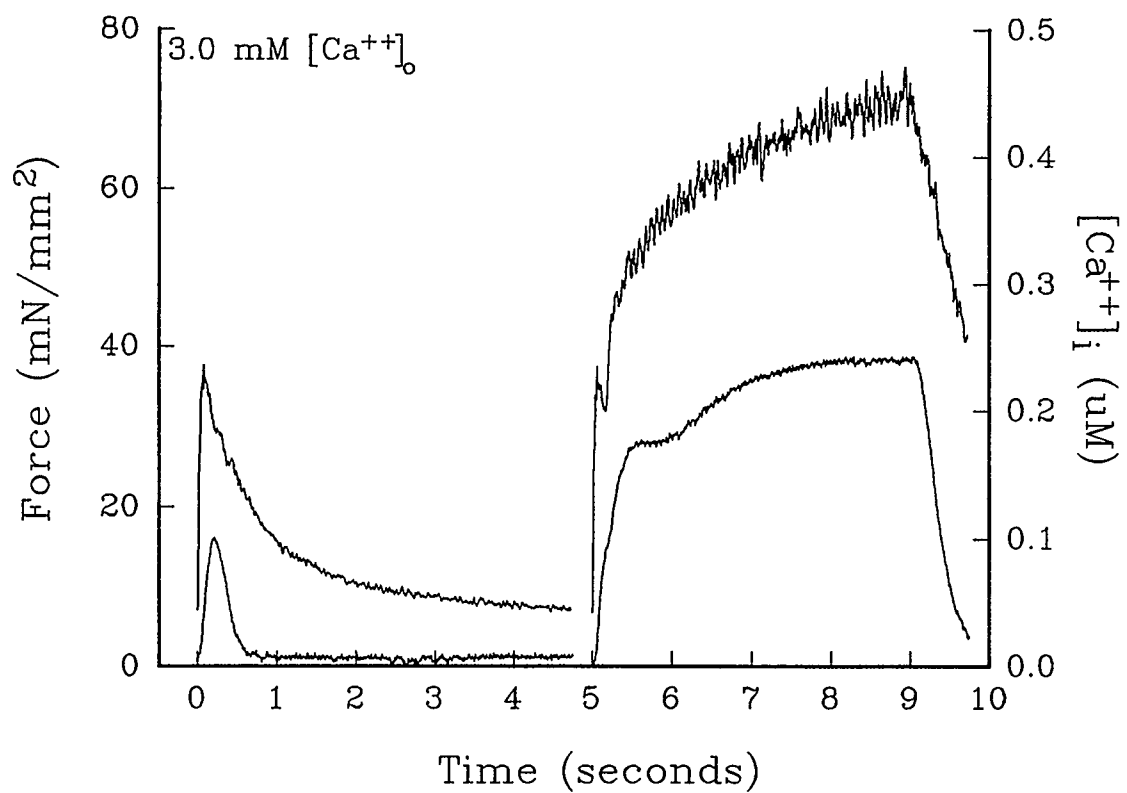


**Figure 5-5:** Force, Fluorescence, and Estimated  $[Ca^{++}]_i$  for the Twitch and Tetanus

Twitch and tetanic force accompanied by their corresponding  $[Ca^{++}]_i$  tracing (A), estimated by conversion of the 340/380 nm signal. Time course of the 340 and 380 nm signal (B). Tracings are from one experiment at 1.6 mM  $[Ca^{++}]_o$ .



the preparation, measurements of fluorescence ratios can be made and estimations of  $[Ca^{++}]_i$  levels can be made under a variety of interventions. Force tracings with corresponding, estimated,  $[Ca^{++}]_i$  values can be seen in figure 5-5. The forces presented are from a twitch, in the presence of CPA, followed by a tetanic contraction (elicited by 12 Hz stimuli, 40 ms duration) with 8.0 mM  $[Ca^{++}]_o$ . This is taken from one representative experiment recorded at the short sarcomere length. A discussion regarding force changes in the twitch and tetanus can be found in chapter 3. The time course of the fluorescence signal, and therefore  $[Ca^{++}]_i$ , closely precedes the force tracing. Notice that at the later portion of the tetanus, a steady state level of force is reached accompanied by a steady state level in the fluorescence. It is this portion of the tetanus that is used in the measurements presented in chapter 6.

## 5.4 Discussion

### 5.4.1 *Autofluorescence*

The values of autofluorescence, for each muscle, is crucial in order to obtain accurate recordings of Fura-2 fluorescence at each wavelength. Therefore, prior to injection of Fura-2 into a muscle, the fluorescence of the muscle alone is measured, which is used later to subtract from the Fura-2 fluorescence before ratioing 340/380 nm. There is no significant difference between muscle lengths or cross-sectional area with regard to autofluorescence.

### 5.4.2 *Dye Fluorescence*

During the time the autofluorescence measurements were taken and the Fura-2 was loaded into the muscle, the muscle was exposed to CPA which altered the shape of the twitch force. Buffering of  $[Ca^{++}]_i$  by Fura-2 in the cytosol with corresponding force reductions have been previously observed (Backx 1989). However, force reductions

resulting from Fura-2 in the cytosol are unlikely due to improved Fura-2 loading techniques (Banijamali 1994). Therefore, force changes from before to after Fura-2 loading are a result of CPA on the SR, as discussed in chapter 3. However, the movement artifact associated with the twitch did not change much and therefore was not considered to be a problem. The increase in fluorescence intensity after the addition of Fura-2 is quite prominent. The signal from 340 nm shows an abrupt increase after stimulation of the muscle and before the increase in force. The signal from 380 nm shows an abrupt decrease after the stimulation with the same time course as the 340 nm signal. The ratio of 340/380 nm is proportional to  $[Ca^{++}]_i$ , and is insensitive to absolute levels of the dye in the muscle (Grynkiewicz et al. 1985). This is important since the amount of dye injected into each muscle varies depending on several factors. With this ratio method it is easy to make comparisons between muscles.

#### *5.4.3 Dye Leakage*

The loss of dye from the each muscle follows a similar time course, independent of the absolute level of dye initially in the muscle. This loss of dye is the same when measured by the fluorescence from illumination at 340, 360, or 380 nm. However, it is best evaluated by 360 nm illumination since this wavelength corresponds to the isobestic point of Fura-2 and is therefore insensitive to  $Ca^{++}$  (Grynkiewicz et al. 1985). It is gratifying to find that resting levels of fluorescence at 340 and 380 nm follow the same trend as 360 nm.

#### *5.4.4 Diastolic Fluorescence Ratio*

The relationship between diastolic ratios and  $[Ca^{++}]_o$  is particularly important in the evaluation of the muscle's health. In the experiments presented here, the ratios during the muscle's rest period have been shown to be maintained at normal levels, low

enough to not activate the myofilaments, until the muscle was exposed to dramatically high  $[Ca^{++}]_o$  levels (16.0 mM). The experiments presented in detail in chapter 6,  $[Ca^{++}]_o$  is increased from 0.25 mM up to a maximum of 8.0 mM, while tetanizing the muscle. The rapid stimuli associated with tetanization and the high  $[Ca^{++}]_o$  causes dramatic increases in  $[Ca^{++}]_i$ , demanding a high level of performance from  $[Ca^{++}]_i$  regulatory mechanisms. Since CPA is added to the muscle preparation, the ability of the SR to take in  $Ca^{++}$  is severely limited. The SR plays a significant role in rat myocardium and therefore to the maintenance of resting  $[Ca^{++}]_i$  levels (Bers 1985, Shattock & Bers 1989). The next contender in the regulation of  $[Ca^{++}]_i$  is the  $Na^+-Ca^{++}$  exchange (Bers et al. 1988, Bassani et al. 1994, Philipson 1985). Because of the reduction in SR activity,  $Ca^{++}$  extrusion via the  $Na^+-Ca^{++}$  exchange is particularly important. If the influx of  $Ca^{++}$  is too great for extrusion mechanisms (the  $Na^+-Ca^{++}$  exchange), then diastolic  $[Ca^{++}]_i$  levels will be elevated, causing moderate activation of the myofilaments. If diastolic  $[Ca^{++}]_i$  levels remain elevated, then the health of the muscle must be questioned. The  $Na^+-Ca^{++}$  exchange can accommodate reductions in SR pumping ability due to  $[Ca^{++}]_i$  elevations providing a favorable gradient for  $Ca^{++}$  extrusion (Bers & Bridge 1989).

#### *5.4.5 Twitch and Tetanus*

The twitch and tetanic contractions are very well matched to  $[Ca^{++}]_i$  levels as indicated in figure 5-5. Once an evaluation of  $[Ca^{++}]_i$  activity associated with force development can be made, then relationships can be established. Such relationships between force and  $Ca^{++}$  are investigated in chapter 6.

### **5.5 Summary of Findings**

1. Resting  $[Ca^{++}]_i$  levels remain in a normal range (<200)nM even in the presence of the SR  $Ca^{++}$ -ATPase inhibitor, CPA. However, resting  $[Ca^{++}]_i$  levels began to rise at

$[Ca^{++}]_o$  of 16.0 mM.

2. Fluorescence measurements and subsequent  $[Ca^{++}]_i$  estimations can be made for a tetanic contraction in cardiac trabeculae, corresponding to values previously found (Gao et al. 1994).

## 5.6 Potential Source of Errors

The measurement of autofluorescence is done just 5-10 minutes after CPA has been added to the solution so that CPA can be exposed to the muscle for a total of about 40 minutes prior to the start of the experimental protocol. During this 30 minutes after autofluorescence measurements, Fura-2 is loaded into the muscle. Therefore, if CPA has any effects on autofluorescence that occurs after it has equilibrated in the muscle for 40 minutes, it will not be accounted for. Changes that could occur could be due to CPA induced increases in [NADH]. This could change the autofluorescence values that are to be subtracted from the Fura-2 fluorescence and lead to inaccurate measurements of  $[Ca^{++}]_i$ . There is no evidence to support such changes and such changes are not likely since measurements of autofluorescence after longer exposure times to CPA do not show much change. However, this cannot be ruled out until it is specifically investigated.

In addition to potential alterations in autofluorescence values in the presence of CPA, autofluorescence values during tetani are not evaluated at all, and values obtained for a twitch prior to Fura-2 loading are used to subtract from tetanic fluorescence values. Fortunately, there is not much variation in the autofluorescence through the course of the twitch which would suggest that additional changes would not occur as stimulation continued as in a tetanic contraction. This consideration as an inaccurate evaluation of autofluorescence also needs to be studied specifically.

Since the primary source of autofluorescence is mitochondrial NADH (Gueth

& Wojciechowski 1986, White & Wittenberg 1993), it is possible that NADH levels could change after the addition of CPA and initiation of tetani. Such changes could arise by the tetani and CPA indirectly affecting mitochondrial activity. CPA's potential effect on the mitochondrial activity would be an indirect result of its actions on the SR. With an impairment of the SR, diastolic  $[Ca^{++}]_i$  could remain elevated for longer periods of time (i.e., prolongation of relaxation), as the  $Na^+-Ca^{++}$  exchange extrudes  $Ca^{++}$  from the cytosol. In addition, large amounts of  $Ca^{++}$  come across the sarcolemma from the rapid stimuli with tetanic contraction causing an elevation in  $[Ca^{++}]_i$ . Elevations in  $[Ca^{++}]_i$  occur for the duration of the tetani (2 to 4.7 seconds) before relaxation is allowed to take place. When the rapid train of stimuli is stopped, the muscle can begin to extrude more  $Ca^{++}$  than is coming in and thus initiate relaxation. The inhibitory actions of CPA on the SR  $Ca^{++}$ -ATPase pump makes extrusion of  $Ca^{++}$  slower, as indicated by a prolongation of relaxation with the addition of CPA, discussed in chapter 3. This sequence of events not only elevates  $[Ca^{++}]_i$ , but maintains this elevated level for an extended period of time. Elevations in  $Ca^{++}$  activate several mitochondrial enzymes (review by McCormack et al. 1990). Such increases ultimately lead to changes in [NADH]. Increases in mitochondrial activity stimulated by increased  $Ca^{++}$  allows the normally functioning cell to match ATP utilization with ATP production (Katz et al. 1987, McCormack & Denton 1990). However, in the case presented here it could potentially alter the muscle's intrinsic fluorescence which is not being accounted for. The fluorescence data presented here agree with data from other laboratories (Yue et al. 1986, Gao et al. 1994), but their results could also be affected by these problems as well. This is probably the most significant potential problem that can be found in the protocols used here. It would then be logical to measure autofluorescence during the course of a tetanic contraction to see if there are indeed alterations in NADH levels.

## Chapter 6

### Steady State Force-Fura-2 Fluorescence at Two Sarcomere Lengths

#### 6.1 Introduction

The force- $[Ca^{++}]_i$  relation for cardiac muscle has traditionally been measured using a skinned fiber preparation. The "skinning" of a cardiac muscle can have several specific meanings but is basically permeabilization of the sarcolemmal and intracellular organelle membranes. The end result is a muscle preparation that is unable to regulate  $Ca^{++}$  levels within the cellular boundaries, therefore the experimenter must provide a  $Ca^{++}$  free bathing solution (i.e., relaxing solution) to mimic "diastole". Activating solutions are then made to mimic various levels of contractile activation or "systole" by containing various levels of free  $Ca^{++}$ . The muscle's force response to an exposure to activating solution is to show an initial rise, then a plateau, when a steady state level of force is achieved. Force declines when the activating solution is replaced with relaxing solution. Using this method, a relation between force and  $[Ca^{++}]$  can be made. These relations can be fit using the sigmoidal function described by Hill, from which the  $EC_{50}$  value and a value for maximum force can be obtained, as indicated in chapter 2 section 2.6. To further look at the response of the myofilaments when exposed to varying  $[Ca^{++}]$ , force measurements are repeated at different sarcomere lengths. This has been done by Kentish et al. (1986) showing a dramatic increase in the sensitivity of the myofilaments to  $Ca^{++}$  (leftward shift of the  $EC_{50}$ ) and increase in maximal force production as the sarcomere length increases. This has provided evidence to support length-dependent activation as the primary mechanism for the Frank-Starling Law of the heart (i.e., dependence of cardiac output on end-diastolic volume). However, the direct relevance of these skinning experiments to the intact myocardium has to be resolved. A series of experiments by Gao et al. (1994) compared changes in force- $[Ca^{++}]$

relations from the same muscle in both the intact and skinned state. In their study, the muscle was first loaded with the fluorescent  $\text{Ca}^{++}$  indicator dye, Fura-2, and then exposed to a high concentration of ryanodine to disrupt sarcoplasmic reticulum function. The muscle could then be tetanized (to achieve a steady state force) at varied  $[\text{Ca}^{++}]_o$  with  $[\text{Ca}^{++}]_i$  being measured by fluorescence. Secondly, the muscle was skinned and exposed to solutions containing varying  $[\text{Ca}^{++}]_o$ 's. This protocol provided the data to generate two force- $[\text{Ca}^{++}]_i$  relations for each muscle; one for the intact and one for the skinned state, ideally they would show no difference. Unfortunately, the relations differed in that the  $\text{EC}_{50}$  showed a rightward shift (decreased  $\text{Ca}^{++}$  sensitivity) with skinning. This suggests that the results from skinned experiments may overestimate the  $[\text{Ca}^{++}]_i$  at which intact muscles operate. In light of this result, it is reasonable to question the force- $[\text{Ca}^{++}]_i$  relation at varying sarcomere lengths obtained in skinned muscles (Kentish et al. 1986). Are the relations quantitatively valid in the intact muscle? It is the purpose of this series of experiments to obtain steady state force- $[\text{Ca}^{++}]_i$  relations at different sarcomere lengths in the intact muscle where  $[\text{Ca}^{++}]_i$  is determined by Fura-2 fluorescence.

### 6.1.1 Hypothesis

The steady state force- $[\text{Ca}^{++}]_i$  relation in the myocardium will undergo a leftward shift in the  $\text{EC}_{50}$  and increase in maximal force production as sarcomere length increases from a short to a long length. The relations in the intact muscle will be qualitatively similar to the skinned fiber experiments of Kentish et al. (1986), however, the absolute  $[\text{Ca}^{++}]_i$  for each relation will be reduced.

## 6.2 Methods

### 6.2.1 Muscle Preparation

Trabeculae were dissected and mounted in the set-up, as described in chapter 2. Each of the trabecula were first stimulated at 1 Hz and allowed to equilibrate for 30-45 minutes at 26°C in HEPES buffered solution with 0.5 mM  $\text{Ca}^{++}$ . The procedures used to measure autofluorescence, inject the dye into the muscle, and record fluorescence have all been extensively described in chapter 2 (section 2.3).

### 6.2.2 Fura-2 Loading and Muscle Stimulation

After the muscle has equilibrated, the HEPES solution superfusing the muscle was changed to one containing 0.25 mM  $\text{Ca}^{++}$  and 30  $\mu\text{M}$  CPA. After 10 minutes, the muscle's autofluorescence was recorded at each wavelength (340, 360, and 380 nm). Fura-2 was then injected with a current of -7.2 to -8.2 nA into the muscle preparation for 20 to 30 minutes (time is dependent on muscle size). After the Fura-2 had been loaded into the muscle, the muscle was stimulated at 1 Hz until a steady level of force was achieved (approximately 5 minutes), then 0.2 Hz stimulation was resumed. Immediately after 0.2 Hz stimulation was resumed, the protocol was begun and Fura-2 fluorescence measurements were taken. Fluorescence measurements were taken for the twitch and tetanus. The tetanus was initiated by introducing a train of stimuli at 12-15 Hz (40 ms duration) for 2 to 4.7 seconds. The length of the stimulus interval was determined based on the time it takes for the force to reach a steady plateau, but the maximum allowance for the duration was 4.7 seconds. The procedure to tetanize the muscle is described in chapter 2 section 2.9.

### 6.2.3 Force- $\text{Ca}^{++}$ Relations

In order to obtain steady state force- $[\text{Ca}^{++}]$  relations in a muscle loaded with

Fura-2 and exposed to 30  $\mu\text{M}$  CPA, the following sequence was followed. First, after the muscle had been loaded with Fura-2, the muscle was illuminated with 340 nm light and the fluorescence was recorded for the twitch and tetanus. The muscle was allowed 1 to 3 minutes, the muscle was illuminated with 380 nm light and the fluorescence was again recorded for the twitch and tetanus. The records obtained from the 340 nm and 380 nm fluorescence for twitch and tetanus were ratioed, this ratio is denoted as  $R_{340/380}$ . Secondly, the  $[\text{Ca}^{++}]_o$  in the bath was increased to the next concentration and the sequence of 340 and 380 nm illumination and recording during the twitch and tetanus were repeated after the force had stabilized to the increased  $[\text{Ca}^{++}]_o$  (approximately 5-8 minutes). The  $[\text{Ca}^{++}]_o$ 's used in the bath for these series of experiments were: 0.25, 0.5, 1.0, 3.0, 8.0, 16.0 mM  $\text{Ca}^{++}$ , and each experiment went from low to high  $[\text{Ca}^{++}]_o$ . In some experiments, not all of these  $[\text{Ca}^{++}]_o$ 's were used. Three fluorescence records at 360 nm were taken through the course of each experiment. The first was taken at the start of the protocol (after fura-2 injection), just before the first 340 nm records were taken in 0.25 mM  $\text{Ca}^{++}$ . The second was taken halfway through the experiment just before the 340 and 380 nm series of experiment at 1.0 or 3.0 mM  $[\text{Ca}^{++}]_o$ . The third 360 nm record was taken after the last 340 and 380 nm record were taken in 8.0 or 16.0 mM  $[\text{Ca}^{++}]_o$ . This series of fluorescence measurements were taken at a long resting sarcomere length (2.3  $\mu\text{m}$ ) and at a short resting sarcomere length (1.9  $\mu\text{m}$ ). The muscle preparations were not truly isometric since shortening as internal shortening did take place (Krueger & Pollack 1975, ter Keurs et al. 1980) making 2.2  $\mu\text{m}$  and 1.8  $\mu\text{m}$  the approximate lengths the muscle contracted to for the long and short sarcomere length, respectively.

## 6.3 Results

### 6.3.1 Tetanus at Long and Short Sarcomere Lengths

In figure 6-1, the tetanic contraction at the short sarcomere length is shown for

1.0, 3.0, and 8.0 mM  $[Ca^{++}]_o$ . The fluorescence ratio ( $R_{340/380}$ ) tracings precede the force tracings in the initial portion of the tetanic contraction. As the tetanus continues, the force and  $R_{340/380}$  both reach a steady state level, however, at the lower  $[Ca^{++}]_o$ , this may take a little bit longer than at higher  $[Ca^{++}]_o$ , when the  $Ca^{++}$  gradient is larger. Figure 6-2 presents tetanic contractions at the long sarcomere length for 1.0, 3.0, and 16.0 mM  $[Ca^{++}]_o$ . In these examples, it is apparent that force is dramatically increased above values obtained at the short sarcomere length ( $p < 0.0001$ ). However, there was no significant difference between  $R_{340/380}$  at the two lengths. The time course of  $R_{340/380}$  for both sarcomere lengths are quite similar, but the force at the long length makes a more significant initial rise to a level that is sustained in contrast to the force fluctuations before a steady state is reached at the short length.

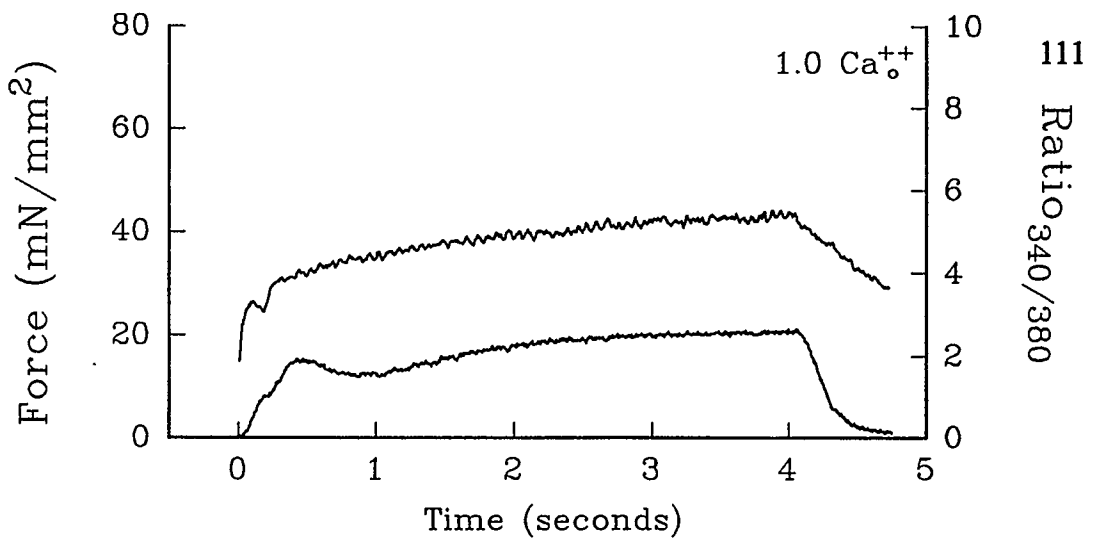
### 6.3.2 Force- $[Ca^{++}]_o$ Relations

When the results for each sarcomere length (short and long) are plotted as a function of force and  $[Ca^{++}]_o$  (figure 6-3A), two distinctly different relationships become apparent. The points obtained at the long sarcomere length show a steep rise in force with increasing  $[Ca^{++}]_o$ . In contrast, the data points from the short sarcomere length show a much less steep rise to  $F_{max}$ . Each experiment was fit with a sigmoid using the modified Hill equation. Each of the parameters from that equation ( $n$ ,  $EC_{50}$ , and  $F_{max}$ ) are listed for both the short and long lengths in table 6-1, as an average of five experiments. The averaged values are then used to make a fit through the averaged data points shown in figure 6-3B. The average  $F_{max}$  was  $107.5 \pm 4.8$  mN/mm<sup>2</sup> for the long sarcomere length and  $78.1 \pm 7.6$  mN/mm<sup>2</sup> for the short sarcomere length ( $p < 0.0001$ ). The long sarcomere length has a significantly lower  $EC_{50}$  of  $0.32 \pm 0.13$  mM  $[Ca^{++}]_o$ , compared to values at the short sarcomere length of  $1.82 \pm 0.38$  mM  $[Ca^{++}]_o$  ( $p < 0.0001$ ). The difference was not significant for  $n$  between the two lengths ( $p = 0.5009$ ).

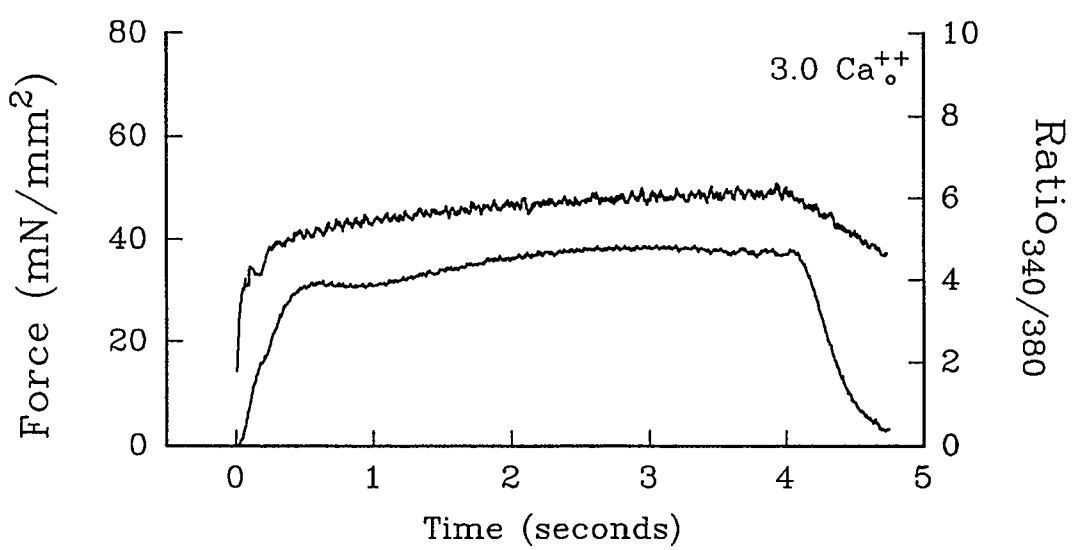
**Figure 6-1: Tetanic Force and Fluorescence Ratio Tracings for the Short Length**

The time course of tetanic force and fluorescence tracings are shown for the short sarcomere length at 1.0 (A), 3.0 (B), and 8.0 (C) mM  $[\text{Ca}^{++}]_o$ .

A



B



C

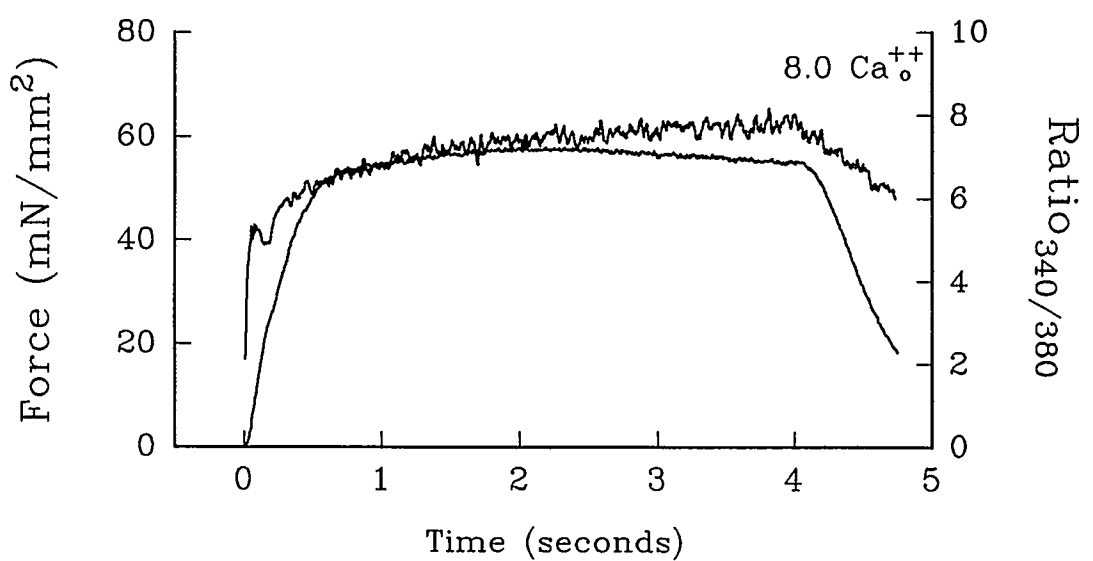
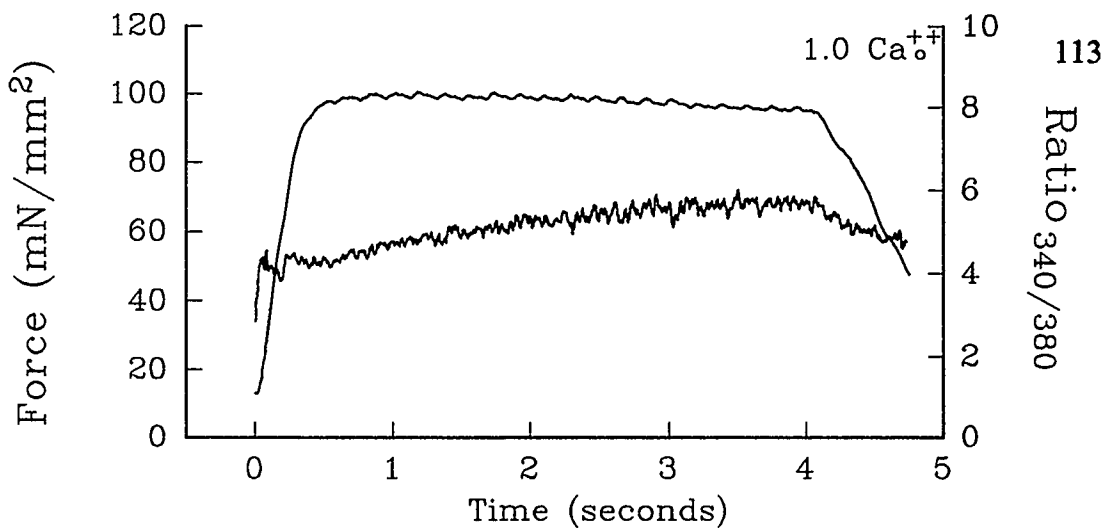


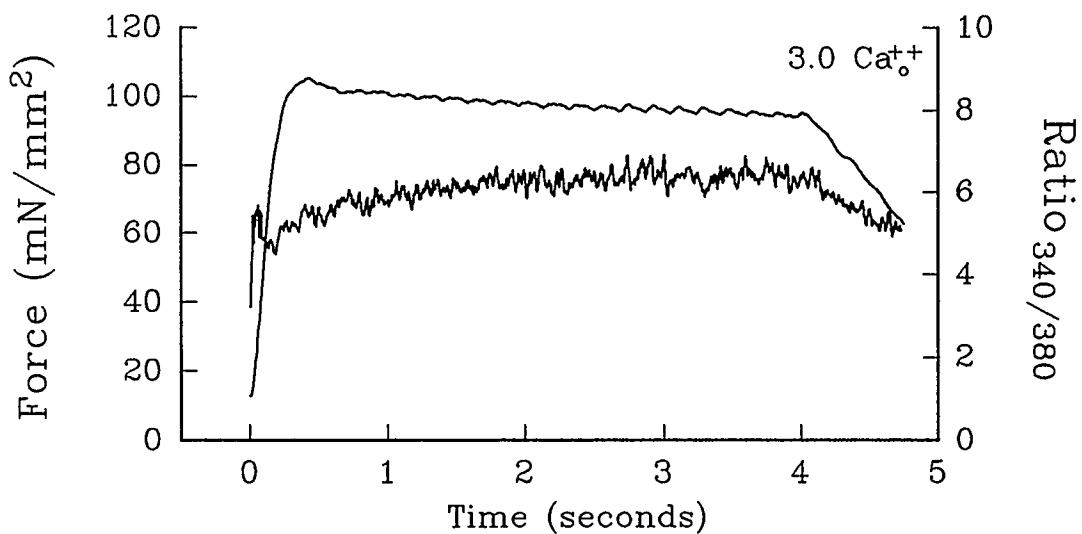
**Figure 6-2: Tetanic Force and Fluorescence Ratio Tracings for the Long Length**

The time course of tetanic force and fluorescence tracings are shown for the long sarcomere length at 1.0 (A), 3.0 (B), and 8.0 (C) mM  $[Ca^{++}]_o$ .

A



B



C

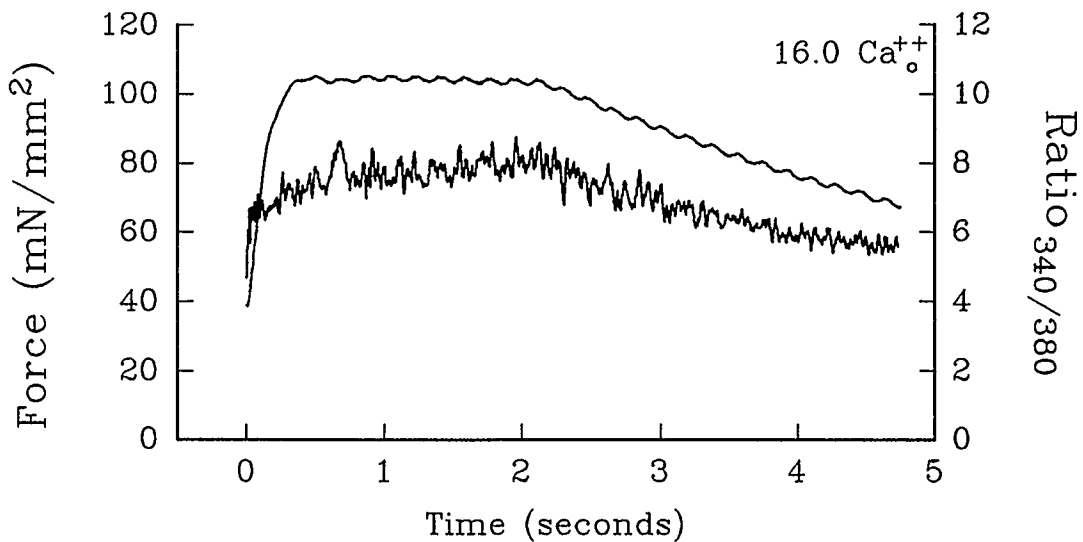
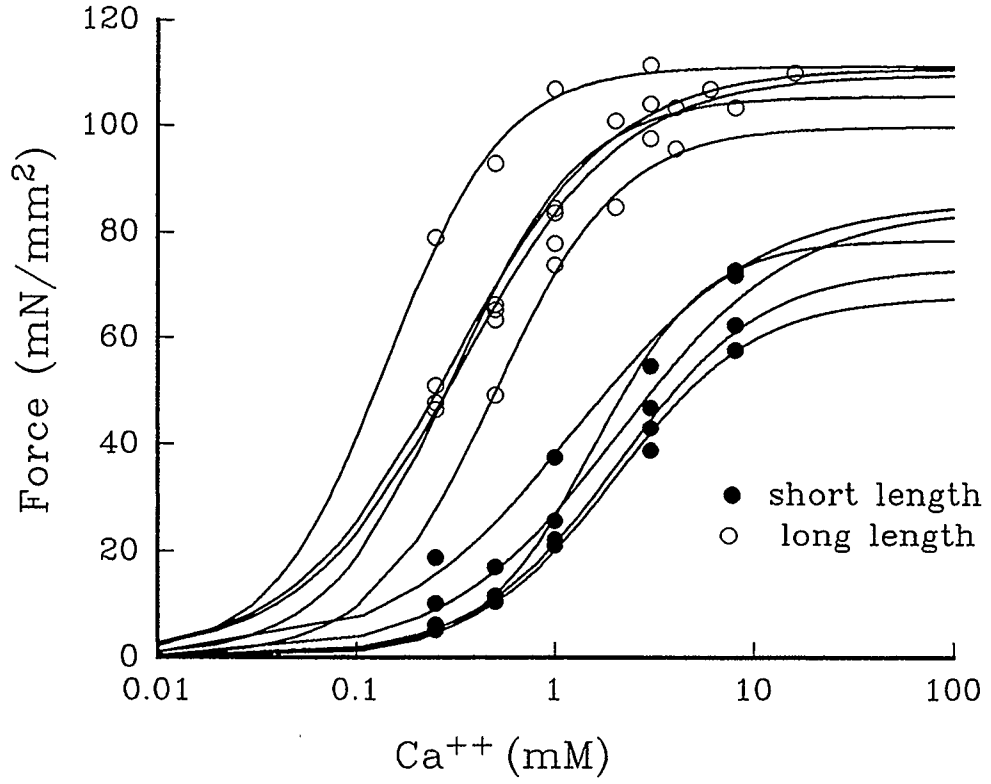


**Figure 6-3: Force-[Ca<sup>++</sup>]<sub>o</sub> Relations at Short and Long Sarcomere Lengths**

Force-[Ca<sup>++</sup>]<sub>o</sub> relations are plotted for the short and long sarcomere lengths are plotted with their corresponding curve fit from the modified Hill equation for each individual experiment (A), and for the mean values of the experiments (B). The data in (B) are expressed as mean±standard error of the mean (n=5).

A



B

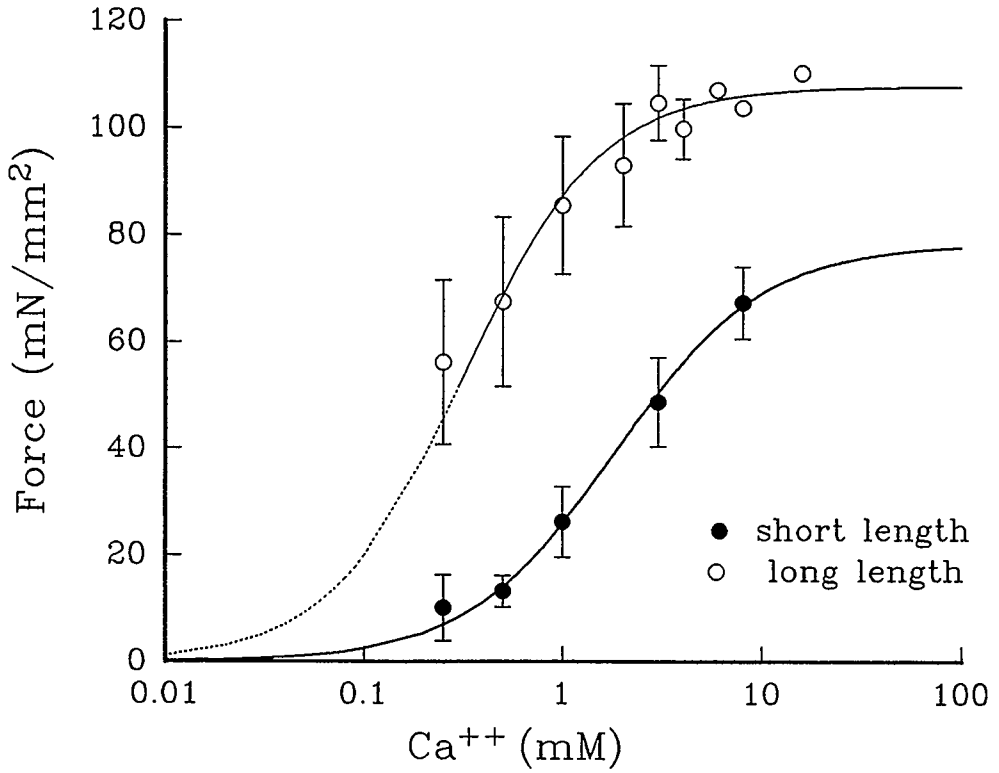


**Table 6-1**

Parameters from the modified Hill equation fit through force-[Ca<sup>++</sup>]<sub>o</sub> relations at short and long sarcomere lengths (mean ± standard error of the mean) from five experiments shown in figure 6-3.

Sarcomere Length	<i>n</i>	EC <sub>50</sub> (mM)	F <sub>max</sub> (mN/mm <sup>2</sup> )
Long	1.28±0.09	0.32±0.06	107.5±2.2
Short	1.18±0.11	1.82±0.17	78.1±3.4
<i>p</i> value*	0.5009	<0.0001	<0.0001

\* difference between short and long sarcomere length is significant if *p*<0.05

### 6.3.3 Force-[Ca<sup>++</sup>]<sub>i</sub> Relations

Using the 340/380 ratio of the fluorescence ( $R_{340/380}$ ) to estimate [Ca<sup>++</sup>]<sub>i</sub>, a force- $R_{340/380}$  relation can be made, which can be converted to force-[Ca<sup>++</sup>]<sub>i</sub>. In figure 6-4, individual data points are plotted and curve fit with a modified Hill equation. The relations are strikingly similar to the force-[Ca<sup>++</sup>]<sub>o</sub> relations previously discussed (figure 6-3). The curve fit for the long sarcomere length was taken as the fit through the averaged data points since it made the best visual fit through the individual data points. The fit for short sarcomere length was derived from the individual data points while  $F_{max}$  was predetermined from previous force-[Ca<sup>++</sup>]<sub>o</sub> relations since  $F_{max}$  was not achieved in the fluorescence experiments.  $F_{max}$  for the long sarcomere length was  $107.1 \pm 4.32$  mN/mm<sup>2</sup> compared to  $86.2 \pm 15.1$  mN/mm<sup>2</sup> for the short sarcomere length. The  $EC_{50}$  (indicated as  $R_{340/380}$ ) shifts right from  $3.80 \pm 0.09$  at the long sarcomere length to  $6.55 \pm 0.60$  at the short sarcomere length ( $p=0.002$ ). The coefficient indicating steepness,  $n$ , is  $5.63 \pm 1.11$  and  $4.50 \pm 0.96$  for the long and short sarcomere length, respectively. These values are displayed in table 6-2 for the force- $R_{340/380}$  relation, as well as values determined for the estimated force-[Ca<sup>++</sup>]<sub>i</sub> relation.

Figure 6-5 shows each individual point used to make the force- $R_{340/380}$  relations in figure 6-4A is plotted in figure 6-5 accompanied with its raw data from the steady state and relaxation portion of the tetanic contraction plotted against its corresponding raw  $R_{340/380}$  values. The raw data tracings from the short length follow the computer derived curve fit through the individual data points very closely. The data points from experiments done at the long length appear to drop more abruptly than is drawn with the computer estimated fit through the data points. This suggests that at the long sarcomere length the steepness of the force-[Ca<sup>++</sup>]<sub>i</sub> relation for the data points may have been underestimated. The scatter is plausible since there are relatively few data points at this lower level where the discrepancy takes place, and the spread of data appears to

**Figure 6-4:** Force-Ratio<sub>340/380</sub> Relations at Short and Long Sarcomere Lengths

Individual data points are displayed for the force-Ratio<sub>340/380</sub> relation at short and long sarcomere lengths plotted with their corresponding curve fit from the modified Hill equation (A). Averaged data expressed as mean  $\pm$  standard error of the mean are shown (B).

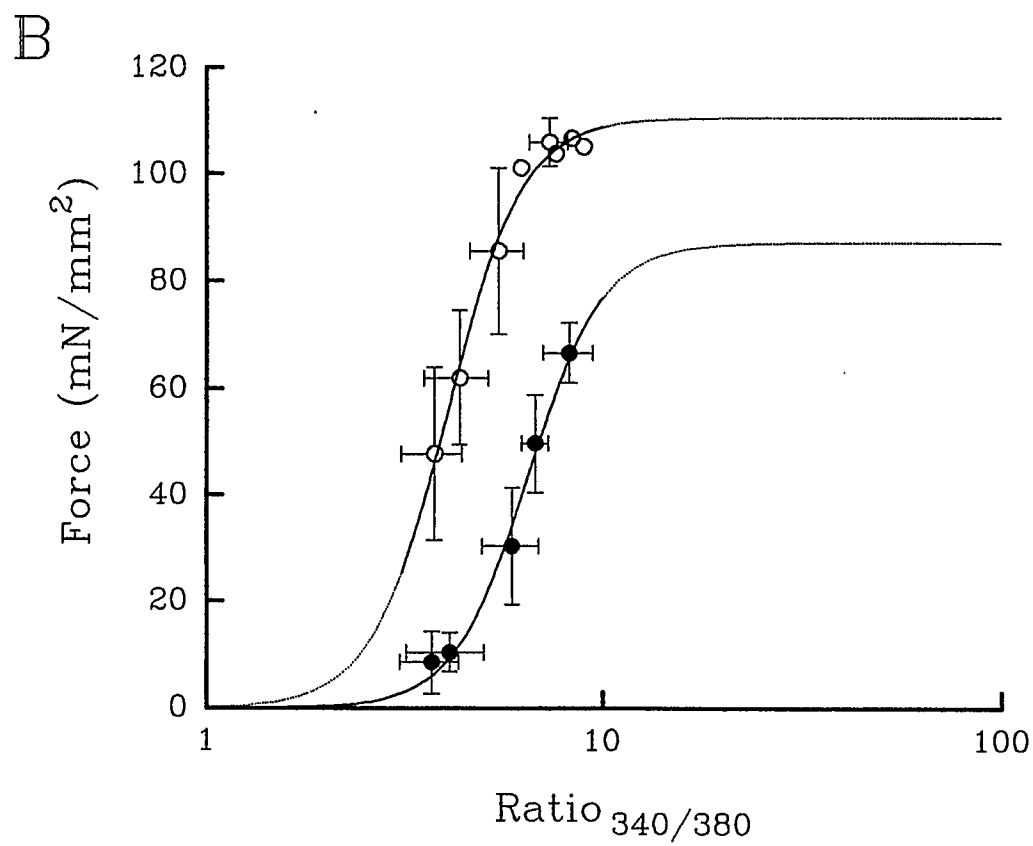
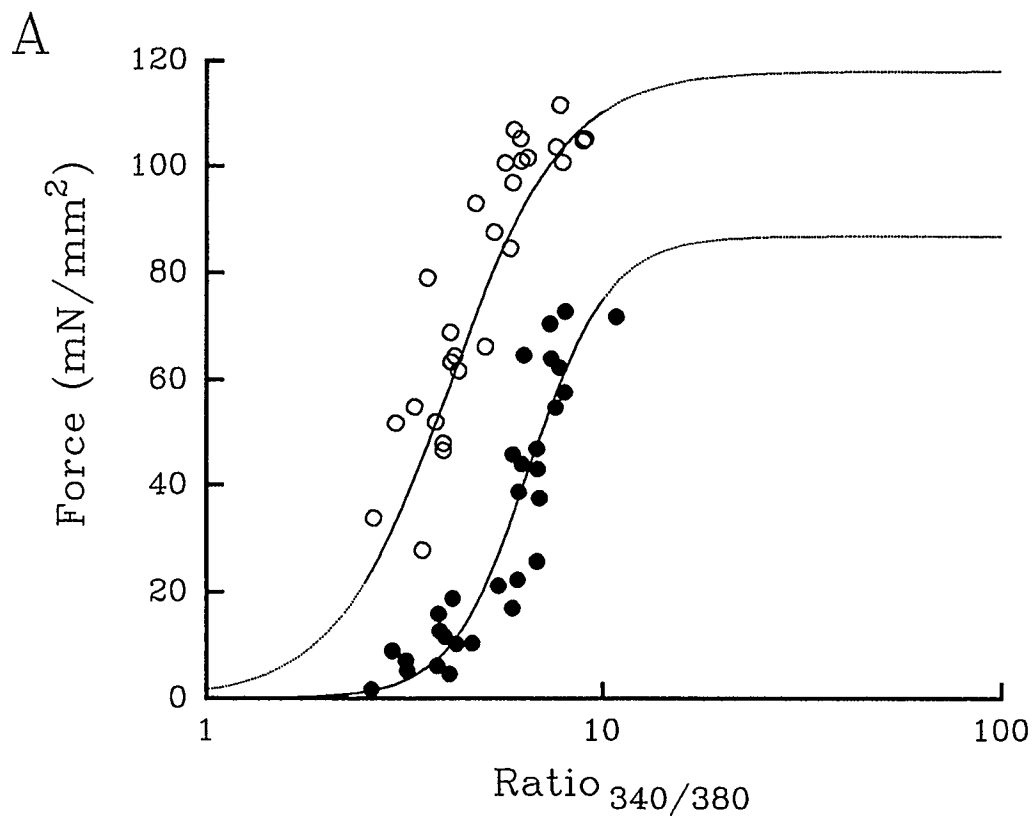


**Figure 6-5: Force- $R_{340/380}$  Relations with Data from Steady State and Relaxation**

Individual data points with curve fit and raw data from the steady state and relaxation portion of the tetanic contraction are displayed for the force- $R_{340/380}$  relation at long (A) and short (B) sarcomere lengths. The individual points and curve fit are the same as for figure 6-4.

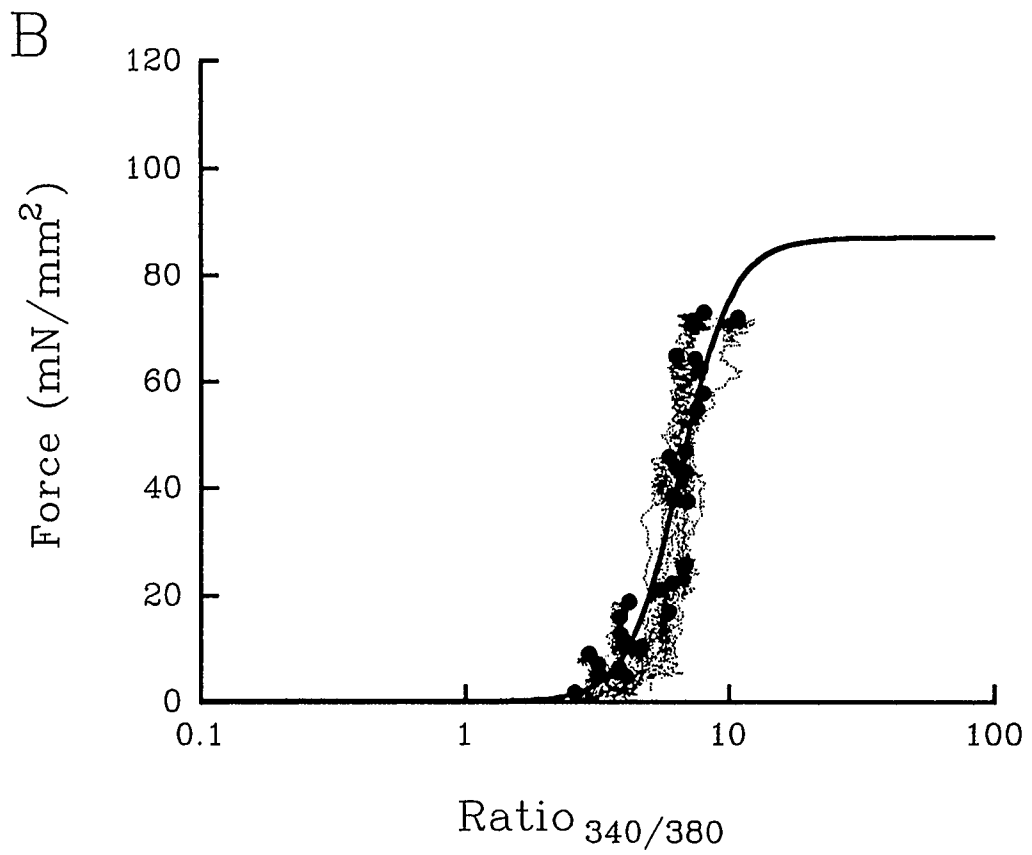
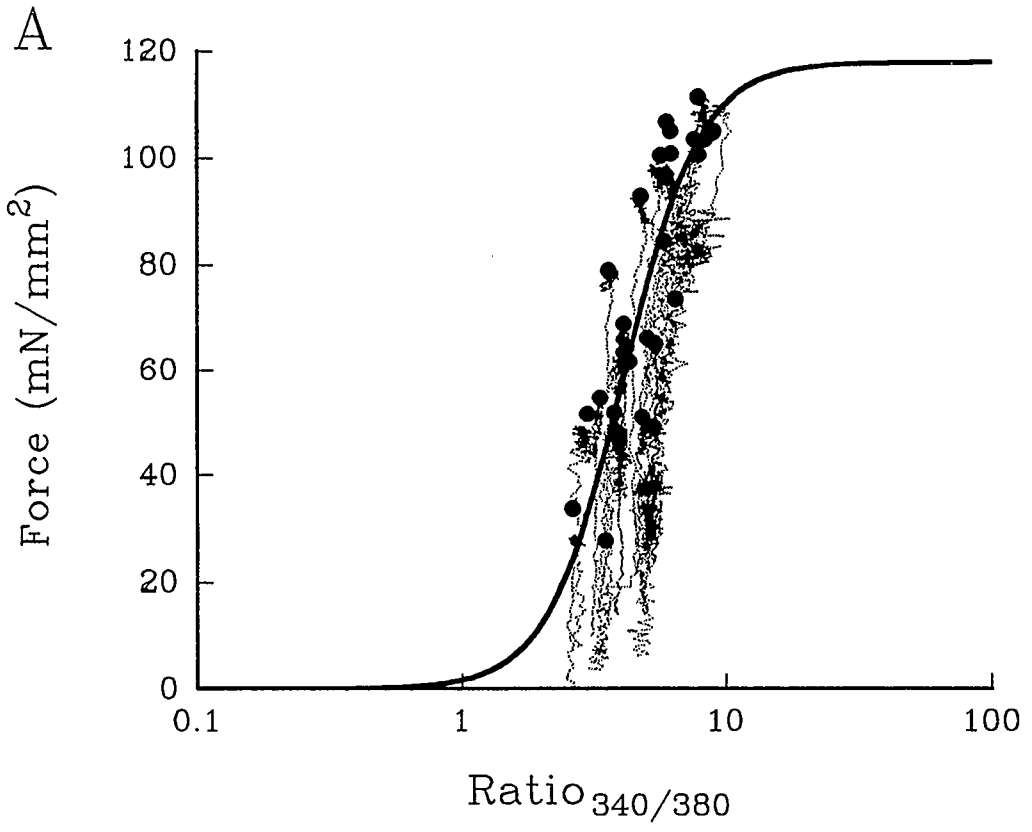


**Table 6-2**

Parameters from the modified Hill equation fit through data points for the force- $R_{340/380}$  and estimated force- $[Ca^{++}]_i$  relations in figures 6-4, 6-5, 6-6, (mean  $\pm$  standard error of the mean).

Relation	<i>n</i>	EC <sub>50</sub>	F <sub>max</sub> (mN/mm <sup>2</sup> )
<b>Force-<math>R_{340/380}</math></b>		<b>(Ratio)</b>	
long length	5.63 $\pm$ 1.11	3.80 $\pm$ 0.09	107.0 $\pm$ 4.3
short length	4.50 $\pm$ 0.96	6.55 $\pm$ 0.60	86.2 $\pm$ 15.1
<i>p</i> value*	0.46	0.002	0.018
<b>Force-<math>[Ca^{++}]_i</math></b>		<b>(<math>\mu</math>M)</b>	
long length	3.64 $\pm$ 0.85	0.21 $\pm$ 0.01	107.0 $\pm$ 5.2
short length	3.19 $\pm$ 0.67	0.49 $\pm$ 0.03	86.2 $\pm$ 5.8
<i>p</i> value*	0.68	0.0002	0.02

\* difference is considered significant if  $p < 0.05$

be greater than measured at the shorter length.

The data points for the force- $R_{340/380}$  can be mathematically converted to an estimated force- $[Ca^{++}]_i$  relation, using numbers derived from the in vitro calibration (discussed in chapter 2 section 2.3.5). This relation can be seen in figure 6-6A. Figure 6-6B shows essentially the same force- $[Ca^{++}]_o$  relation as in figure 6-3, except only the experiments in which the fluorescence data had been obtained are shown. Seeing these relations together allow differences and similarities to be seen when force is plotted against  $[Ca^{++}]_o$  and  $[Ca^{++}]_i$ . The relation qualitatively appears to be much steeper for  $[Ca^{++}]_i$ . However, quantitative evaluations are difficult since the force- $[Ca^{++}]_o$  relation has  $[Ca^{++}]$  in millimol/liter while the force- $[Ca^{++}]_i$  relation plots  $[Ca^{++}]$  as micromol/liter.

#### *6.3.4 Relationship Between $[Ca^{++}]_o$ and $[Ca^{++}]_i$*

In figure 6-7, steady state  $R_{340/380}$  is converted to an estimated  $[Ca^{++}]_i$  and plotted against  $[Ca^{++}]_o$  ( $[Ca^{++}]_o$  plotted on a log scale). The relation between  $[Ca^{++}]_i$  and  $\log [Ca^{++}]_o$  is linear with the same slope for both sarcomere lengths. The average values from both the long and short lengths are shown, the two relations are not statistically different. The linearity of this relation between  $[Ca^{++}]_i$  and  $\log [Ca^{++}]_o$  represents the balance of  $Ca^{++}$  transport across the sarcolemmal membrane.

## **6.4 Discussion**

### *6.4.1 Short and Long Sarcomere Lengths*

The development of tetanic force is accomplished by: 1) rapid stimulation causing an influx of  $Ca^{++}$  across the sarcolemma, 2) inability of the SR to accumulate any incoming cytosolic  $Ca^{++}$ , and 3) help from the  $Na^+$ - $Ca^{++}$  exchange. The influx of  $Ca^{++}$  increases with increasing stimulation (Allen & Blinks 1978, Noble & Shimoni 1980, Boyett & Fedida 1984, Frampton et al. 1991) and increased  $[Ca^{++}]_o$  (Kirby et al. 1989).

**Figure 6-6: Force-[Ca<sup>++</sup>]<sub>i</sub> and Force-[Ca<sup>++</sup>]<sub>o</sub> Relations at Short and Long Lengths**

Force-Ratio<sub>340/380</sub> relations from figure 6-4 were converted to create these force-[Ca<sup>++</sup>]<sub>i</sub> relations for both the short and long sarcomere lengths (A). The force-[Ca<sup>++</sup>]<sub>o</sub> relation is the same as presented in figure 6-3B (B).

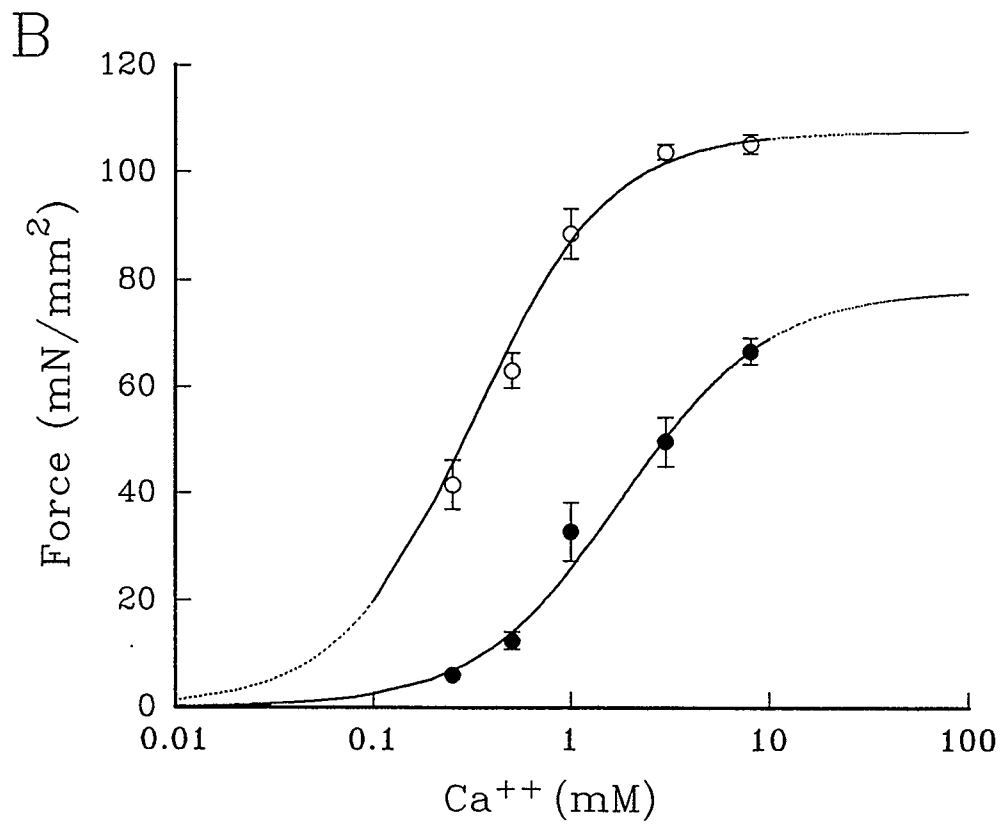
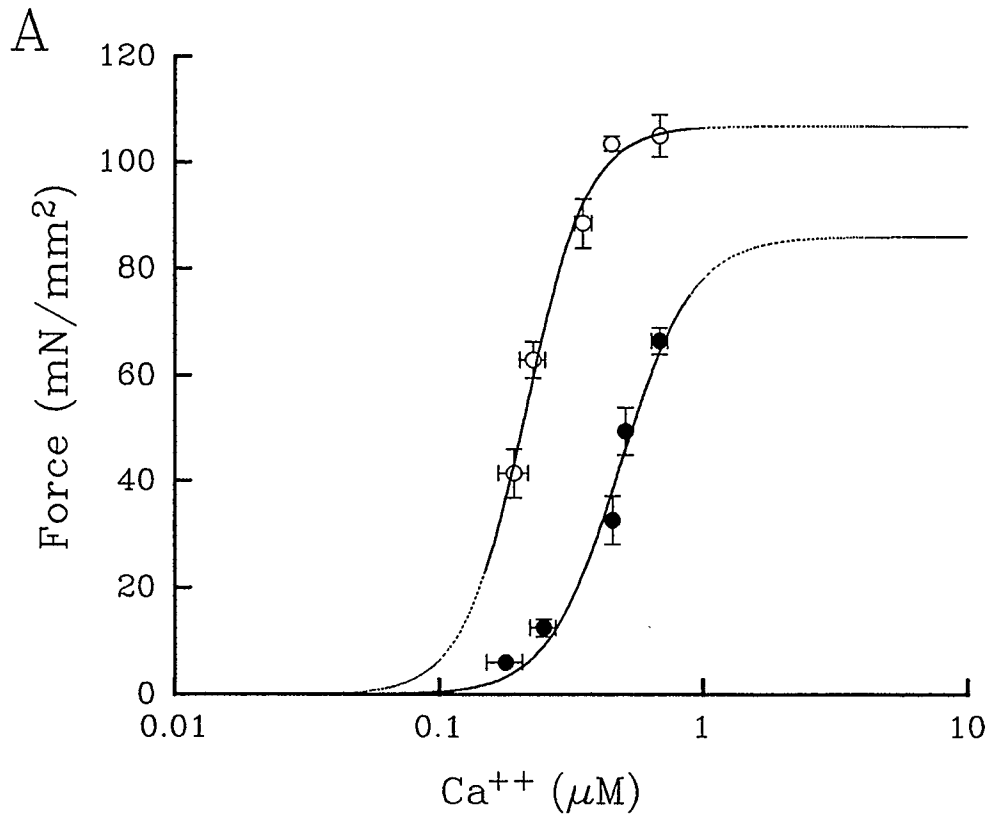
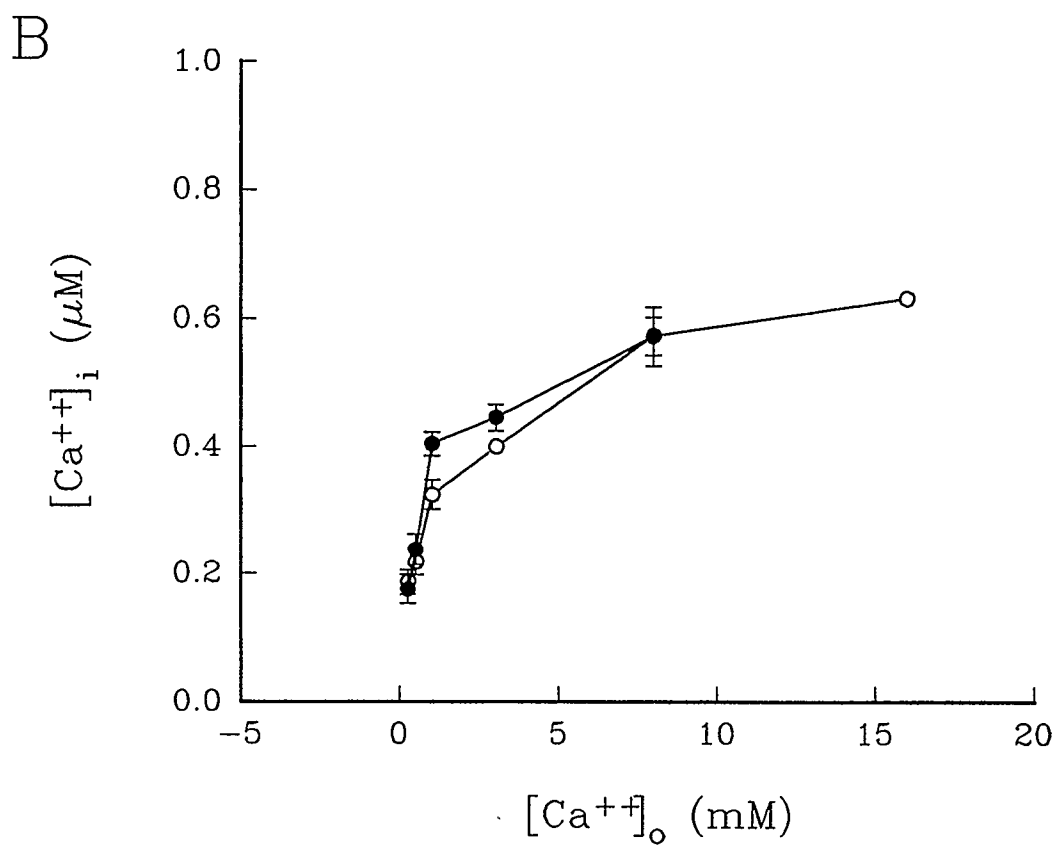
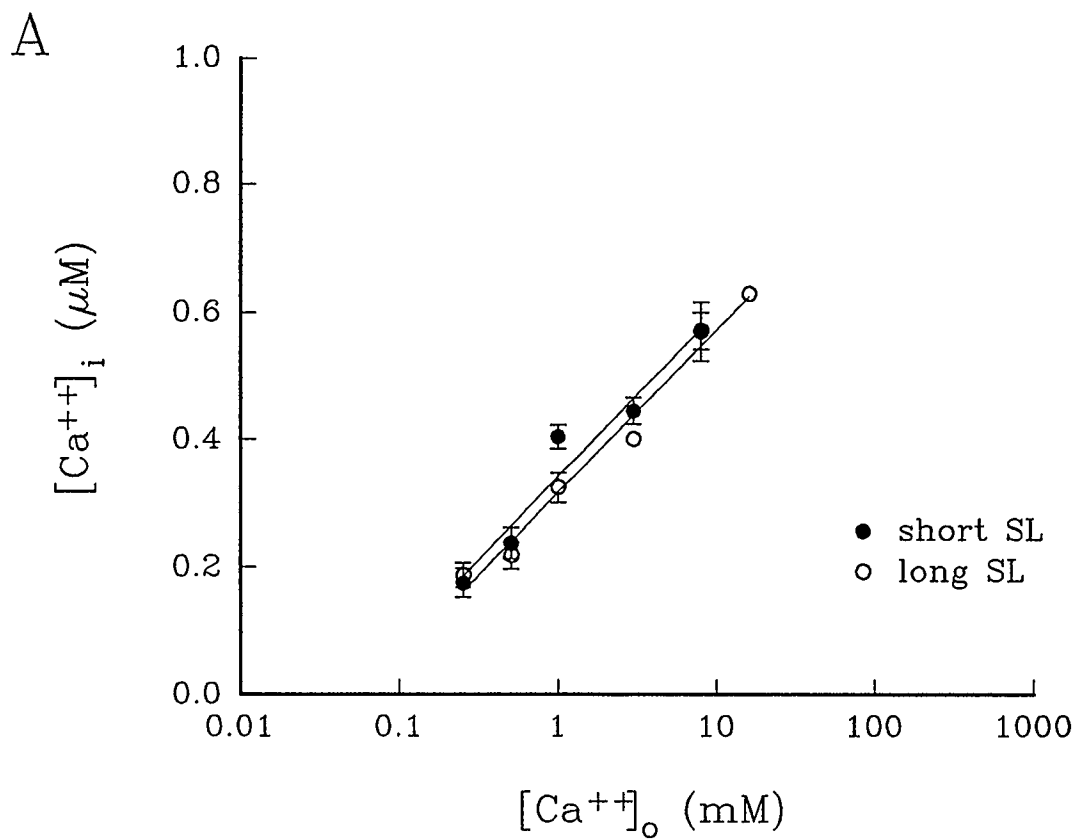


**Figure 6-7:** Steady State  $[Ca^{++}]_i$  vs.  $[Ca^{++}]_o$ .

(A)  $[Ca^{++}]_i$  from the tetanic plateau is plotted against the  $[Ca^{++}]_o$ . This shows a linear relation, that are not statistically different for the two sarcomere lengths. (B) The same data presented on a linear scale. Note there is only one data point for 16.0 mM  $[Ca^{++}]_o$  at the long sarcomere length, and the error bars for the 8.0 mM  $[Ca^{++}]_o$  data point, at the long sarcomere length, are so small that they are not seen over the size of the symbol.



Inhibition of the SR  $\text{Ca}^{++}$ -ATPase is achieved by the addition of 30  $\mu\text{M}$  CPA (Goeger et al. 1988), discussed in detail in chapter 3. Increasing  $[\text{Ca}^{++}]_i$  from the  $\text{Na}^+$ - $\text{Ca}^{++}$  exchange can occur by either a reduction in  $\text{Ca}^{++}$  extrusion or an influx of  $\text{Ca}^{++}$  through the exchanger resulting from an increased  $[\text{Na}^+]_i$  and membrane potential changes (reviewed by Eisner & Lederer 1985). The effect of membrane depolarization is greater with longer pulses (Eisner & Lederer 1985) which becomes important when one considers that 40 ms pulse duration is used to tetanize the muscle here. Thus, with rapid stimulation, the net effect of the  $\text{Na}^+$ - $\text{Ca}^{++}$  exchange is to promote  $\text{Ca}^{++}$  accumulation in the cells (Mullins 1979, Boyett et al. 1987) which could augment steady state force levels. Steady state levels of force take longer to achieve when  $[\text{Ca}^{++}]_o$  is low and at short sarcomere lengths. Tetanic contractions at the short length are marked by a drop in force in the early phase of the contraction, where  $\text{Ca}^{++}$  influx at the short length may not be large enough to overcome SR sequestration. This is in contrast to the long length where the force immediately reaches a level of force that is maintained until stimulation is ceased. These differences may be due to the reduced  $\text{Ca}^{++}$  binding to the myofilaments at the shorter length (Hofmann & Fuchs 1988), allowing more to remain in the cytosol, whereas at the long length the myofilaments have a higher affinity for  $\text{Ca}^{++}$  so steady state force can be achieved more easily than at shorter lengths.

#### *6.4.2 Force- $[\text{Ca}^{++}]_o$ Relations*

From a  $F_{\text{max}}$  at the long sarcomere length of 107.5  $\text{mN}/\text{mm}^2$  a drop to 78.1  $\text{mN}/\text{mm}^2$  at the short sarcomere length was seen. Reductions in  $F_{\text{max}}$  with decreasing sarcomere length have been found before in skeletal muscle (Gordon et al. (1966), Moss (1979) and in cardiac muscle (Allen et al. 1974, Gordon & Pollack 1980, ter Keurs et al, 1980). Force-length relations in skeletal muscle can be explained using the sliding filament theory, by the degree of actin overlap (discussed in Gordon et al. 1966). At a

length of 80% optimal length, 80-90% of maximum force is achieved. In contrast, cardiac muscle can only produce about 10% of  $F_{\max}$  at 80% of optimal length making the force-length relation much steeper in cardiac compared to skeletal muscle. Such differences have been attributed to a length-dependent activation property of cardiac muscle (reviewed in Allen & Kentish 1985). As the level of activation of cardiac muscle increases, the force-length relation becomes less steep in both intact and skinned fibers (Fabiato 1975, Kentish et al. 1986). Tetanization of intact cardiac muscle at maximal  $[Ca^{++}]_o$ , as presented here, should have eliminated any variability in muscle activation by providing the muscle with enough  $Ca^{++}$  to generate a maximal force at any length (short or long). The results presented here show a 25% reduction in  $F_{\max}$  as sarcomere length was reduced to 1.85  $\mu\text{m}$ , from an optimal length of 2.3  $\mu\text{m}$  (which is about an 80% reduction). It would be expected that since the muscle is maximally activated, the level of myofilament activation would be indifferent to length so that maximum force would drop with sarcomere length on the basis of physical factors, similar to skeletal muscle, as found by Fabiato and Fabiato (1975). Since it is reported that with a 20% reduction in sarcomere length, there is a 25% reduction of  $F_{\max}$  in tetanized cardiac muscle instead of the 10% reduction of  $F_{\max}$  as seen in tetanized skeletal muscle, length-dependent activation must still have some degree of contribution to cardiac force development. However, the forces presented here for the long length are overestimated because it includes passive force for the resting length (2.3  $\mu\text{m}$ ) instead of the smaller passive force for the active length (2.2  $\mu\text{m}$ ). Thus, if the differences between the passive force was subtracted, then the difference in  $F_{\max}$  is in the range of 10% as found in skinned cardiac (Fabiato & Fabiato 1975) and tetanized skeletal muscle (Gordon et al. 1966, Moss et al. 1970). Thus, at maximal activation, cardiac muscle behaves in a similar fashion compared to maximally activated skeletal muscle with regard to the dependence of force production on sarcomere length.

### 6.4.3 Force-[Ca<sup>++</sup>]<sub>i</sub> Relations

The significant increase in force at the long sarcomere length relative to the short sarcomere length at all [Ca<sup>++</sup>]<sub>o</sub>'s without an accompanying increase in the R<sub>340/380</sub> lends support to the length-dependent activation of the myofilaments. The length-tension relation at submaximal [Ca<sup>++</sup>]<sub>i</sub>'s is steeper in cardiac muscle than skeletal muscle (reviewed by Allen & Kentish 1985). Experiments using skinned cardiac muscle, have found length-dependent Ca<sup>++</sup> binding to the myofilaments (Hofmann & Fuchs 1988). This length dependency of Ca<sup>++</sup> binding can be directly attributed to the number of crossbridges attached to actin (Hofmann & Fuchs 1987, Guth & Potter 1987, Zot & Potter 1989), which in turn is affected by sarcomere length (Gordon et al. 1966). In a study by Allen and Kentish (1988) using aequorin to indicate [Ca<sup>++</sup>]<sub>i</sub> in skinned cardiac muscle, a rise in [Ca<sup>++</sup>]<sub>i</sub> was seen when the muscle was quickly released (shortened), which was reduced again when the muscle was stretched back to the original length, suggesting a reduction in the affinity of the myofilaments to Ca<sup>++</sup> at the shorter length. The results here, in intact muscle, show a large increase in force from short to long sarcomere length with no change in [Ca<sup>++</sup>]<sub>i</sub>. These changes in force without [Ca<sup>++</sup>]<sub>i</sub> changes suggests that Ca<sup>++</sup> binding to myofilaments remained the same but the response of the myofilaments to Ca<sup>++</sup> bound was altered. Such a change could be seen by a shift in the EC<sub>50</sub> or sensitivity of the myofilaments for Ca<sup>++</sup> as determined from force-[Ca<sup>++</sup>]<sub>i</sub> relations with different sarcomere lengths. This response has been observed in skinned cardiac trabeculae by Kentish et al. (1986). Kentish et al. (1986) have shown a drop in F<sub>max</sub> from 86.3 mN/mm<sup>2</sup> (2.15 μm sarcomere length) to 63.2 mN/mm<sup>2</sup> (1.85 μm sarcomere length), as well as an increase in EC<sub>50</sub> from 3.8 μM to 6.8 μM, for these two sarcomere lengths. The changes presented here, from similar sarcomere lengths in intact preparations show F<sub>max</sub> drops from 107.5 mN/mm<sup>2</sup> to 78.1 mN/mm<sup>2</sup> with an increase in the EC<sub>50</sub> from 0.2 μM to 0.4 μM. Qualitatively, the two studies are very similar, but

the quantitative differences are likely due to the nature of the methods used (i.e., skinned vs. intact). Such differences between skinned and intact preparations have been found by Gao et al. (1994) indicating that the intact preparation is much more sensitive to  $\text{Ca}^{++}$  than the skinned preparation.

Raw data plotted for the long sarcomere length (figure 6-5A) shows that the relation between force and  $[\text{Ca}^{++}]_i$  is much steeper than predicted by the curve fit through the data points since the raw data show a much more abrupt fall in force in the terminal relaxation period. The raw data from the short sarcomere length (figure 6-5B) follow the curve fit very well, suggesting that this steep relationship at the short length is indeed valid. However, force- $\text{Ca}^{++}$  curves obtained in skinned fibers at this length have been shown to be less steep (Kentish et al. 1986). Force- $[\text{Ca}^{++}]_i$  relations accompanied with data from the steady state and relaxation phase of the tetanic contractions provide evidence that there is a direct interaction between  $[\text{Ca}^{++}]_i$  and force development that can only be accurately detected when a quasi-equilibrium between troponin C and  $\text{Ca}^{++}$  is achieved. Such a state of quasi-equilibrium is found when the relation between force and  $\text{Ca}^{++}$  is not dominated by the kinetics of excitation-coupling mechanisms such as rapid SR  $\text{Ca}^{++}$  release, troponin C binding, and SR  $\text{Ca}^{++}$  uptake. Such mechanisms dominate in the normal cardiac twitch, where the peak of the measured  $\text{Ca}^{++}$  transient precedes peak force (Backx & ter Keurs 1993). With such rapid kinetics it is difficult to establish an accurate relationship between the amount of  $\text{Ca}^{++}$  necessary to activate the myofilaments and produce a given amount of force. As the time course of  $[\text{Ca}^{++}]_i$  and force slow down, a relation between the two can be made, as has been done for a  $[\text{Ca}^{++}]_i$ -cell length relation by Spurgeon et al. (1992). The steady state nature of tetanic contractions also provide a more spatially uniform distribution of  $[\text{Ca}^{++}]_i$  and allow a better correlation between force development and  $[\text{Ca}^{++}]_i$  (Cannell & Allen 1984).

#### 6.4.4 Relationship Between $[Ca^{++}]_o$ and $[Ca^{++}]_i$

Increases in  $[Ca^{++}]_i$  above the buffering capacity of the cells causes damage. In most muscles, such damage has been found in the preparations here when  $[Ca^{++}]_o$  is increased to 16.0 mM. This was seen by tetanic force accompanied by a contracture development, indicated by a rise in passive force, in the presence of 16.0 mM  $[Ca^{++}]_o$ , at the long sarcomere length. This is the reason why only measurements up to 8.0 mM  $Ca^{++}$  are reported here. It is at this point that the cellular  $Ca^{++}$  regulatory mechanisms are inadequate to compete with the large influx of  $Ca^{++}$  with each twitch stimulation, not to mention the influx of  $Ca^{++}$  accompanying tetanic stimulation.

The linear relation between  $[Ca^{++}]_i$  and  $[Ca^{++}]_o$  suggests that all of the membrane  $Ca^{++}$  transport and  $Ca^{++}$  buffering mechanisms are able to consistently maintain a balance of influx and efflux for a range of  $[Ca^{++}]_i$  from 0.18 to 0.63  $\mu$ M and  $[Ca^{++}]_o$  from 0.25 to 8.0 mM. This could protect the muscle from  $Ca^{++}$  overload. Two major  $Ca^{++}$  buffering mechanisms, within the cytosol, are the SR and mitochondria. The SR is a likely candidate to take up cytosolic  $Ca^{++}$  even in the presence of CPA because high levels of  $Ca^{++}$  decreased the effectiveness of CPA on the SR  $Ca^{++}$ -ATPase (Seidler et al. 1989), and therefore reduce the degree of inhibition by CPA. The mitochondria are sensitive to  $[Ca^{++}]_i$  levels so they can to match energy supply with energy usage, which they determines by  $Ca^{++}$  levels (Katz et al. 1987, McCormack et al. 1990). At  $[Ca^{++}]_i$  greater than 1  $\mu$ M, the mitochondria begin to act as a buffer and take up  $Ca^{++}$ , thus removing it from the cytosol (Fry et al. 1984).

### 6.5 Summary of Findings

Force- $[Ca^{++}]_i$  relations during steady state force development, show a reduction in  $EC_{50}$  and  $F_{max}$  as sarcomere length decreases, although the steepness of the relation is retained at short sarcomere lengths. Plotting force- $[Ca^{++}]_i$  relations with data from

the steady state period of the tetanic contractions show a good correlation with curve fit estimations. This suggests that during the steady state and relaxation phase of the tetanic contraction the kinetics of cytosolic  $\text{Ca}^{++}$  movement is slow enough for intracellular  $\text{Ca}^{++}$  binding to achieve a state of quasi-equilibrium. Therefore, during this time, the relationship between  $[\text{Ca}^{++}]_i$  and force can be evaluated.

The evaluation of the relationship between force and  $[\text{Ca}^{++}]_i$  at different sarcomere lengths have validated the role of length-dependent activation of cardiac myofilaments. This property of the myofilaments is the basis for the Frank-Starling relation and the end-systolic pressure-volume relation in whole hearts.

## 6.6 Potential Sources of Error

- 1) The amount the muscle shortens during contraction increases as force development increases. This results in shorter active sarcomere lengths for tetani at higher  $[\text{Ca}^{++}]_i$ . These variations in active sarcomere lengths are not accounted for in these experiments. This would tend to underestimate  $F_{\text{max}}$  because the force and degree of shortening were greatest. Active sarcomere lengths during  $F_{\text{max}}$  were then shorter than desired (i.e., active sarcomere length being 2.1  $\mu\text{m}$  instead of 2.2  $\mu\text{m}$  as preferred).
- 2) Passive force recorded during the muscle's resting period, at the long sarcomere length (2.3  $\mu\text{m}$ ), was included in the measurement of active force ( $F_{\text{total}} = F_{\text{active}} + F_{\text{passive}}$ ). This would be an inaccurate estimate of passive force if the preparation was truly isometric. However, during activation, shortening does occur in this preparation (Krueger & Pollack 1975). The actual measurement of force would then correspond to a shorter sarcomere length, than the length measured at rest. Since the muscle was at a shorter length for the active force measurement, the corresponding passive force is also smaller (Kentish et al. 1986). However, the passive force corresponding to the resting length is used to calculate total force. This would cause the measurement of

active force to be overestimated.

3) The force- $[Ca^{++}]_i$  relations obtained at the short sarcomere length would be more convincing if a measurement of maximal  $[Ca^{++}]_i$  ( $R_{340/380}$ ) had been made. The curve fit through the data points provides a reasonable evaluation of the relation between force and  $[Ca^{++}]_i$  at the short length, however, a better quantitative comparison to the long length could be made with this additional measurement. Although fluorescence measurements were not taken at the short sarcomere length's  $F_{max}$ , previously measured  $F_{max}$  was used to obtain a curve fit through the data. This provided adequate means to evaluate  $EC_{50}$  changes using Hill fit parameters.

## Chapter 7

### Conclusion

#### Relevance of Findings

The Frank-Starling relation is a fundamental property of the heart. This is based on measurements of isovolumic pressure at different ventricular volumes (Frank) and cardiac output at varying right atrial pressures (Starling). The mechanical basis for these observations are the force-sarcomere length relations of the myofilaments (Fabiato 1975). Changing the length of a muscle alters the amount of force the muscle can produce. Two primary effects of length on cardiac muscle were observed in skinned fibers. The first observation was a reduction in the amount of maximal force the muscle could generate as the sarcomere length was reduced (Fabiato 1975, Kentish et al. 1986). The second observation indicated length effects on myofilament  $\text{Ca}^{++}$  binding properties, as shown by a reduction in the amount of  $\text{Ca}^{++}$  needed to generate a half-maximal force ( $\text{EC}_{50}$ ) (Kentish et al. 1986). This reduction in  $\text{EC}_{50}$  suggested that the myofilaments were more sensitive to the available  $\text{Ca}^{++}$  at longer lengths than at shorter lengths. Thus, length-dependent effects on the muscle are a result of the interaction between force and  $\text{Ca}^{++}$  binding properties.

The findings of the study presented here validate observations, from skinned fiber experiments, in an intact muscle preparation. Steady state forces and corresponding  $[\text{Ca}^{++}]_i$  from rest to maximal activation were measured at two sarcomere lengths. Increasing sarcomere length resulted in a significant augmentation of force over the entire range of  $[\text{Ca}^{++}]_i$ 's studied. However, there was no significant increase in  $[\text{Ca}^{++}]_i$  measured at the two lengths. These findings show that increasing length allows more force to be generated at a constant  $[\text{Ca}^{++}]_i$ . This provides the basis for the length-dependent sensitivity of the myofilaments for  $\text{Ca}^{++}$  (Allen & Kentish 1985).

The experiments presented here were done with a primary concern of removing

potential extraneous factors that could alter myofilament sensitivity. A SR  $\text{Ca}^{++}$ -ATPase inhibitor was used to eliminate the SR since this would also eliminate unnecessary ATP use, minimizing  $\text{H}^+$  and inorganic phosphate accumulation, since it has been shown that they can alter myofilament binding properties. In addition, CPA was tested directly on the myofilaments, using skinned fibers, to test if it had any effects on myofilament sensitivity. Results showed no alterations in the force generation or  $\text{Ca}^{++}$  sensitivity of the myofilaments.

Thus, findings presented here contribute to understanding the basic mechanisms of the Frank-Starling relation.

### **Technical Improvements and Future Studies**

1. Measurements of autofluorescence during tetani would allow the concern regarding NADH changes during the course of the tetanic contraction to either be quantified or eliminated (if there were no NADH changes). Until such an evaluation is made, the muscle's true autofluorescence during tetani will not be known and will remain a potential source of error in fluorescence measurements.
2. Refinements in the protocol for tetanization of cardiac muscle could be made if both CPA and ryanodine are used together. This could provide an easier means to tetanize the muscle with the added benefit of eliminating SR ATP utilization.
3. Cardiac tetani can be used to further investigate the relation between force, length, and  $\text{Ca}^{++}$  binding of the myofilaments. Repeating the study by Allen and Kentish (1988), in intact preparations, by inducing a quick release during the period of steady state force while simultaneously measuring  $[\text{Ca}^{++}]_i$ . This would provide a means to again test the sensitivity of the myofilaments for  $\text{Ca}^{++}$  at different lengths and support the findings already presented here.
4. Elimination of the SR and development of steady state force and  $[\text{Ca}^{++}]_i$  can

provide an interesting framework to study changes of other ions within the cytosol such as  $\text{Na}^+$ . Elimination of the primary relaxation mechanism, the SR, causes the  $\text{Na}^+$ - $\text{Ca}^{++}$  exchange to become the main regulator of relaxation. Using an intracellular  $\text{Na}^+$  ( $\text{Na}^+$ ) indicator to measure  $[\text{Na}^+]_i$  during the steady state and relaxation phase of a tetanic contraction would provide an interesting method of evaluating the  $\text{Na}^+$ - $\text{Ca}^{++}$  exchange. ☺

## References

- Agata N, Tanaka H, Shigenobu K. Possible action of cyclopiazonic acid on myocardial sarcoplasmic reticulum: inotropic effects on neonatal and adult rat heart. *Br J Pharmacol.* 1993;108:571-572.
- Allen DG, Blinks JR. Calcium transients in aequorin-injected frog cardiac muscle. *Nature.* 1978;273:509-513.
- Allen DG, Blinks JR. The interpretation of light signals from aequorin-injected skeletal and cardiac muscle cells: a new method of calibration. In: Ashley CC, Campbell AK, eds. *Detection and measurement of free  $Ca^{++}$  in cells.* Amsterdam: Elsevier/North-Holland Biomedical Press; 1979:159-174.
- Allen DG, Jewell BR, Murray JW. The contribution of activation processes to the length-tension relation of cardiac muscle. *Nature.* 1974;248:606-607.
- Allen DG, Kentish JC. The cellular basis of the length-tension relation in cardiac muscle. *J Mol Cell Cardiol.* 1985;17:821-840.
- Allen DG, Kentish JC. Calcium concentration in the myoplasm of skinned ferret ventricular muscle following changes in muscle length. *J Physiol.* 1988;407:489-503.
- Allen DG, Kurihara S. The effects of muscle length on intracellular calcium transients in mammalian cardiac muscle. *J Physiol.* 1982;327:79-94.
- Backx PH. *Force sarcomere relation in cardiac myocardium (PhD Thesis).* The University of Calgary; 1989.
- Backx PH, ter Keurs HEDJ. Fluorescent properties of rat cardiac trabecule microinjected with fura-2 salt. *Am J Physiol.* 1993;264:H1098-H1110.
- Banijamali HS. *Force-Interval Relation in Rat Heart. (PhD Thesis).* University of Calgary; 1994.
- Bassani JW, Bassani RA, Bers DM. Relaxation in rat and rabbit cardiac cells: species-dependent difference in cellular mechanisms. *J Physiol.* 1994;476:279-293.

Baudet S, Shaolian R, Bers DM. Effects of thapsigargin and cyclopiazonic acid on twitch force and sarcoplasmic reticulum content of rabbit ventricular muscle. *Circ Res*. 1993;73(5):813-819.

Becker PL, Fay FS. Photobleaching of fura-2 and its effect on determination of calcium concentrations. *Am J Physiol*. 1987;253:613-618.

Bers DM. Calcium influx and sarcoplasmic reticulum calcium release in cardiac muscle activation during postrest recovery. *Am J Physiol*. 1985;248:H366-H381.

Bers DM. *Excitation-contraction coupling and cardiac contractile force*. Boston/London: Kluwer Academic; 1991.

Bers DM, Bridge JHB. Relaxation of rabbit ventricular muscle by Na-Ca exchange and sarcoplasmic reticulum calcium pump: Ryanodine and voltage sensitivity. *Circ Res*. 1989;65:334-342.

Bers DM, Christensen DM, Nguyen TX. Can Ca entry via Na-Ca exchange directly activate cardiac contraction. *J Mol Cell Cardiol*. 1988;20:405-414.

Boyett MR, Fedida D. A decrease of the second inward current, rather than an increase in transient outward current, causes action potential shortening at low stimulus rates in sheep Purkinje fibers. *J Physiol*. 1984;346:76P.

Boyett MR, Hart G, Levi AJ, Roberts A. Effects of repetitive activity on developed force and intracellular sodium in isolated sheep and dog Purkinje fibres. *J Physiol*. 1987;388:295-322.

Brandt PW, Diamond MS, Rutchik JS. Co-operative interactions between troponin-tropomyosin units extend the length of the thin filament in skeletal muscle. *J Mol Biol*. 1987;195:885-896.

Bucx JJJ. *Ischemia of the heart: a study of sarcomere dynamics and cellular metabolism*. (PhD Thesis). Erasmus University Rotterdam; 1993.

Cannell MB, Allen DG. Model of calcium movements during activation in the sarcomere of frog skeletal muscle. *Biophys J*. 1984;45:913-925.

Capogrossi MC, Stern MD, Spurgeon HA, Lakatta EG. Spontaneous Ca<sup>2+</sup> release from the sarcoplasmic reticulum limits Ca<sup>2+</sup>-dependent twitch potentiation in individual cardiac myocytes. A mechanism for maximum inotropy in the myocardium. *J Gen Physiol*.

1988;91:133-155.

Capogrossi MC, Stern MD, Spurgeon HA, Lakatta EG. Spontaneous calcium release from the sarcoplasmic reticulum limits calcium-dependent twitch potentiation in individual cardiac myocytes. *J Gen Physiol.* 1988;91:133-155.

Cleemann L, Morad M. Role of Ca<sup>++</sup> channel in cardiac excitation-contraction coupling in the rat: evidence from Ca<sup>++</sup> transients and contraction. *J Physiol.* 1991;432:283-312.

de Tombe PP. *Determinants of velocity of sarcomere shortening in mammalian myocardium. (Thesis).* Calgary: The university of Calgary; 1989.

Drake-Holland AJ, Noble MIM, Pieterse M, Schouten VJA, Seed WA, ter Keurs HEDJ, Wohlfart B. Cardiac action potential duration and contractility in the intact dog heart. *J Physiol.* 1983;345:75-85.

Eisner DA, Lederer WJ. Na-Ca exchange: stoichiometry and electrogenicity. *Am J Physiol.* 1985;248:189-202.

Eisner DA, Lederer WJ, Vaughan-Jones RD. The control of tonic tension by membrane potential and intracellular sodium activity in the sheep cardiac Purkinje fibre. *J Physiol.* 1983;335:723-743.

Eisner DA, Lederer WJ, Vaughan-Jones RD. The quantitative relationship between twitch tension and intracellular sodium activity in sheep Purkinje fibres. *J Physiol.* 1984;355:251-266.

Endo M. Mechanism of action of caffeine on the sarcoplasmic reticulum of skeletal muscle. *Proc Jpn Acad.* 1975;51:479-484.

Fabiato A. Calcium-induced release of calcium from the cardiac sarcoplasmic reticulum. *Am J Physiol.* 1983;245:C1-C14.

Fabiato A. Effects of ryanodine in skinned cardiac cells. *Fed Proc.* 1985;44:2970-2976.

Fabiato A. Time and calcium dependence of activation and inactivation of calcium-induced release of calcium from the sarcoplasmic reticulum of a skinned canine cardiac Purkinje cell. *J Gen Physiol.* 1985;85:247-289.

Fabiato A, Fabiato F. Activation of skinned cardiac cells: Subcellular effects of cardioactive

drugs. *Eur J Cardiol*. 1973;1:143-155.

Fabiato A, Fabiato F. Contractions induced by a calcium-triggered release of calcium from the sarcoplasmic reticulum of single skinned cardiac cells. *J Physiol*. 1975;249:469-495.

Fabiato A, Fabiato F. Calcium-induced release of calcium from the sarcoplasmic reticulum of skinned cells from adult human, dog, cat, rabbit, rat, and frog hearts and from fetal and new-born rat ventricles. *Ann NY Acad Sc*. 1978;307:491-522.

Fabiato A, Fabiato F. Effects of pH on the myofilaments and the sarcoplasmic reticulum of skinned cells from cardiac and skeletal muscles. *J Physiol*. 1978;276:233-255.

Fabiato A, Fabiato F. Calculator programs for computing the composition of the solutions containing multiple metals and ligands used for experiments in skinned muscle cells. *J Physiol*. 1979;75(5):463-505.

Fabiato F. Dependence of the contractile activation of skinned cardiac cells on the sarcomere length. *Nature*. 1975;256:54-56.

Forman R, Ford LE, Sonnenblick EH. Effect of muscle length on the force-velocity relationship of tetanized cardiac muscle. *Circ Res*. 1972;31:195-206.

Fry CH, Powell T, Twist VW, Ward JPT. Net calcium exchange in adult rat ventricular: An assesment of mitochondrial calcium accumulating capacity. *Proc R Soc Lond*. 1984;223:223-238.

Gagov H, Duridanova D, Boev K. Inhibition of  $Ca^{2+}$  current in ileal cells by cyclopiazonic acid and ryanodine. *Eur J Pharmacol*. 1993;243:19-24.

Gao WD, Backx PH, Azan-Backx M, Marban E. Myofilament  $Ca^{2+}$  sensitivity in intact versus skinned rat ventricular muscle. *Circ Res*. 1994;74:408-415.

Goeger D, Riley R. Interaction of cyclopiazonic acid with rat skeletal muscle sarcoplasmic reticulum vesicles. *Biochemical Pharmacology*. 1989;38, No.22:3995-4003.

Goeger D, Riley R, Dorner J, Cole R. Cyclopiazonic acid inhibition of the  $Ca^{2+}$  -transport ATPase in rat skeletal muscle sarcoplasmic reticulum vesicles. *Biochemical Pharmacology*. 1988;37, No.5:978-981.

- Gordon AM, Huxley AF, Julian FJ. The variation in isometric tension with sarcomere length in vertebrate muscle fibres. *J Physiol.* 1966;184:170-192.
- Gordon AM, Pollack GH. Effects of calcium on the sarcomere length-tension relation in rat cardiac muscle. *Circ Res.* 1980;47:610-619.
- Grynkiewicz G, Poenie M, Tsien RY. A new generation of  $\text{Ca}^{++}$  indicators with greatly improved fluorescence properties. *J Biol Chem.* 1986;260:3440-3450.
- Gueth K, Wojciechowski R. Perfusion cuvette for the simultaneous measurement of mechanical optical and energetic parameters of skinned muscle fibres. *Pflugers Arch.* 1986;407:552-557.
- Guth K, Potter JD. Effect of rigor and cycling cross-bridges on the structure of troponin C and on the  $\text{Ca}^{++}$  affinity of the  $\text{Ca}^{++}$ -specific regulatory sites in skinned rabbit psoas fibers. *J Biol Chem.* 1987;262/28:13627-13635.
- Hannon JD, Martyn DA, Gordon AM. Effects of cycling and rigor crossbridges on the conformation of cardiac troponin C. *Circ Res.* 1991;71:984-991.
- Harrison SM, Bers DM. Correction of proton and Ca association constants of EGTA for temperature and ionic strength. *Am J Physiol.* 1989;256/25:C1250-C1256.
- Harrison SM, McCall E, Boyett MR. The relationship between contraction and intracellular sodium in rat and guinea-pig ventricular myocytes. *J Physiol.* 1992;449:517-550.
- Hibberd MG, Jewell BR. Calcium- and length-dependent force production in rat ventricular muscle. *J Physiol.* 1982;329:527-540.
- Hofmann PA, Fuchs F. Effect of length and cross-bridge attachment on  $\text{Ca}^{++}$  binding to cardiac troponin-C. *Am J Physiol.* 1987a;253:90-96.
- Hofmann PA, Fuchs F. Evidence for a force-dependent component of calcium binding to cardiac troponin-C. *Am J Physiol.* 1987b;253:541-546.
- Hofmann PA, Fuchs F. Bound calcium and force development in skinned cardiac muscle bundles: Effect of sarcomere length. *J Mol Cell Cardiol.* 1988;20:667-677.
- Holroyde MJ, Robertson SP, Johnson JD, Solaro RJ, Potter JD. The calcium and magnesium

binding sites on cardiac troponin and their role in the regulation of myofibrillar adenosine triphosphatase. *J Biol Chem.* 1980;255:11688-11693.

Hove-Madsen L, Bers D. Sarcoplasmic Reticulum  $Ca^{2+}$  Uptake and Thapsigargin Sensitivity in Permeabilized Rabbit and Rat Ventricular Myocytes. *Circ Res.* 1993;73, No.5:820-828.

Huchet C, Leoty C. Effects of cyclopiazonic acid on  $Ca^{2+}$  -activated tension production in skinned skeletal muscle fibres of the ferret. *Eur J Pharmacol.* 1993;241:41-46.

Janczewski AM, Lakatta EG. Thapsigargin inhibits  $Ca^{++}$  uptake and  $Ca^{++}$  depletes sarcoplasmic reticulum in intact cardiac myocytes. *Am J Physiol.* 1993;265:H517-H522.

Jewell BR, Kentish JC. Dithiothreitol reduces the deterioration of skinned preparations of cardiac muscle. *J Physiol.* 1981;319:83P-84P.

Katz LA, Koretsky AB, Balaban RS. Activation of dehydrogenase activity and cardiac respiration: a  $^{31}P$ -NMR study. *Am J Physiol.* 1988;255:H185-H188.

Kentish JC. The inhibitory effects of monovalent ions on force development in detergent-skinned ventricular muscle from guinea-pig. *J Physiol.* 1984;352:353-374.

Kentish JC. The effects of inorganic phosphate and creatine phosphate on force production in skinned fibres from rat ventricle. *J Physiol.* 1986;370:585-604.

Kentish JC, Stienen GJM. Differential effects of length on maximum force production and myofibrillar ATPase activity in rat skinned cardiac muscle. *J Physiol.* 1994;475:175-184.

Kentish JC, ter Keurs HEDJ, Allen DG. The contribution of myofibrillar properties to the sarcomere length-force relationship of cardiac muscle. In: ter Keurs HEDJ, Noble MIM, eds. *Starling's Law of the Heart Revisited*. Kluwer Academic Publishers; 1988:

Kentish JC, ter Keurs HEDJ, Ricciardi L, Bucx JJJ, Noble MIM. Comparison between the sarcomere length-force relations of intact and skinned trabeculae from rat right ventricle. *Circ Res.* 1986;58:755-768.

Kirby MS, Orchard C, Boyett MR. The control of calcium influx by cytoplasmic calcium in mammalian heart cells. *Mol Cell Biochem.* 1989;89:109-113.

Kirby MS, Sagara Y, Gaa S, et.al. . Thapsigargin Inhibits Contraction and  $Ca^{2+}$  Transient in

Cardiac Cells by Specific Inhibition of the Sarcoplasmic Reticulum  $\text{Ca}^{2+}$  Pump. *J Biol Chem.* 1992;267:12545-12551.

Kort AA, Capogrossi MC, Lakatta EG. Frequency, amplitude, and propagation velocity of spontaneous calcium-dependent contractile waves in intact adult rat cardiac muscle and isolated myocytes. *Circ Res.* 1985;57:844-855.

Krueger JW, Pollack GH. Myocardial sarcomere dynamics during isometric contraction. *J Physiol.* 1975;251:627-643.

Kuhn HJ, Bletz C, Ruegg JC. Stretch-induced increase in the  $\text{Ca}^{++}$  sensitivity of myofibrillar ATPase activity in skinned fibers from pig ventricles. *Pflugers Arch.* 1990;415:741-746.

Kurebayashi N, Ogawa Y. Discrimination of  $\text{Ca}^{2+}$ -ATPase activity of the sarcoplasmic reticulum from actomyosin-type ATPase activity of myofibrils in skinned mammalian skeletal muscle fibres: distinct effects of cyclopiazonic acid on the two ATPase activities. *J Muscle Res Cell Motil.* 1991;12:355-365.

Landesberg A, Sideman S. Coupling calcium binding to troponin C and cross-bridge cycling in skinned cardiac cells. *Am J Physiol.* 1994;266:H1260-H1271.

Lee JA, Allen DG. *Modulation of cardiac calcium sensitivity.* New York: Oxford Medical Publications; 1993.

Lytton J, Westlin M, Hanley MR. Thapsigargin inhibits the sarcoplasmic reticulum or endoplasmic reticulum  $\text{Ca}$ -ATPase family of calcium pumps. *J Biol Chem.* 1991;266(26):17067-17071.

Marban E, Kusuoka H, Yue DT, Weisfeldt ML, Gil Wier W. Maximal  $\text{Ca}^{2+}$ -activated force elicited by tetanization of ferret papillary muscle and whole heart: mechanism and characteristics of steady contractile activation in intact myocardium. *Circ Res.* 1986;59:262-269.

Martell AE, Smith RM. *Critical stability constants.* New York & London: Plenum Press; 1974:

Mashima H. Tetanic contraction and tension-length relation of frog ventricular muscle. *Jpn J Physiol.* 1977;27:321-335.

Mason M, Garcia-Rodriguez C, Grinstein S. Coupling between Intracellular  $\text{Ca}^{2+}$  Stores and

- the  $Ca^{2+}$  Permeability of the Plasma Membrane. *J Biol Chem*. 1991;266,No.31:20856-20862.
- McCormack JG, Denton RM. The role of mitochondrial  $Ca^{++}$  transport and matrix  $Ca^{++}$  in signal transduction in mammalian tissue. *Biochim Biophys Acta*. 1990;1018:287-291.
- McCormack JG, Halestrap AP, Denton RM. Role of calcium ions in regulation of mammalian intramitochondrial metabolism. *Physiol Rev*. 1990;70:391.
- Metzger JM, Moss RL. Kinetics of a  $Ca^{++}$ -sensitive crossbridge state transition in skeletal muscle fibers. *J Gen Physiol*. 1991;98:233-248.
- Miller DJ, Smith GL. EGTA purity and the buffering of calcium ions in physiological solutions. *Am J Physiol*. 1984;246:C160-C166.
- Miller DJ, Smith GL. The contractile behaviour of EGTA- and detergent-treated heart muscle. *J Muscle Res Cell Motil*. 1985;6:541-568.
- Moore GA, McConkey DJ, Kass GEN, O'Brien PJ, Orrenius S. 2,5-Di(tert-butyl)-1,4-benzohydroquinone- a novel inhibitor of liver microsomal  $Ca^{++}$  sequestration. *FEBS Lett*. 1987;224:331-336.
- Morad M, Goldman Y. Excitation-contraction coupling in heart muscle: membrane control of development of tension. *Prog Biophys Molec Biol*. 1973;27:257-313.
- Morad M, Goldman YE, Trentham DR. Rapid photochemical inactivation of  $Ca^{++}$ -agonists shows that  $Ca^{++}$  entry directly activates contraction in frog heart. *Nature*. 1983;304:635-638.
- Moss RL. Sarcomere-length-tension relations of frog skinned muscle fibres during calcium activation at short lengths. *J Physiol*. 1979;292:177-192.
- Moss RL.  $Ca^{++}$  Regulation of Mechanical Properties of Striated Muscle. *Circ Res*. 1992;70:865-884.
- Moss RL, Giulian GG, Greaser ML. The effects of partial extraction of TnC upon the tension-pCa relationship in rabbit skinned skeletal muscle fibers. *J Gen Physiol*. 1985;86:585-600.
- Mullins LJ. The generation of electric currents in cardiac fibers by sodium/calcium exchange. *Am J Physiol*. 1979;236:C103-C110.

Nayler WG, Dunnett J, Burian W. Further observations on species-determined differences in the calcium-accumulating activity of cardiac microsomal fractions. *J Mol Cell Cardiol.* 1975;7:663-675.

Nguyen TT. *ATP hydrolysis by cardiac actomyosin.* University of Calgary; 1994.

Noble D, Shimoni Y. The calcium and frequency dependence of the slow inward current "staircase" in frog atrium. *J Physiol.* 1981;310:57-75.

Orchard CH, Kentish JC. Effects of changes in pH on the contractile function of cardiac muscle. *Am J Physiol.* 1990;258:C967-C981.

Pan B, Solaro RJ. Calcium-binding Properties of Troponin C in Detergent-skinned Heart Muscle Fibers. *J Biol Chem.* 1987;262:7839-7849.

Perreault CL, Mulieri LA, Alpert NR, Ransil BJ, Allen PD, Morgan JP. Cellular basis of negative inotropic effect of 2,3-butanedione monoxime in human myocardium. *Am J Physiol.* 1992;263:H503-H510.

Pery-Man N, Chemla D, Coirault C, Riou B, Lecarpentier Y. A comparison of cyclopiazonic acid and ryanodine effects on cardiac muscle relaxation. *Am J Physiol.* 1993;265:1364-1372.

Philipson KD. Sodium-calcium exchange in plasma membrane vesicles. *Ann Rev Physiol.* 1985;47:561-571.

Potter JD, Gergely J. The calcium and magnesium binding sites on troponin and their role in the regulation of myofibrillar adenosine triphosphatase. *J Biol Chem.* 1975;250:4628-4633.

Ricciardi L, Bucx JJJ, ter Keurs HEDJ. Effects of acidosis on force-sarcomere length and force-velocity relations of rat cardiac muscle. *Cardiovasc Res.* 1986;20:117-123.

Robertson SP, Johnson JD, Holroyde MJ, Kranias EG. The effect of troponin I phosphorylation on the Ca-binding properties of the Ca-regulatory site of bovine cardiac troponin. *J Biol Chem.* 1982;257:260-263.

Roe MW, Lemasters JJ, Herman B. Assessment of fura-2 for measurements of cytosolic free calcium. *Cell Calcium.* 1990;11:63-73.

Ruegg JC. The dependence of muscle contraction and relaxation on the intracellular concentration of free calcium ions. In: Ruegg JC, ed. *Calcium in Muscle activation*. Berlin: Springer-Verlag; 1988:59-82.

Schouten VJA. *Excitation-contraction coupling in heart muscle*. The Netherlands: 1985.

Schouten VJA, Bucx JJJ, de Tombe PP, ter Keurs HEDJ. Sarcolemma, sarcoplasmic reticulum, and sarcomeres as limiting factors in force production in rat heart. *Circ Res*. 1990;67:913-922.

Schouten VJA, Deen JK, Tombe PP, Verveen AA. Force-interval relationship in heart muscle of mammals. A calcium compartment model. *Biophys J*. 1987;51:13-26.

Schramm M, Thomas G, Towart R, Frankowiac G. Novel dihydropyridine with positive inotropic action through activation of calcium channels. *Nature (Lond)*. 1983;309:535-537.

Seidler NW, Jona I, Vegh M, Martonosi A. Cyclopiazonic acid is a specific inhibitor of the  $Ca^{++}$ -ATPase of sarcoplasmic reticulum. *J Biol Chem*. 1989;264:17816-17823.

Shattock MJ, Bers DM. Rat vs. rabbit ventricle: Ca flux and intracellular Na assessed by ion-selective microelectrodes. *Am J Physiol*. 1989;256:C813-C822.

Shima H, Blaustein MP. Modulation of evoked contractions in rat arteries by ryanodine, thapsigargin, and cyclopiazonic acid. *Circ Res*. 1992;70:968-977.

Snedecor GW, Cochran WG. *Statistical Methods*. Iowa State University Press; 1967:

Spurgeon HA, DuBell WH, Stern MD, Sollott SJ, Ziman BD, Silverman HS, Capogrossi MC, Talo A, Lakatta EG. Cytosolic calcium and myofilaments in single rat cardiac myocytes achieve a dynamic equilibrium during twitch relaxation. *J Physiol Lond*. 1992;447:83-102.

Sutko JL, Kenyon JL. Ryanodine modification of cardiac muscle responses to potassium-free solutions. *J Gen Physiol*. 1983;82:385-404.

Sutko JL, Willerson JT. Ryanodine alteration of the contractile state of rat ventricular myocardium. *Circ Res*. 1980;46:332-343.

Suzuki M, Muraki K, Imaizumi Y, Watanabe M. Cyclopiazonic acid, an inhibitor of the sarcoplasmic reticulum  $Ca^{2+}$ -pump, reduces  $Ca^{2+}$ -dependent  $K^{+}$  currents in guinea-pig smooth muscle cells. *Br J Pharmacol*. 1992;107:134-140.

- Sweitzer NK, Moss RL. The effect of altered temperature on  $Ca^{++}$  sensitive force in skinned single cardiac myocytes: Evidence for force dependence of thin filament activation. *J Gen Physiol*. 1990;96:1221-1245.
- ter Keurs HEDJ, Rijnsburger WH, van Heuningen R, Nagelsmit MJ. Tension development and sarcomere length in rat cardiac trabeculae: Evidence of length-dependent activation. *Circ Res*. 1980;46:703-714.
- Thastrup O, Cullen PJ, Drobak BK, et.al. . Thapsigargin, a tumor promoter, discharges intracellular  $Ca^{2+}$  stores by specific inhibition of the endoplasmic reticulum. *Proc Natl Acad Sci USA*. 1990;87:2466-2470.
- Tobacman LS. Activation of actin-cardiac myosin subfragment 1 MgATPase rate by  $Ca^{++}$  shows cooperativity intrinsic to the thin filament. *Biochemistry*. 1987;20:492-497.
- Tobacman LS, Saywer D. Calcium binds cooperatively to the regulatory sites of the cardiac thin filament. *J Biol Chem*. 1990;265(2):931-939.
- Tsien RY. Fluorescence probes of cell signaling. *Ann Rev Neurosci*. 1989;12:227-253.
- Uyama Y, Imaizumi Y, Watanabe M. Effects of cyclopiazonic acid, a novel  $Ca^{2+}$  -ATPase inhibitor, on contractile responses in skinned ileal smooth muscle. *Br J Pharmacol*. 1992;106:208-214.
- Uyama Y, Imaizumi Y, Watanabe M. Cyclopiazonic acid, an inhibitor of  $Ca^{2+}$  -ATPase in sarcoplasmic reticulum, increases excitability in ileal smooth muscle. *Br J Pharmacol*. 1993;110:565-572.
- Watanabe J, Karibe A, Horiguchi S, Keitoku M, Satoh S, Takishima T, Shirato K. Modification of myogenic intrinsic tone and  $[Ca^{++}]_i$  of rat isolated arterioles by ryanodine and cyclopiazonic acid. *Circ Res*. 1993;73:465-472.
- White RL, Wittenberg BA. NADH fluorescence of isolated ventricular myocytes: Effect of pacing, myoglobin, and oxygen supply. *Biophys J*. 1993;65:196-204.
- Wohlfart B. *Interval-strength relations of mammalian myocardium interpreted as altered kinetics of activator  $Ca^{++}$  during the cardiac cycle (Thesis)*. The University of Lund, Sweden; 1982.

- Wohlfart B, Noble MIM. The cardiac excitation-contraction cycle. *Pharmac Ther.* 1982;16:1-43.
- Wrzosek A, Schneider H, Grueninger S, Chiesi M. Effect of Thapsigargin on cardiac muscle cells. *Cell Calcium.* 1992;13:281-292.
- Wuytack F, Raeymaekers L. The  $Ca^{2+}$ -Transport ATPases from the Plasma Membrane. *J Bioenerg Biomembr.* 1992;24,No.3:285-300.
- Yue DT, Marban E, Wier G. Relationship between force and intracellular [Ca] in tetanized mammalian heart muscle. *J Gen Physiol.* 1986;87:223-242.
- Zot AS, Potter JD. Reciprocal coupling between troponin C and myosin crossbridge attachment. *Biochemistry.* 1989;28:6751-6756.
- Zot AS, Potter JD. Structural aspects of troponin-tropomyosin regulation of skeletal muscle contraction. *Ann Rev Biophys Biophys Chem.* 1987;16:535-559.
- Zot HG, Potter JD. Purification of Actin from Cardiac Muscle. *Prep Biochem.* 1981;11:381-395.